# Short-Lived Radical Characterisation: Novel Radical Trap Synthesis, Application and Methodology Development

Supporting Information

Peter J. H. Williams

University of York

Chemistry

January 2022

# List of supporting information contents

# List of supporting information tables

# List of supporting information figures

# SI1. Chemicals

*2,2,6,6*-Tetramethylpiperidine 1-oxyl (TEMPO•, 98%, Acros Organics), cyclohexanecarboxaldehyde (97%, Acros Organics) pyrrolidine (99%, Sigma-Aldrich), iron(iii) chloride (97%, Sigma-Aldrich), methyltriphenylphosphonium bromide (98%, Sigma-Aldrich), sodium bis(trimethylsilyl)amide (1.0 M in dry THF, Sigma-Aldrich), allyl iodide (98%, Sigma-Aldrich), sodium sulfite (≥98%, Sigma-Aldrich), 2,2,6,6-tetramethylpiperidine (TMP, >98%, Alfa Aesar), allyl bromide (97%, Sigma-Aldrich), potassium iodide (≥99.0%, Sigma-Aldrich), *meta*-chloroperoxybenzoic acid (*m*-CPBA, ≤77%, Sigma-Aldrich), 2-(bromomethyl)acrylic acid (98%, Sigma-Aldrich), *O*-(benzotriazol-1-yl)-*N*,*N*,*N'*,*N'*-tetramethyluronium hexafluorophosphate (HBTU, 98%, Alfa Aesar), *N*,*N*-diisopropylethylamine (DIPEA, ≥99%, Sigma-Aldrich), cyclohexylamine (>98%, Alfa Aesar), sodium iodide (>99%, Thermo Scientific), methyl 2-(bromomethyl)acrylate (>97%, TCI), cyclooctylamine (97%, Sigma-Aldrich), 1-decanamine (≥99.0%, Sigma-Aldrich), ethanolamine (≥98%, Sigma-Aldrich), 1,3,4,6-tetra-*O*-acetyl-2-amino-2-deoxy-β-D-glucopyranose hydrochloride (≥98%, Alfa Aesar), ethylenediamine (99%, Alfa Aesar), 1,8-diaminoctane (98%, Sigma-Aldrich), 4,7,10-trioxa-1,13-diaminotridecane (97%, Sigma-Aldrich), Boc anhydride (>99%, Acros Organics), D-biotin (>98%, Fluorochem), trifluoroacetic acid (≥99.0%, Sigma-Aldrich), *N*,*N*-dimethylethylenediamine (≥98%, Sigma-Aldrich), iodomethane (99%, Sigma-Aldrich) and (3-aminopropyl)tris(trimethylsiloxy)silane (95%, Fluorochem) were used for TART synthesis without further purification.

1-Dodecanethiol (≥98%, Sigma-Aldrich), azobisisobutyronitrile (AIBN, 98%, Sigma-Aldrich), lead(iv) oxide (99.998%, Sigma-Aldrich), isopentyl nitrite (97%, Alfa Aesar), diisopropylamine (99%, Acros Organics), dibutylamine (≥98%, Sigma-Aldrich), *N*-chlorosuccinimide (NCS, 98%, Sigma-Aldrich), octanoic acid (≥99%, Sigma-Aldrich), silver nitrate (≥99.0%, Sigma-Aldrich), bromine (≥95%, Sigma-Aldrich), 4-methylstyrene (96%, Sigma-Aldrich), diphenylphosphine oxide (97%, Sigma-Aldrich), 4-chloroaniline (98%, Sigma-Aldrich), iodine (≥99.8%, Sigma-Aldrich), *p*-anisic acid (≥99%, Sigma-Aldrich), tribasic potassium phosphate (>97%, Thermo Scientific), styrene (99%, Acros Organics), tris(2,2'-bipyrazine)ruthenium(II) hexafluorophosphate (95%, Strem), benzyl mercaptan (99%, Sigma-Aldrich), thiophenol (>99%, Alfa Aesar), 3-methoxythiophenol (98%, Sigma-Aldrich), cyclohexanethiol (97%, Sigma-Aldrich), methyl thiosalicylate (97%, Acros Organics), *tert*-butylthiol (99%, Sigma-Aldrich), methylenecyclohexane (98%, Acros Organics), 1-methylcyclohexene (97%, Sigma-Aldrich), allyl chloride (98%, Sigma-Aldrich), phenylacetylene (98%, Fluorochem), ethyl *trans*-cinnamate (98%, Acros Organics), sodium acetate (≥99%, Alfa Aesar), iron(II) sulfate heptahydrate (≥99%, Sigma-Aldrich), hydrogen peroxide (30wt.%, Fischer Chemical), *tert*-butanol (≥99.0%, Sigma-Aldrich), thymine (97%, Alfa Aesar), D(+)-glucose (≥99.5%, Sigma-Aldrich), L-ascorbic acid (99%, Sigma-Aldrich), cyclohexene (≥98%, Fischer Chemical), α-pinene (98%, Sigma-Aldrich), Celite® Analytical Filter Aid II (CAFA II, Sigma-Aldrich), *p*-toluenesulfonic acid (≥98.5%, Sigma-Aldrich), dodecamethylpentasiloxane (97%, Sigma-Aldrich), Galden™ HT270 (Fluorochem) and *n*-nonane (99%, Acros Organics) were used for radical trapping without further purification.

Water (LC-MS grade, ≥99.9%, Fischer Chemical), acetonitrile (LC-MS grade, ≥99.9%, Fischer Chemical), formic acid (LC-MS grade, ≥99%, Fischer Chemical), tetrabutylammonium hexafluorophosphate (98%, Sigma-Aldrich), water-$d_2$ (99.9 atom % D, Sigma-Aldrich), formic acid-$d_2$ (95 wt.% in $D_2O$, 98% atom % D, Sigma-Aldrich) were used for MS characterisation without further purification.

# SI2. Synthesis

## SI2.1. Grantham TART

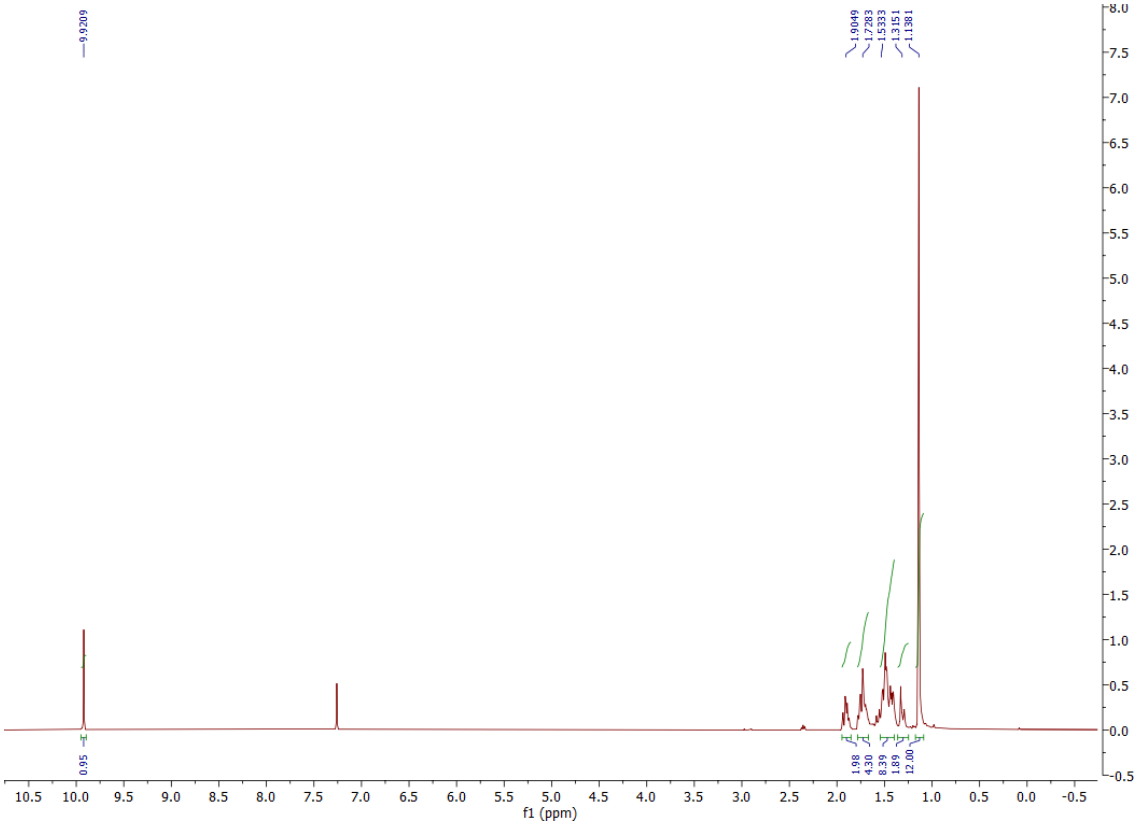


Figure SI1: 1-[(2,2,6,6-Tetramethylpiperidin-1-yl)oxy]cyclohexane-1-carbaldehyde $^{1}H$ NMR spectrum ($CDCl_3$, 400 MHz, 298 K).

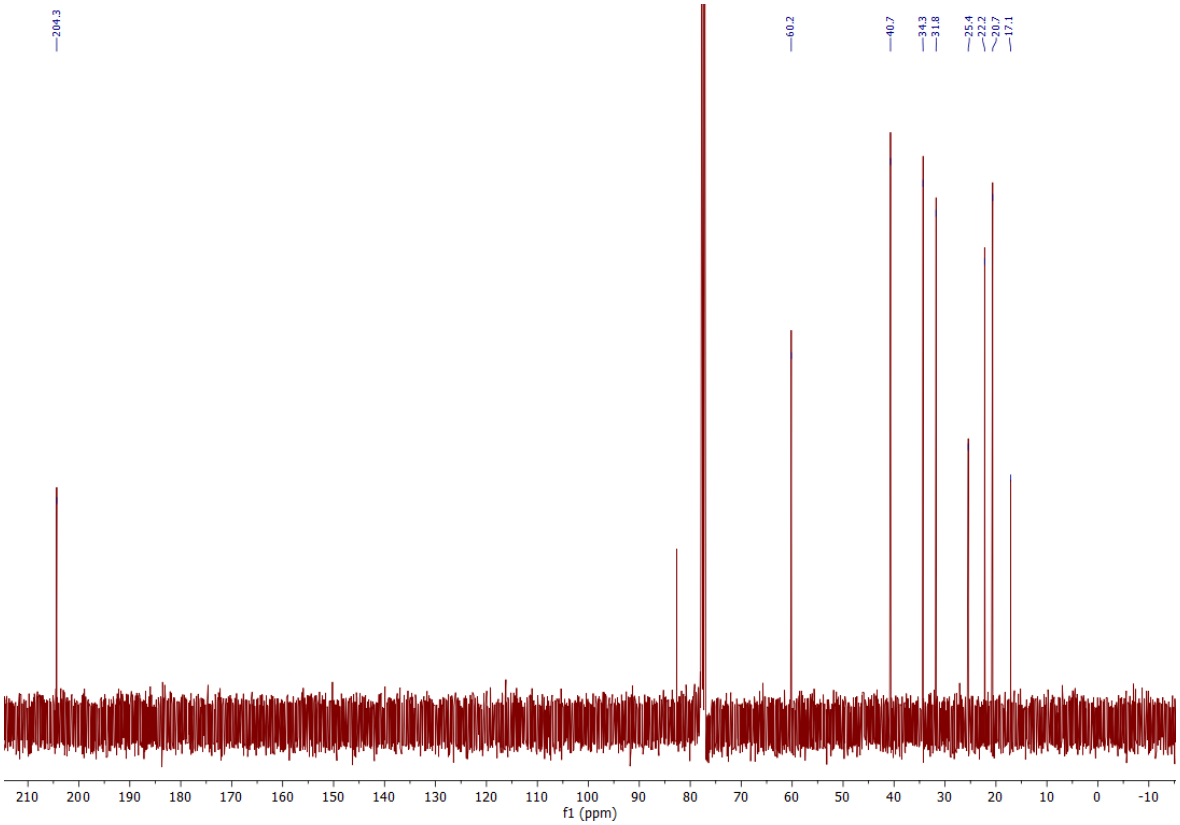


Figure SI2: 1-[(2,2,6,6-Tetramethylpiperidin-1-yl)oxy]cyclohexane-1-carbaldehyde $^{13}C$ NMR spectrum ($CDCl_3$, 100 MHz, 298 K).

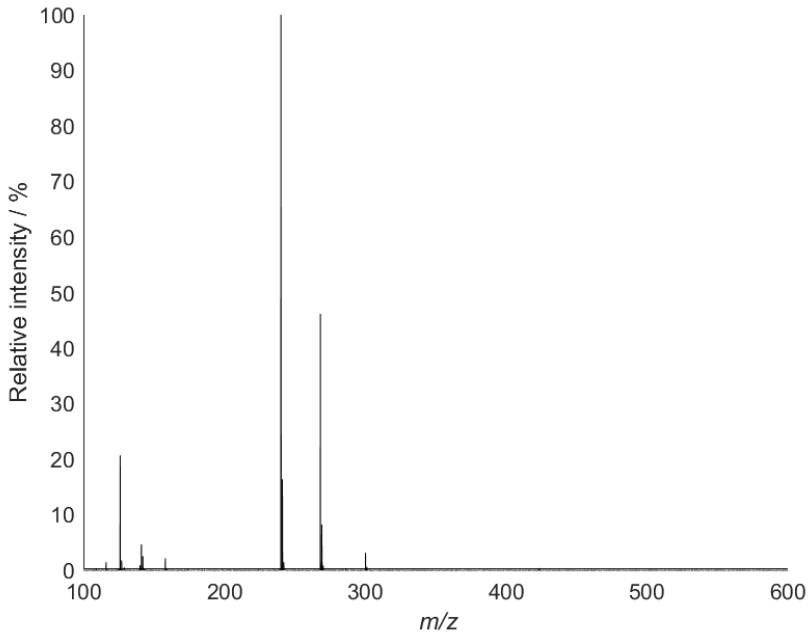


Figure SI3: 1-[(2,2,6,6-Tetramethylpiperidin-1-yl)oxy]cyclohexane-1-carbaldehyde mass spectrum (Pos ESI).

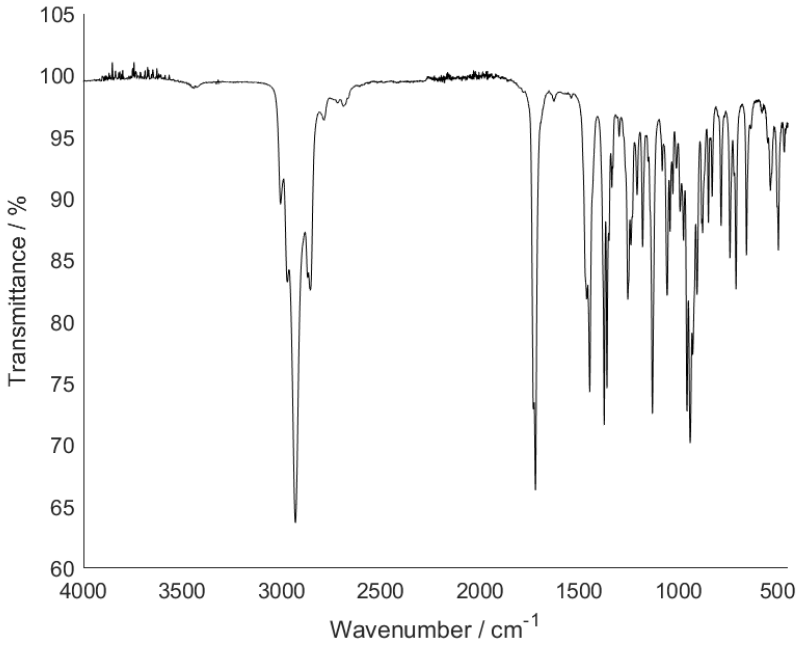


Figure SI4: 1-[(2,2,6,6-Tetramethylpiperidin-1-yl)oxy]cyclohexane-1-carbaldehyde IR spectrum.

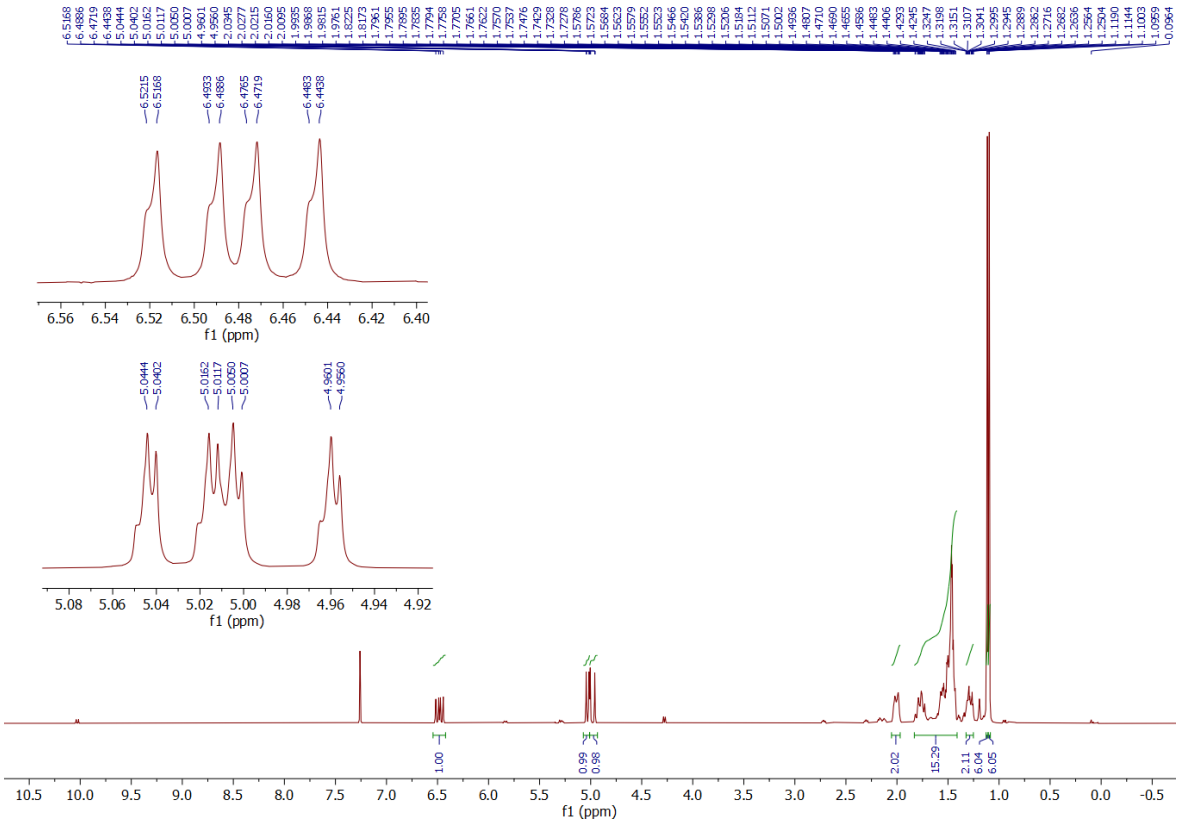


Figure SI5: Grantham TART $^{1}$H NMR spectrum ($CDCl_3$, 400 MHz, 298 K).

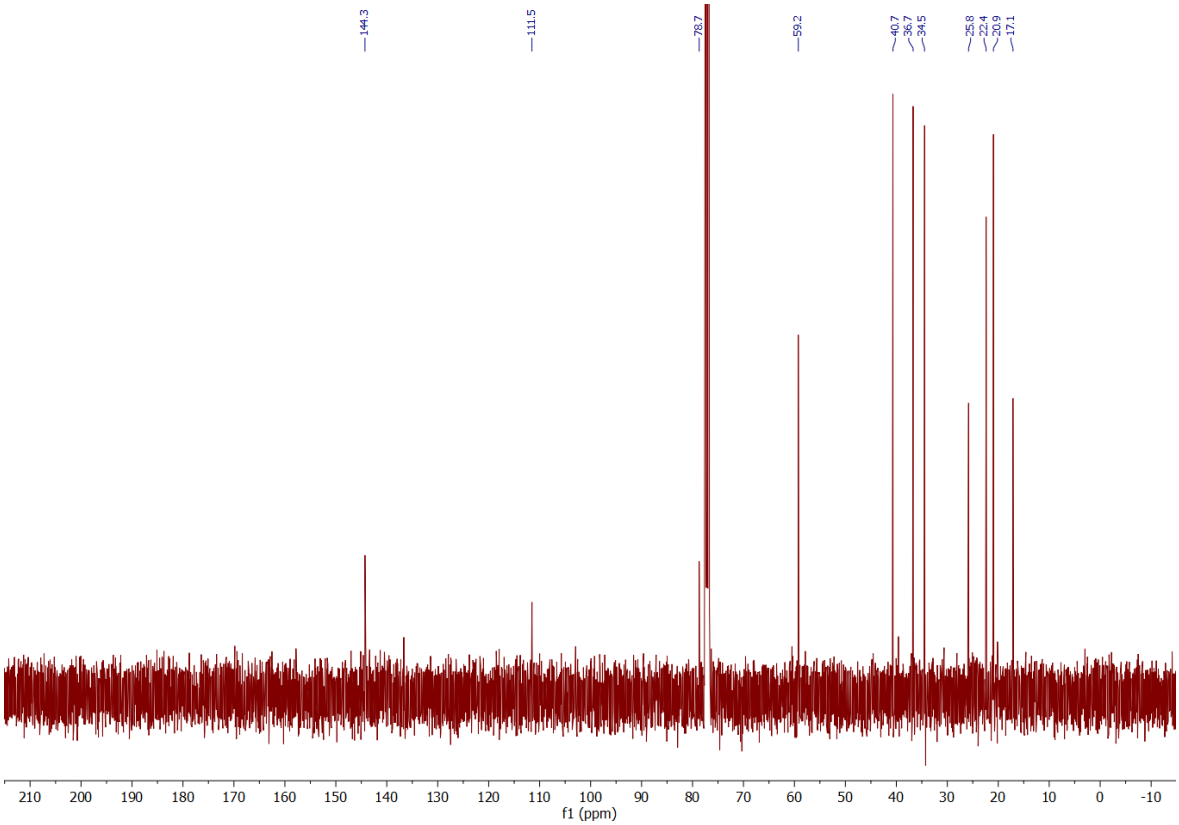


Figure SI6: Grantham TART $^{13}C$ NMR spectrum ($CDCl_3$, 100 MHz, 298 K).

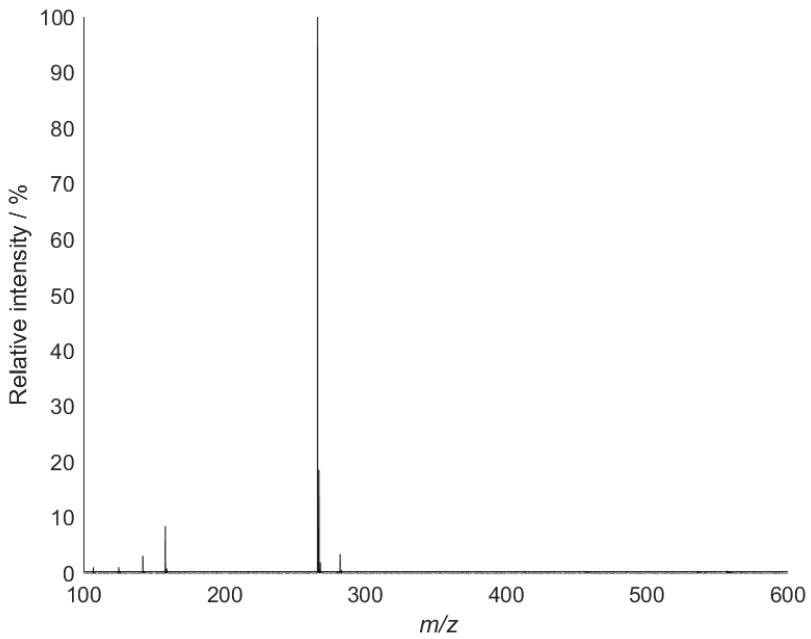


Figure SI7: Grantham TART mass spectrum (Pos ESI).

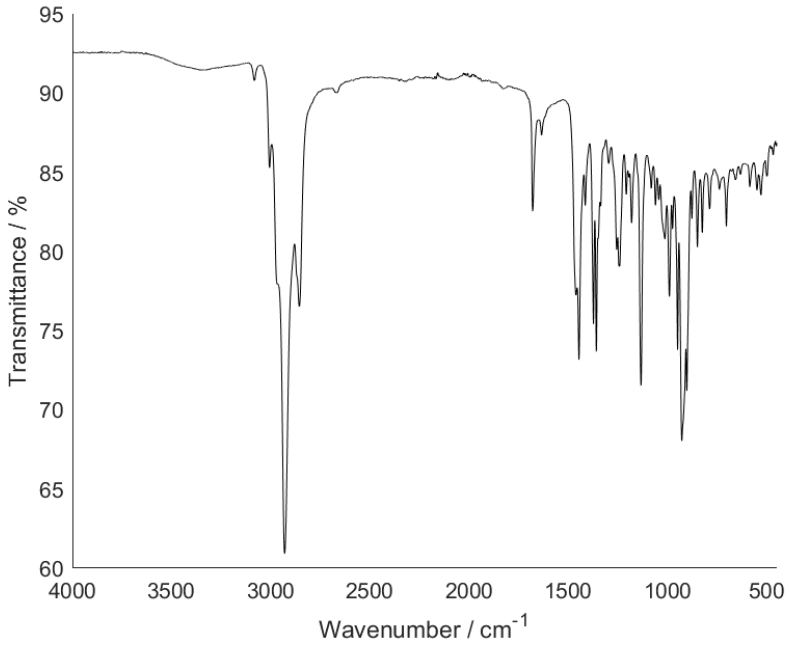


Figure SI8: Grantham TART IR spectrum.

## SI2.2. Allyl-TEMPO

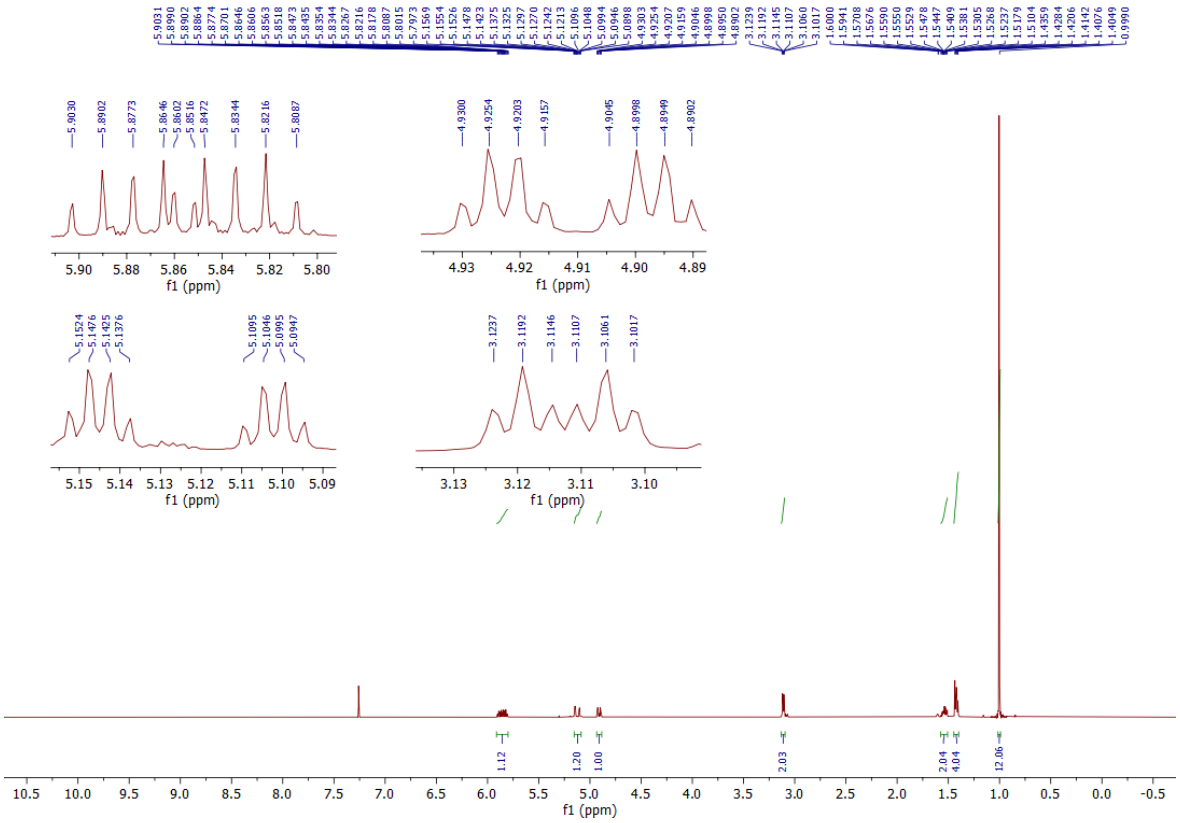


Figure SI9: Allyl-TMP $^{1}$H NMR spectrum ($CDCl_3$, 400 MHz, 298 K).

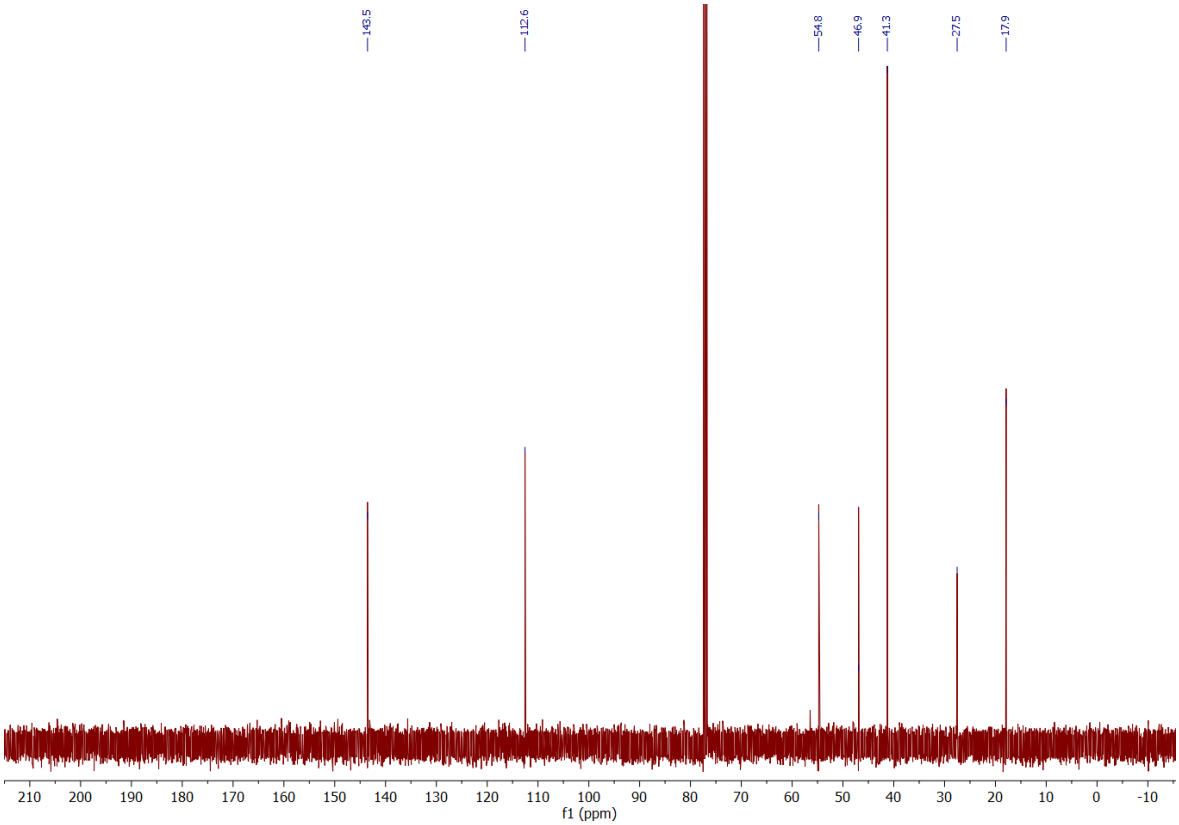


Figure SI10: Allyl-TMP $^{13}C$ NMR spectrum ($CDCl_3$, 100 MHz, 298 K).

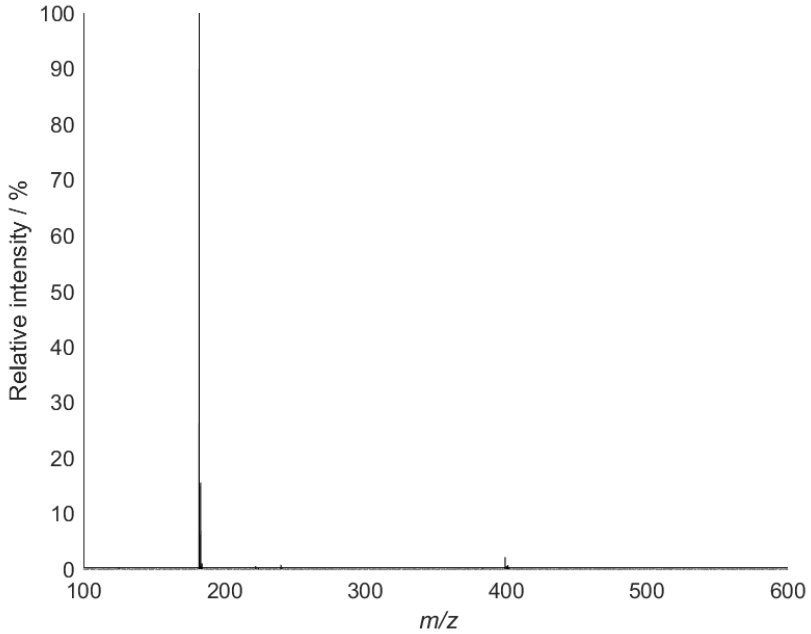


Figure SI11: Allyl-TMP mass spectrum (Pos ESI).

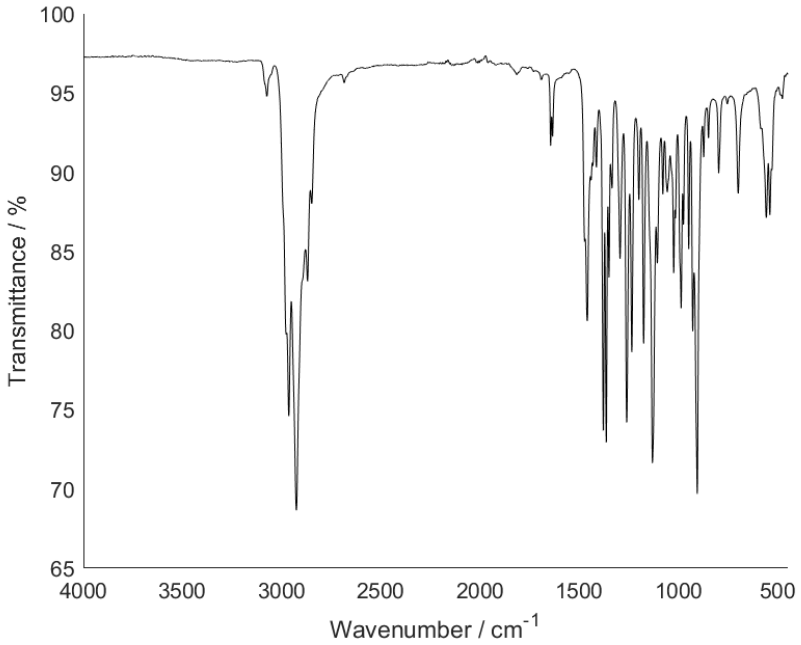


Figure SI12: Allyl-TMP IR spectrum.

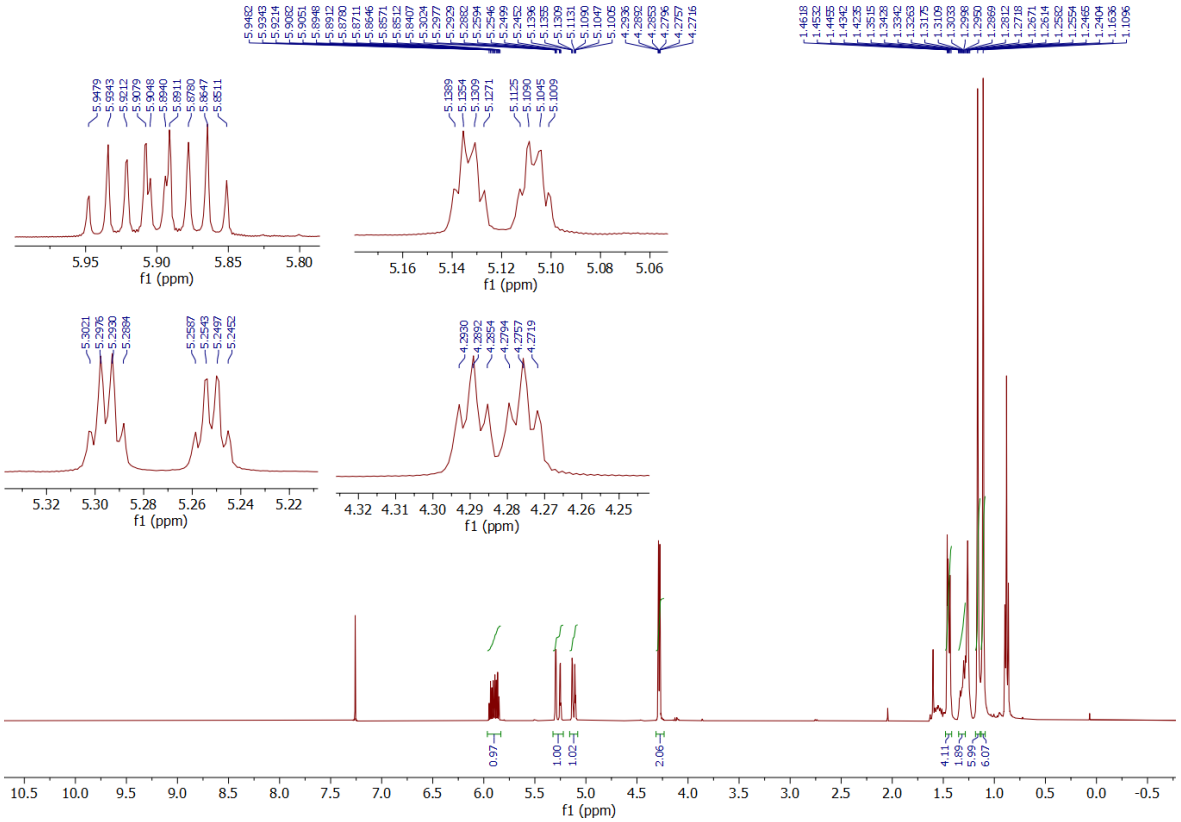


Figure SI13: Allyl-TEMPO $^{1}H$ NMR spectrum ($CDCl_3$, 400 MHz, 298 K).

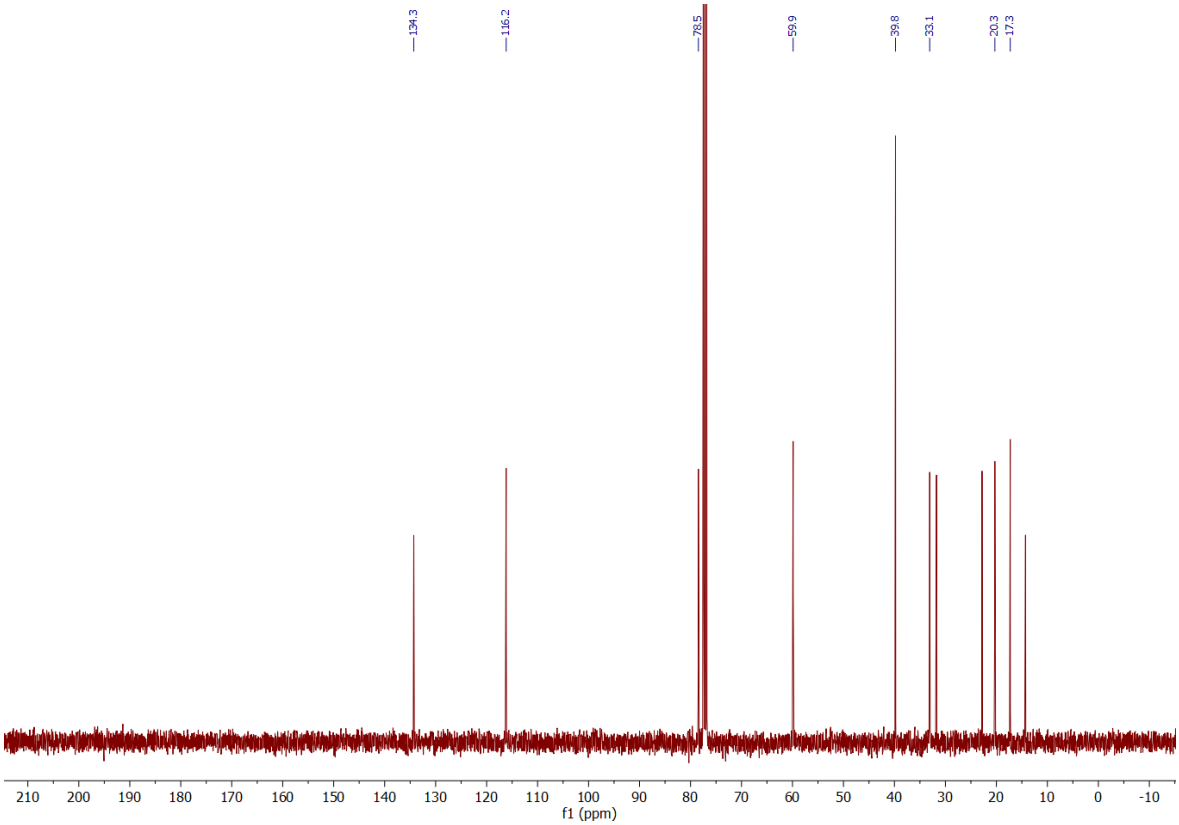


Figure SI14: Allyl-TEMPO $^{13}C$ NMR spectrum ($CDCl_3$, 100 MHz, 298 K).

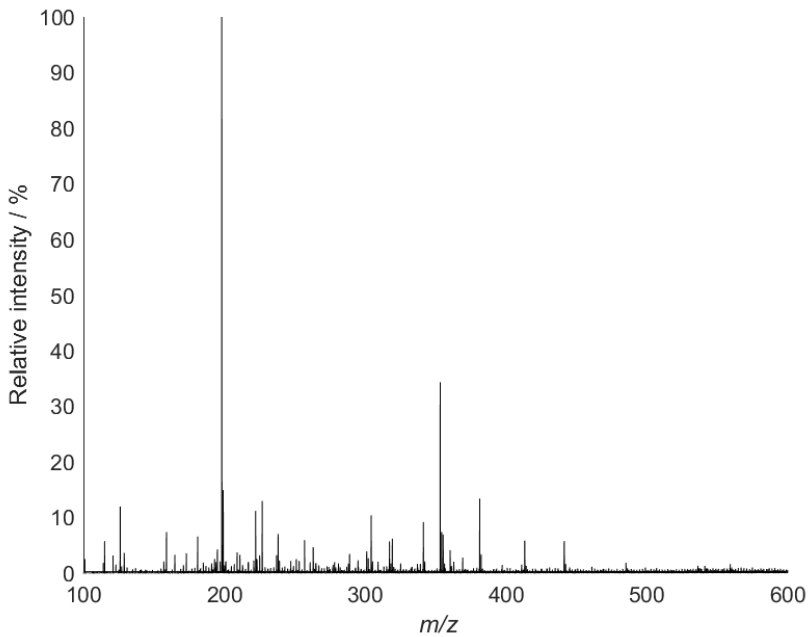


Figure SI15: Allyl-TEMPO mass spectrum (Pos ESI).

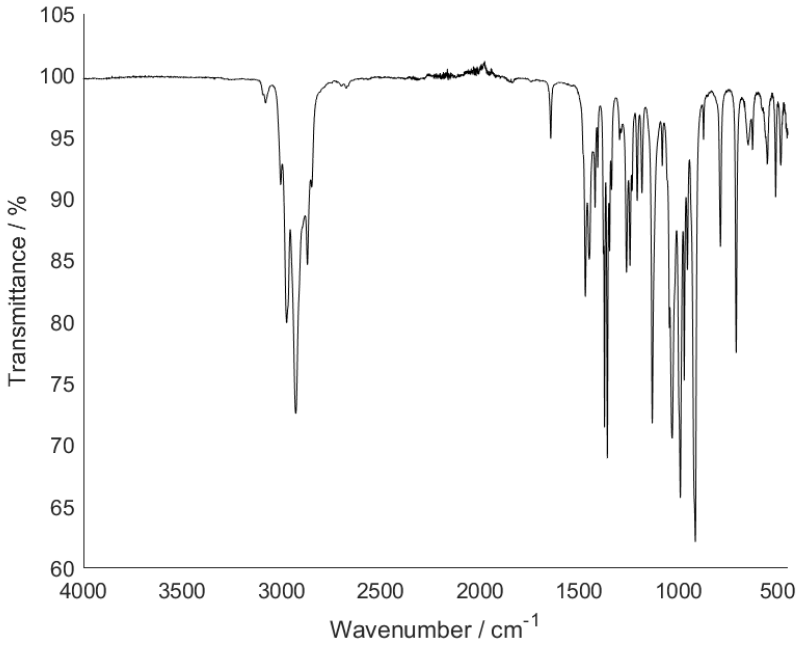


Figure SI16: Allyl-TEMPO IR spectrum.

## SI2.3. Abandoned 2-(bromomethyl)acrylic acid nucleophilic substitution by TMP and Meisenheimer rearrangement

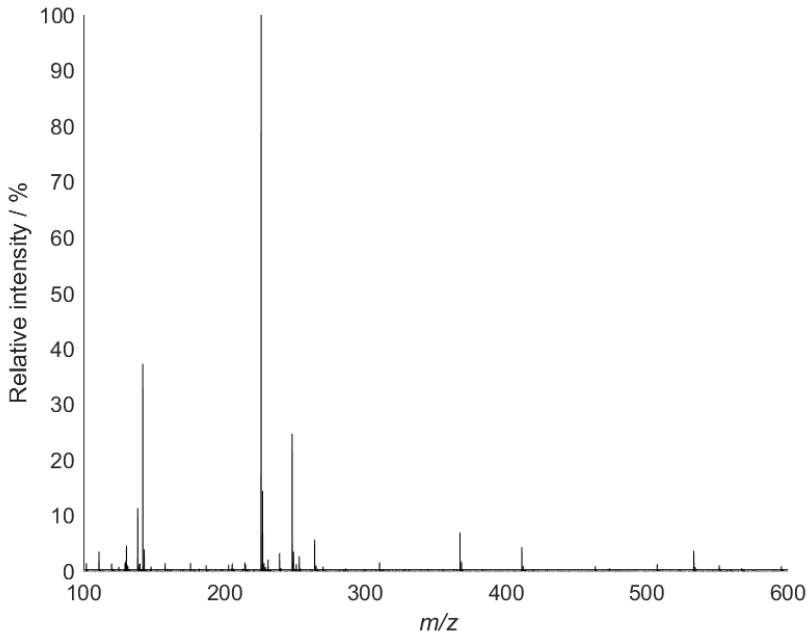


Figure SI17: 2-(TMPmethyl)acrylic acid mass spectrum (Pos ESI).

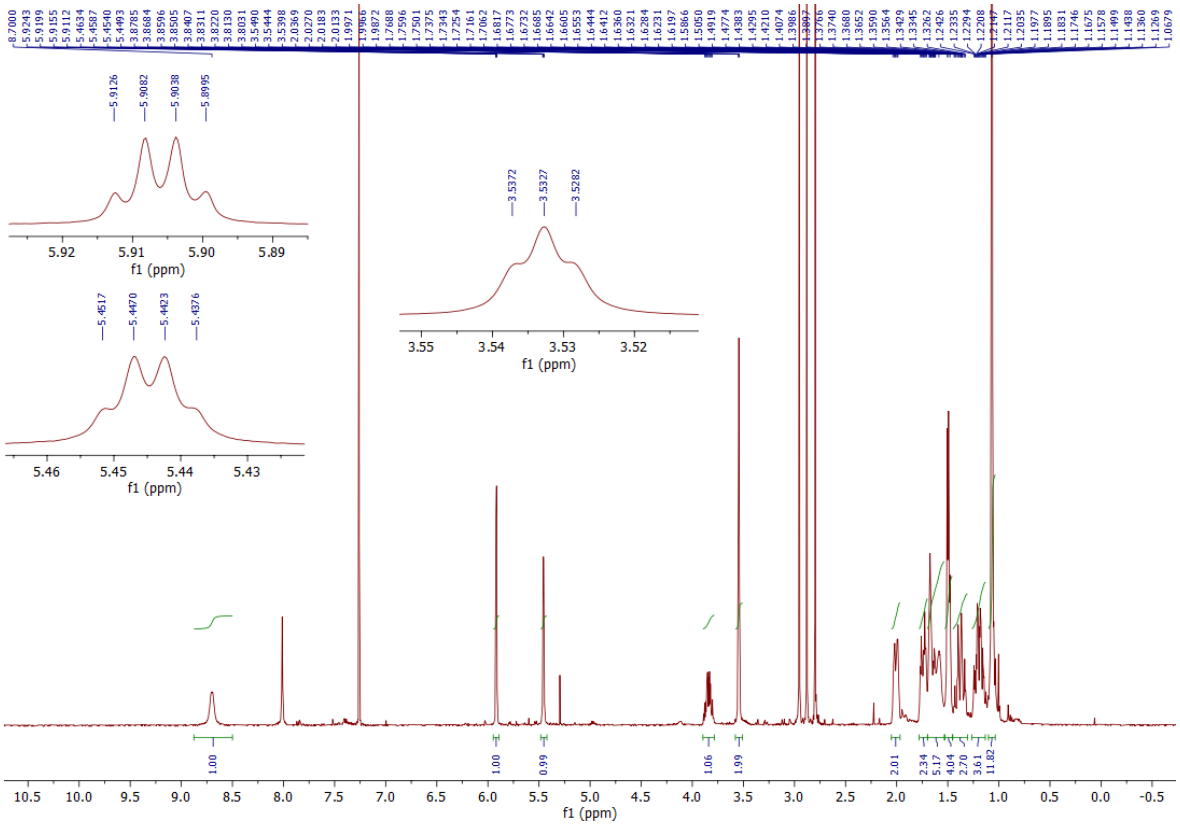


Figure SI18: *N*-Cyclohexyl-2-([2,2,6,6-tetramethylpiperidine]methyl)acrylamide $^{1}$H NMR spectrum ($CDCl_3$, 400 MHz, 298 K).

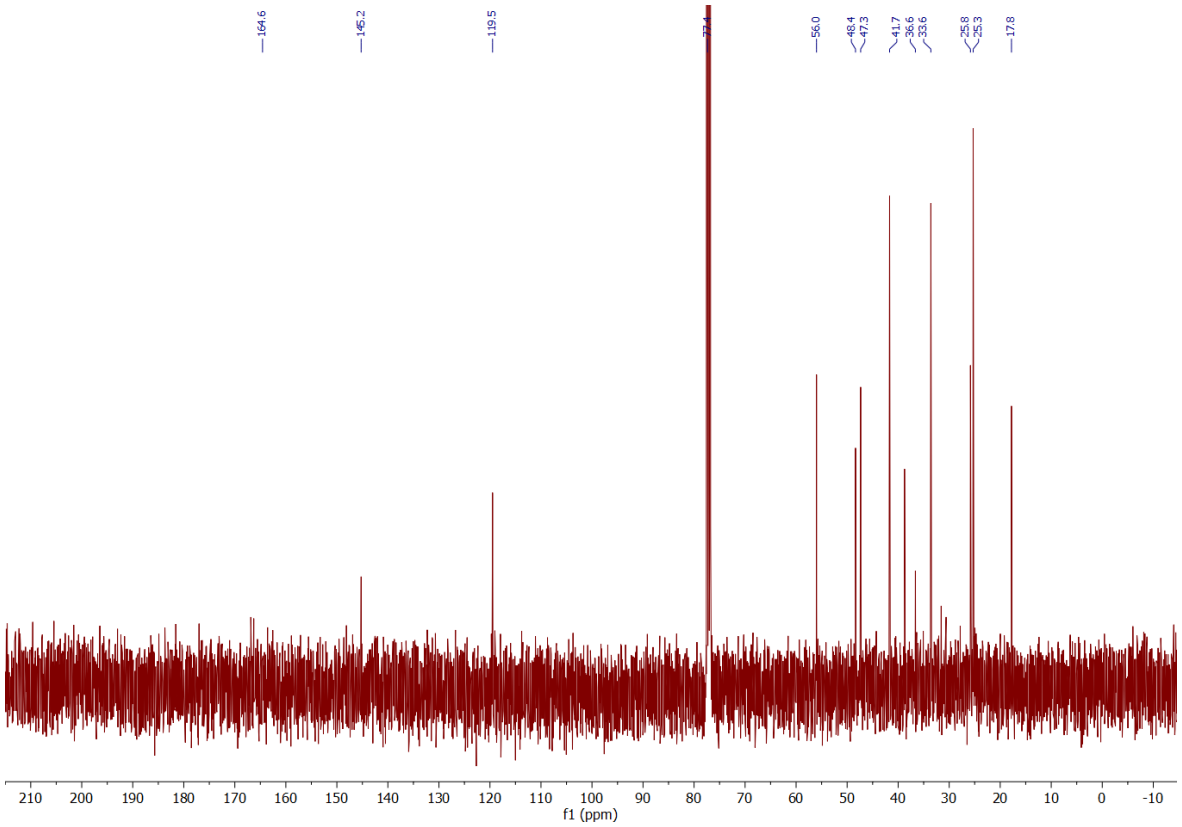


Figure SI19: *N*-Cyclohexyl-2-([2,2,6,6-tetramethylpiperidine]methyl)acrylamide $^{13}$C NMR spectrum ($CDCl_3$, 100 MHz, 298 K).

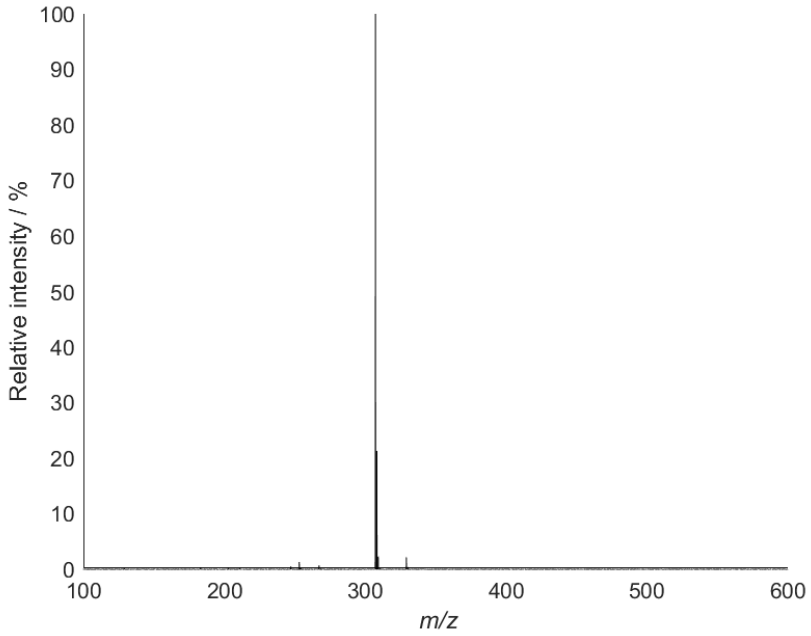


Figure SI20: *N*-Cyclohexyl-2-([2,2,6,6-tetramethylpiperidine]methyl)acrylamide mass spectrum (Pos ESI).

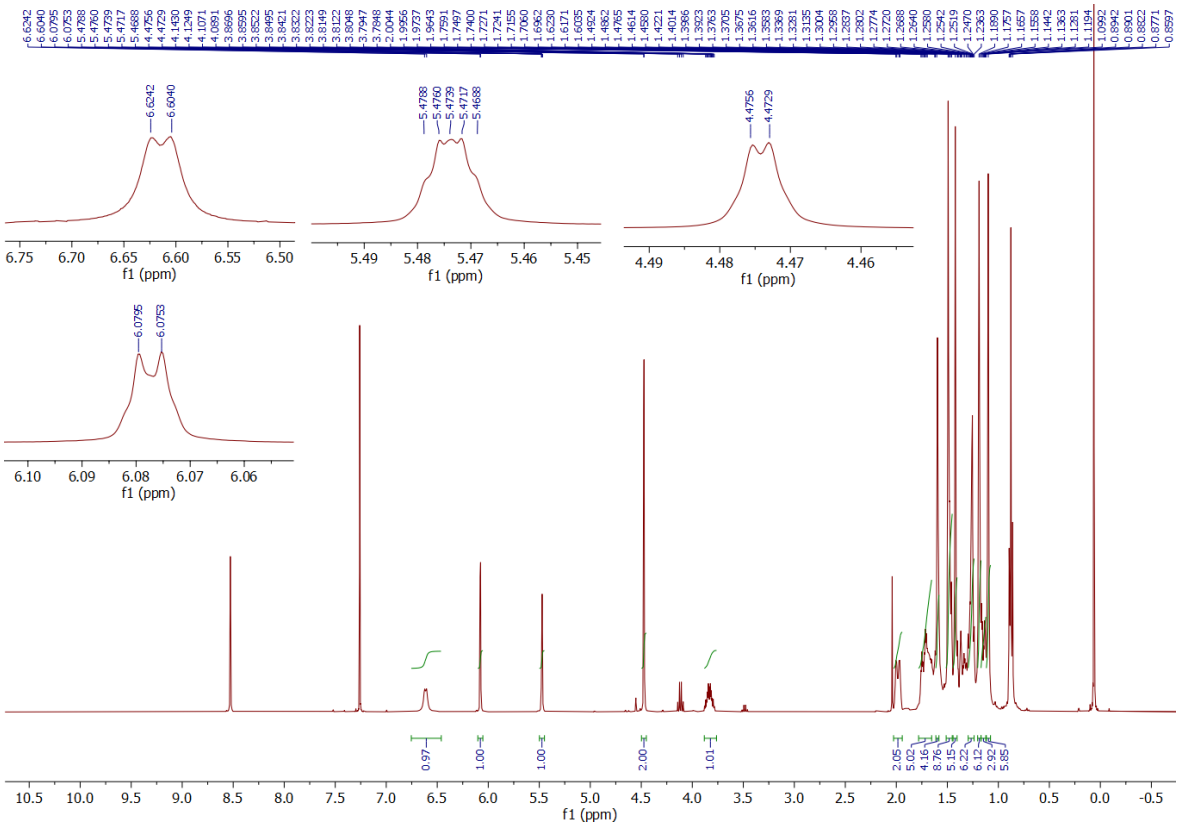


Figure SI21: CHANT $^{1}$H NMR spectrum ($CDCl_3$, 400 MHz, 298 K).

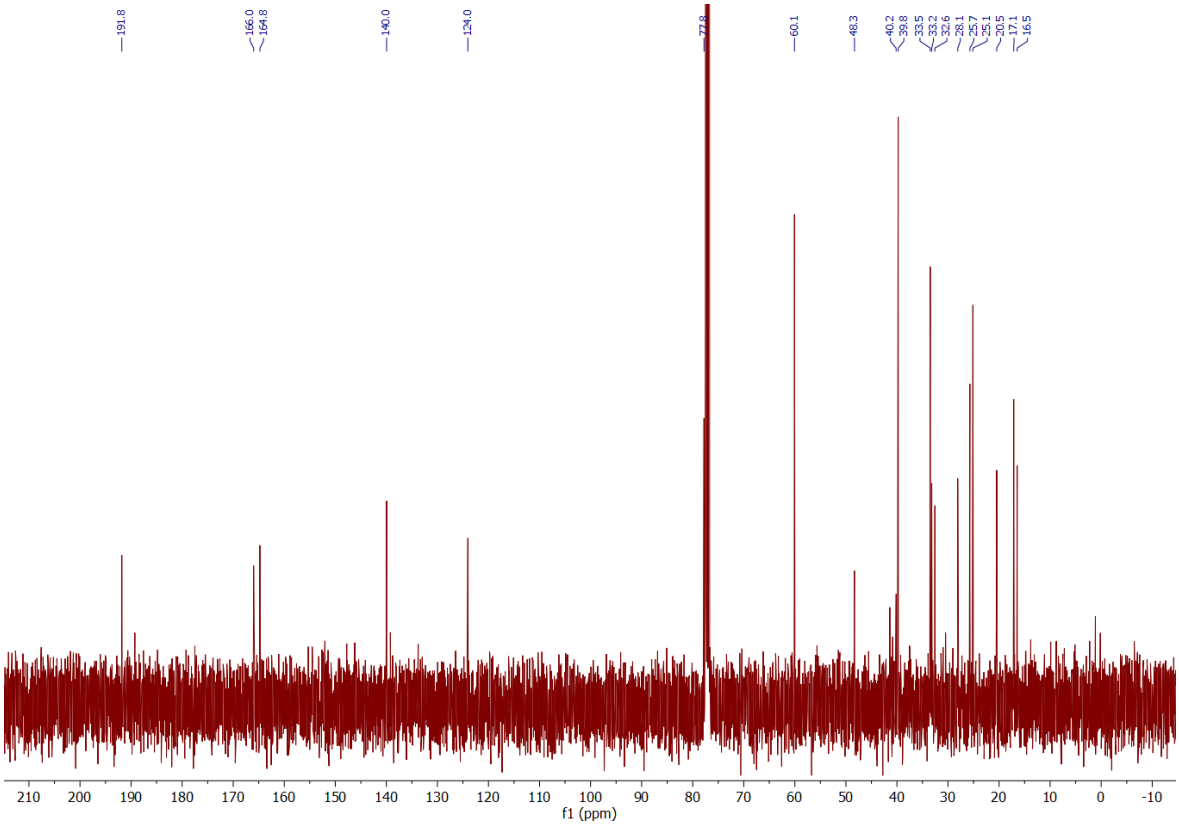


Figure SI22: CHANT $^{13}C$ NMR spectrum ($CDCl_3$, 100 MHz, 298 K).

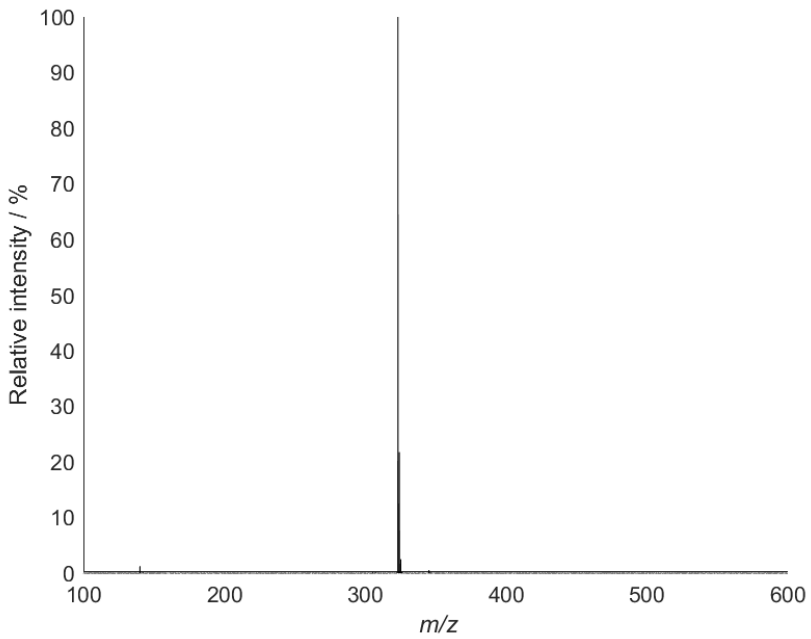


Figure SI23: CHANT mass spectrum (Pos ESI).

## SI2.4. Unsuccessful 2-(bromomethyl)acrylic acid UV irradiation

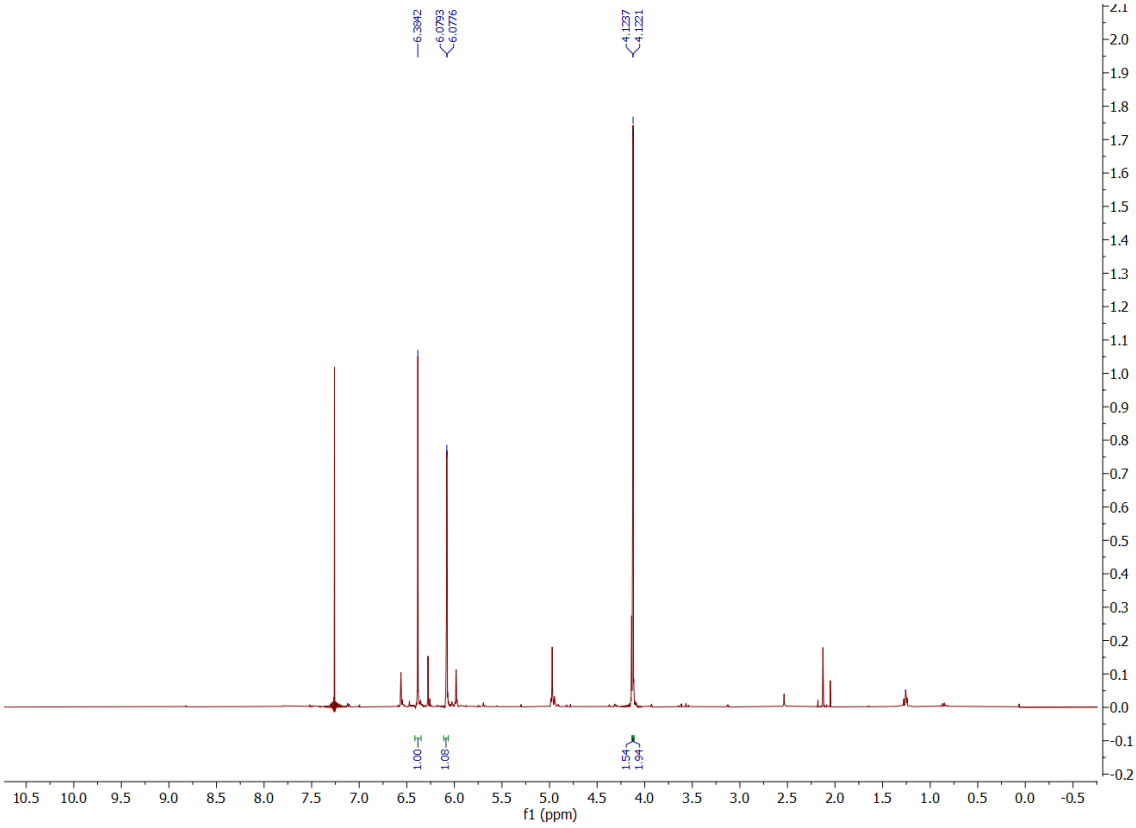


Figure SI24: 2-(Iodomethyl)acrylic acid $^{1}H$ NMR spectrum ($CDCl_3$, 400 MHz, 298 K).

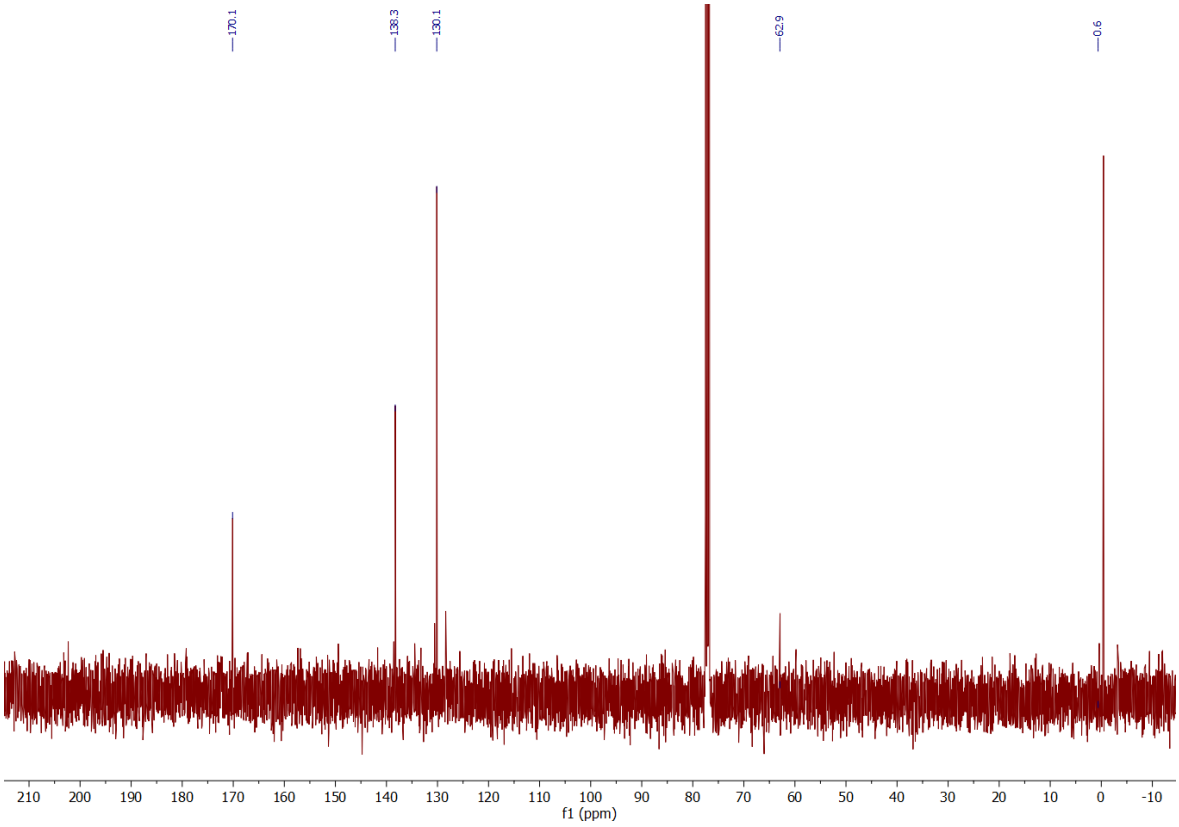


Figure SI25: 2-(Iodomethyl)acrylic acid $^{13}C$ NMR spectrum ($CDCl_3$, 100 MHz, 298 K).

## SI2.5. Methyl 2-(TEMPOmethyl)acrylate

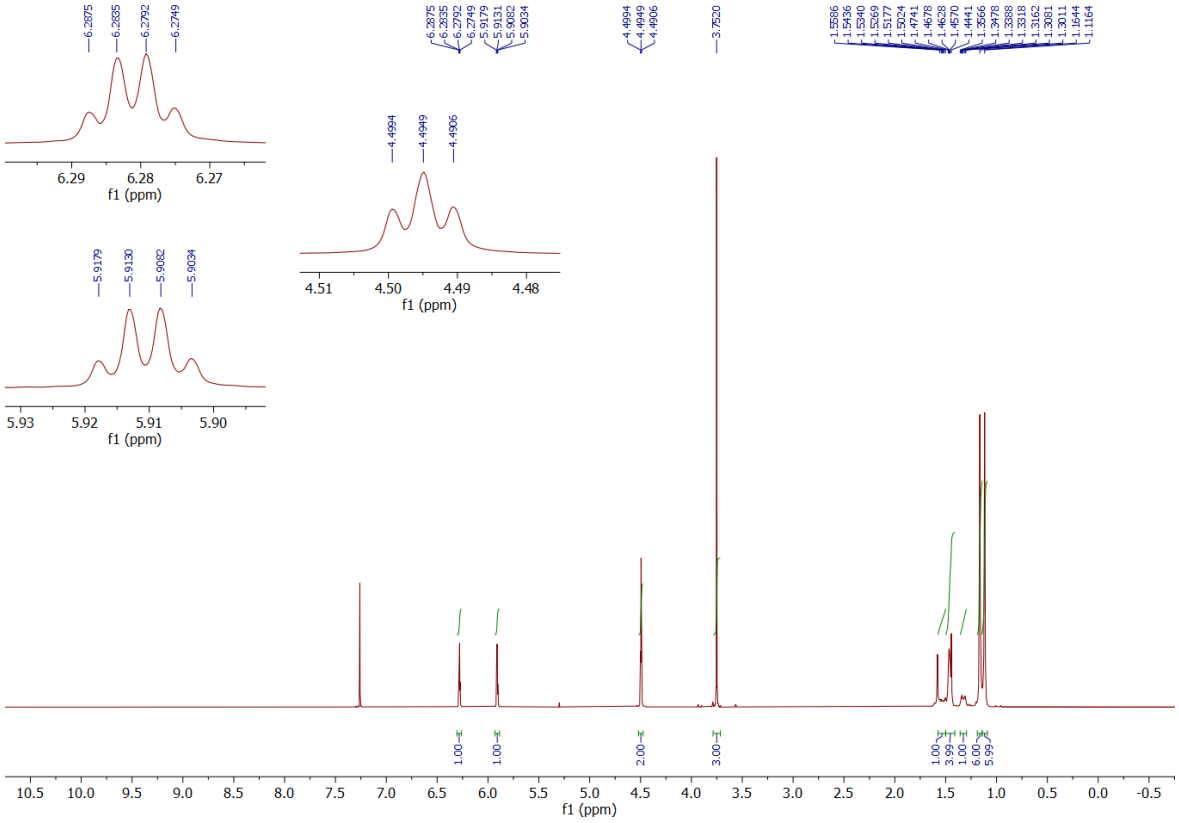


Figure SI26: Methyl 2-(TEMPOmethyl)acrylate $^{1}H$ NMR spectrum ($CDCl_3$, 400 MHz, 298 K).

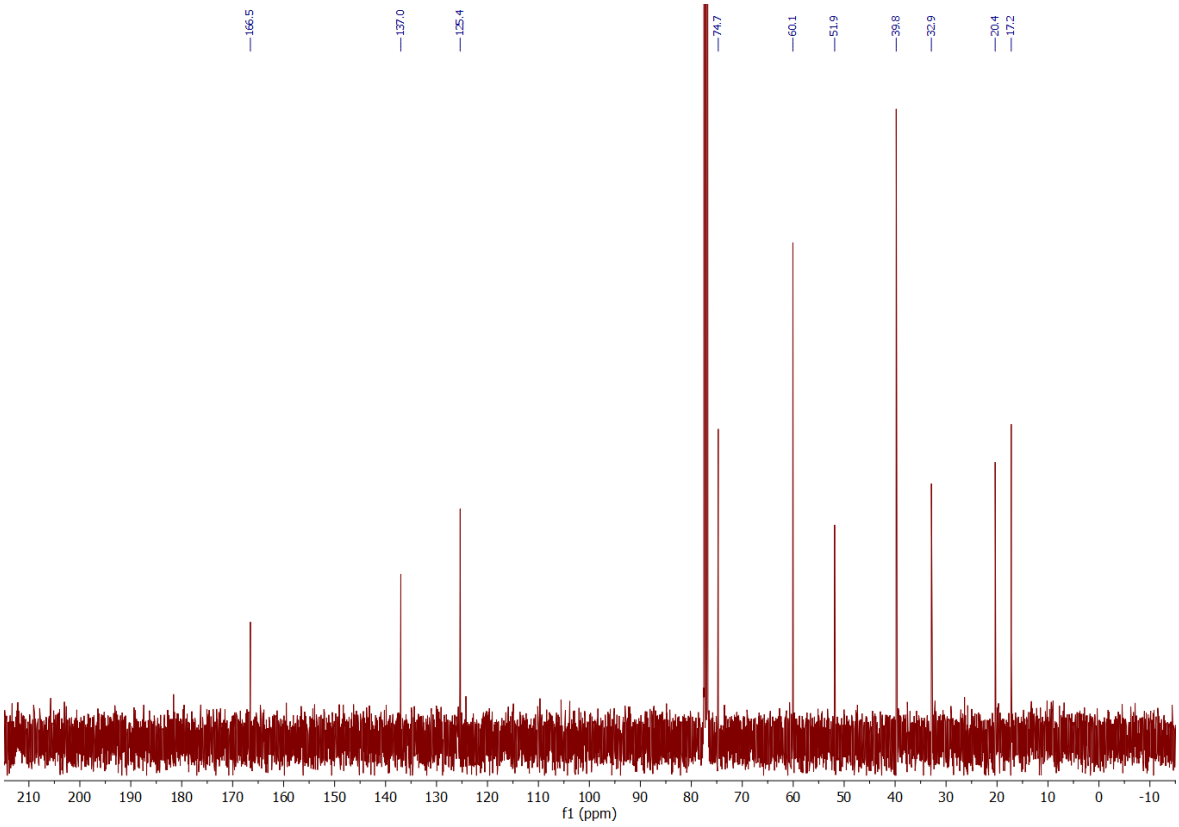


Figure SI27: Methyl 2-(TEMPOmethyl)acrylate $^{13}C$ NMR spectrum ($CDCl_3$, 100 MHz, 298 K).

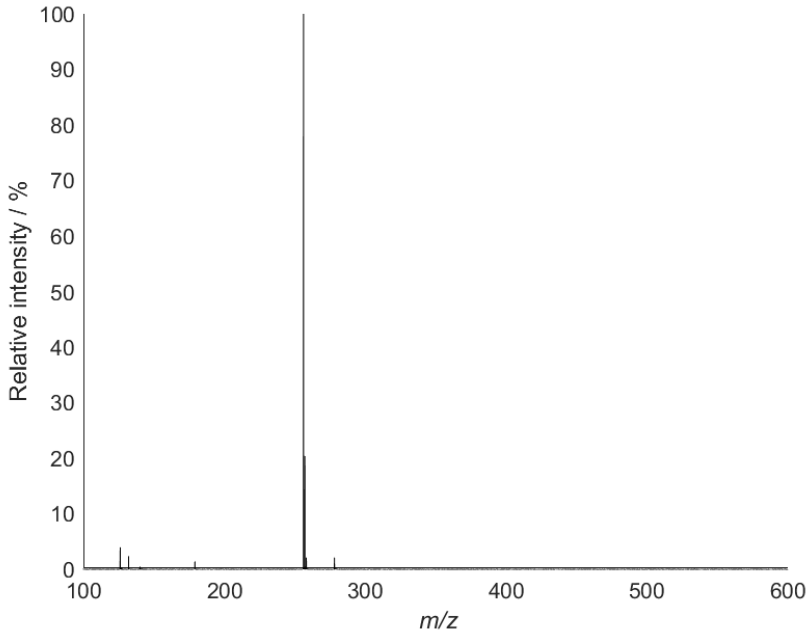


Figure SI28: Methyl 2-(TEMPOmethyl)acrylate mass spectrum (Pos ESI).

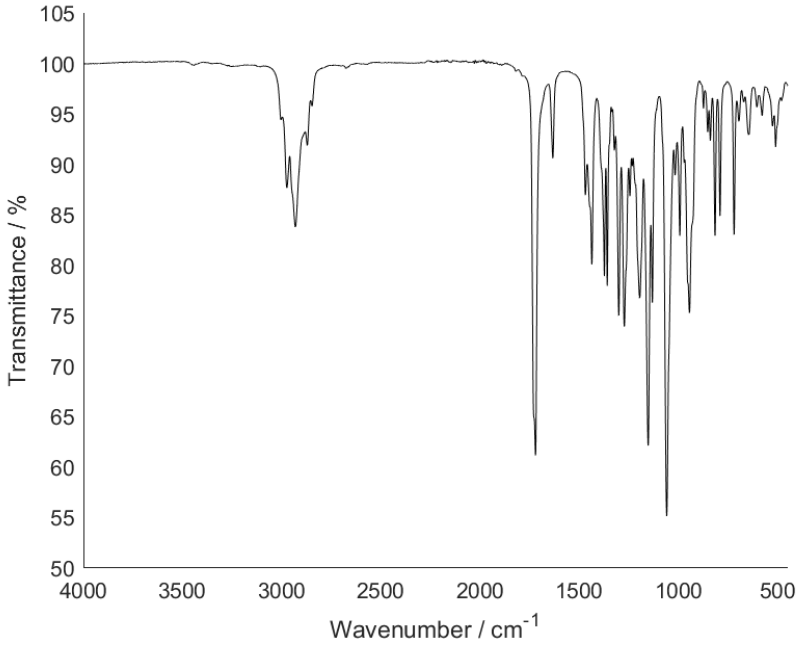


Figure SI29: Methyl 2-(TEMPOmethyl)acrylate IR spectrum.

## SI2.6. 2-(TEMPOmethyl)acrylic acid

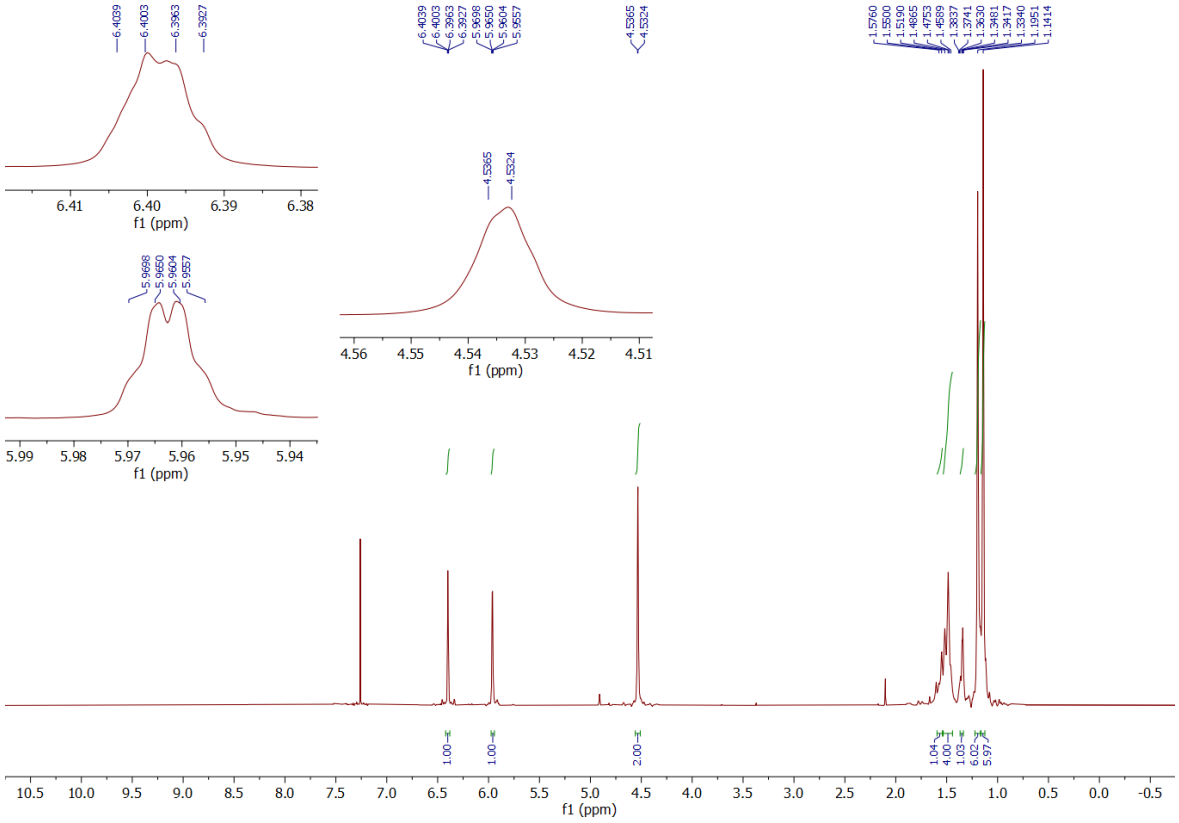


Figure SI30: 2-(TEMPOmethyl)acrylic acid $^{1}$H NMR spectrum ($CDCl_3$, 400 MHz, 298 K).

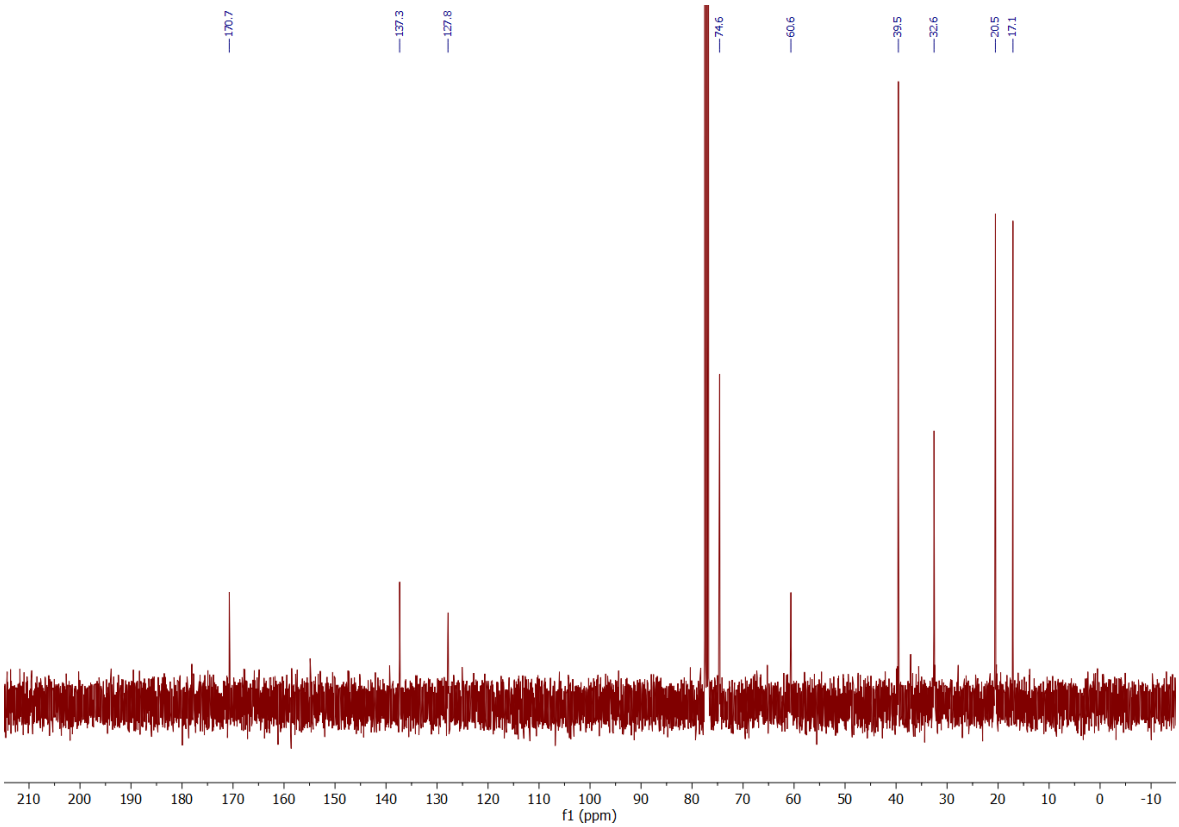


Figure SI31: 2-(TEMPOmethyl)acrylic acid $^{13}$C NMR spectrum ($CDCl_3$, 100 MHz, 298 K).

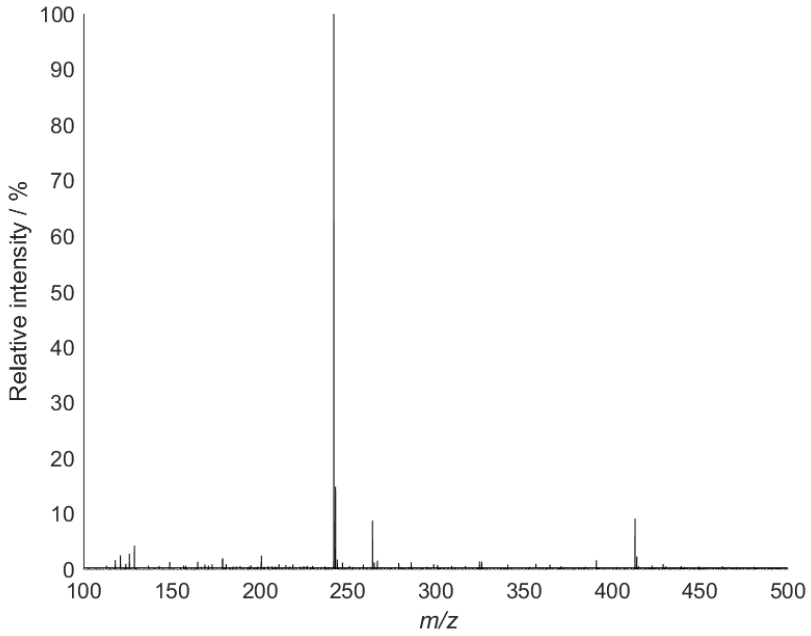


Figure SI32: 2-(TEMPOmethyl)acrylic acid mass spectrum (Pos ESI).

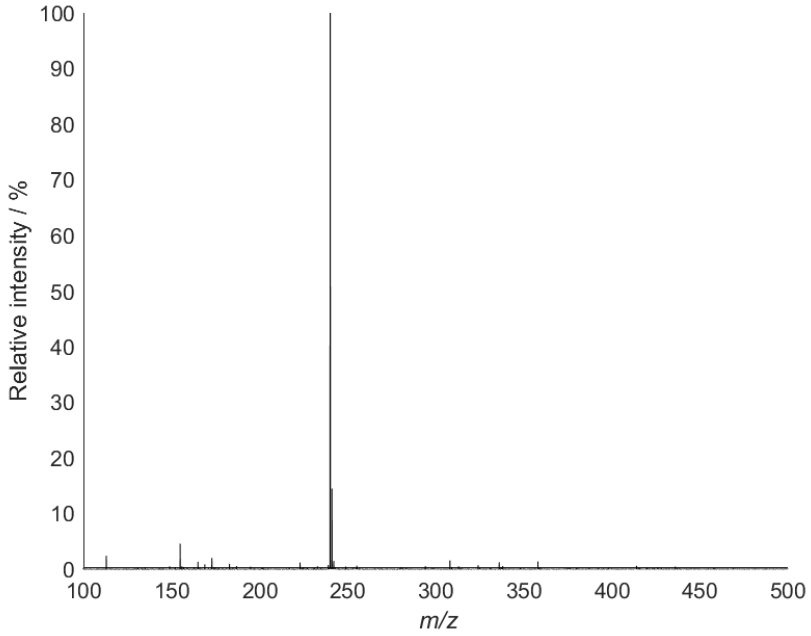


Figure SI33: 2-(TEMPOmethyl)acrylic acid ESI (-ve) mass spectrum.

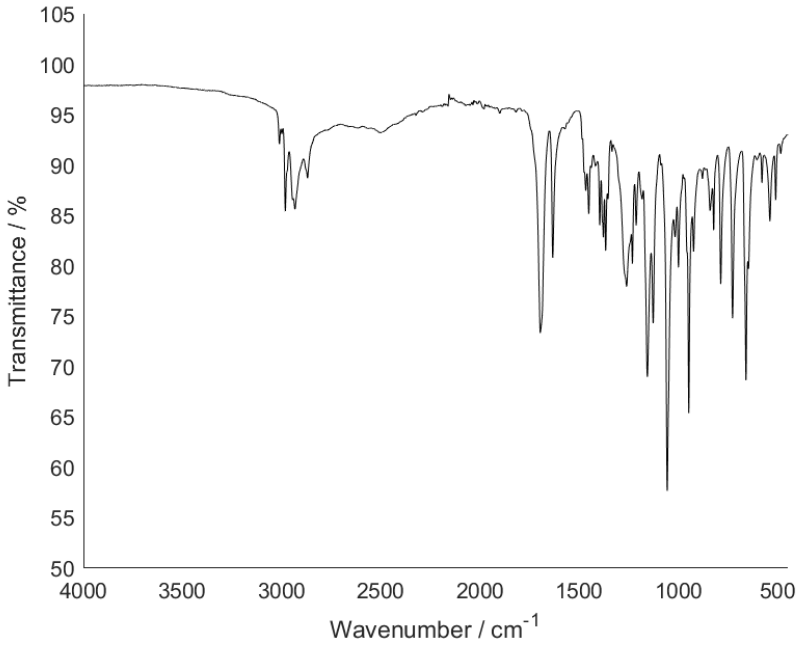


Figure SI34: 2-(TEMPOmethyl)acrylic acid IR spectrum.

## SI2.7. CHANT

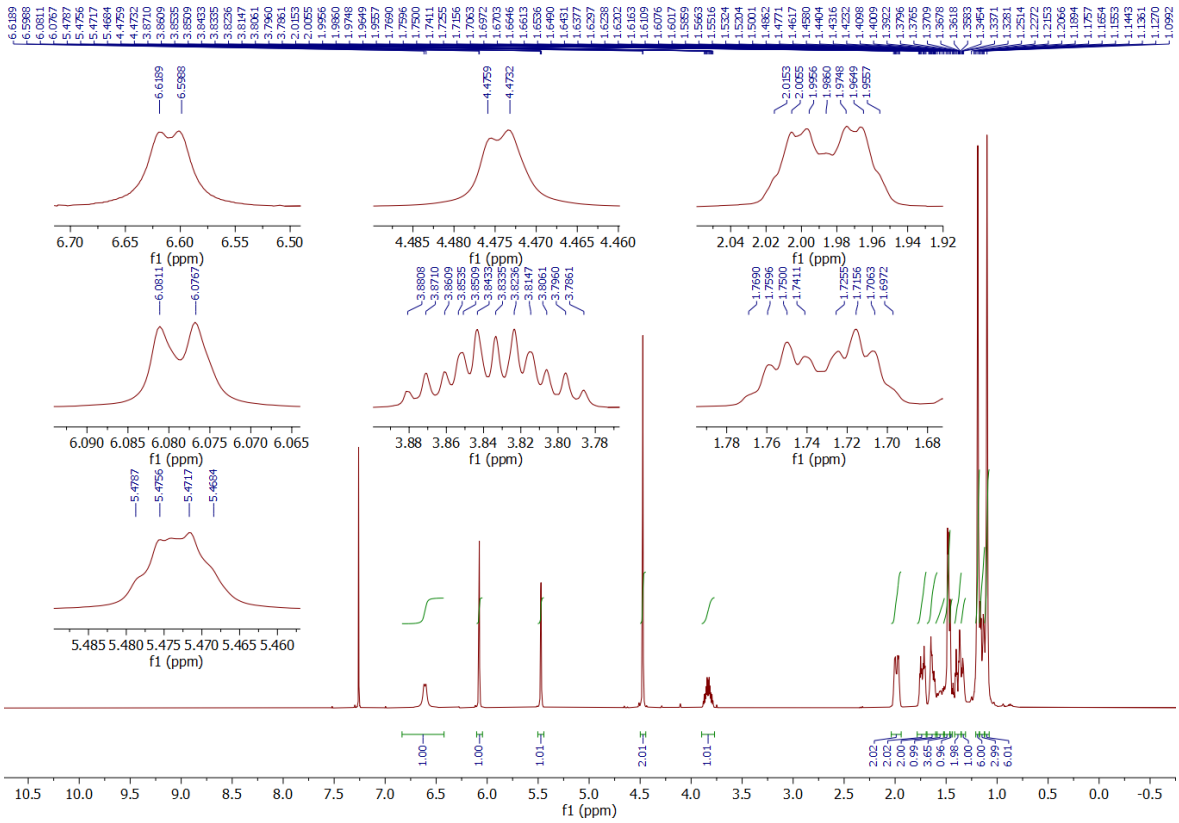


Figure SI35: CHANT $^{1}$H NMR spectrum ($CDCl_3$, 400 MHz, 298 K).

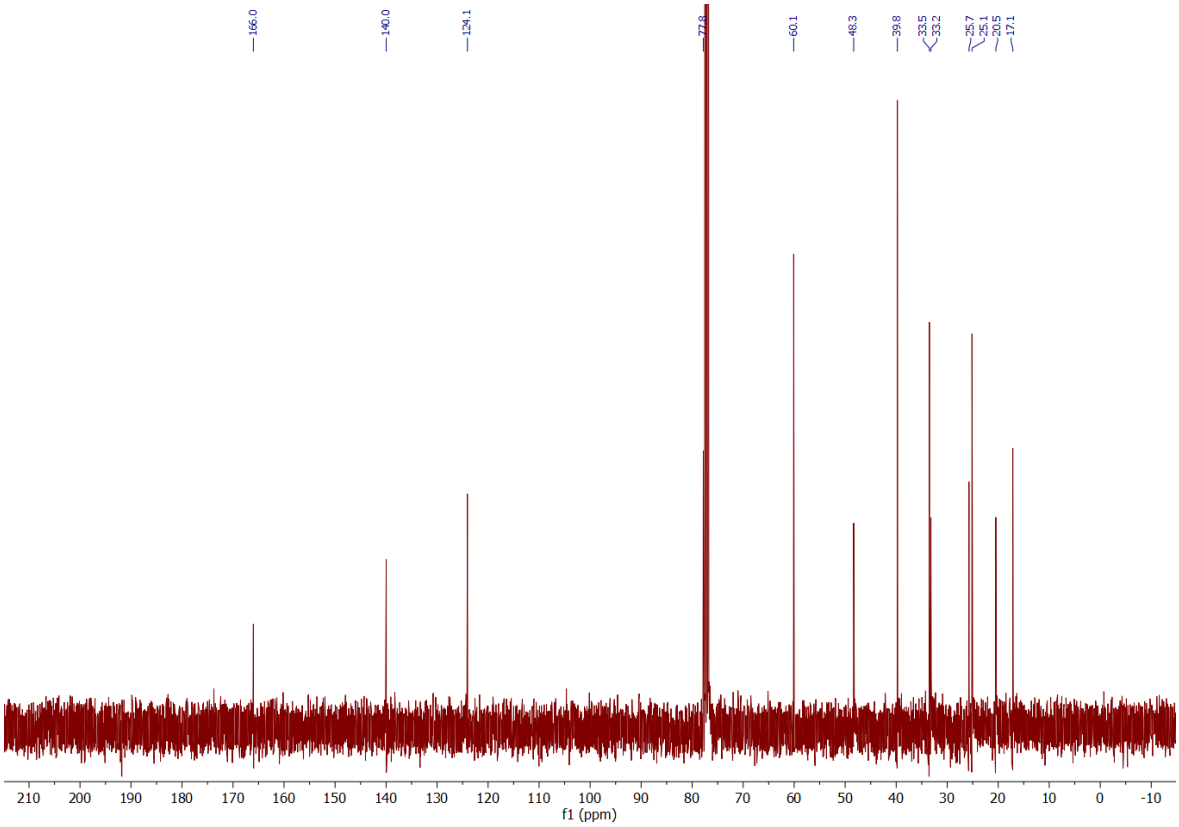


Figure SI36: CHANT $^{13}C$ NMR spectrum ($CDCl_3$, 100 MHz, 298 K).

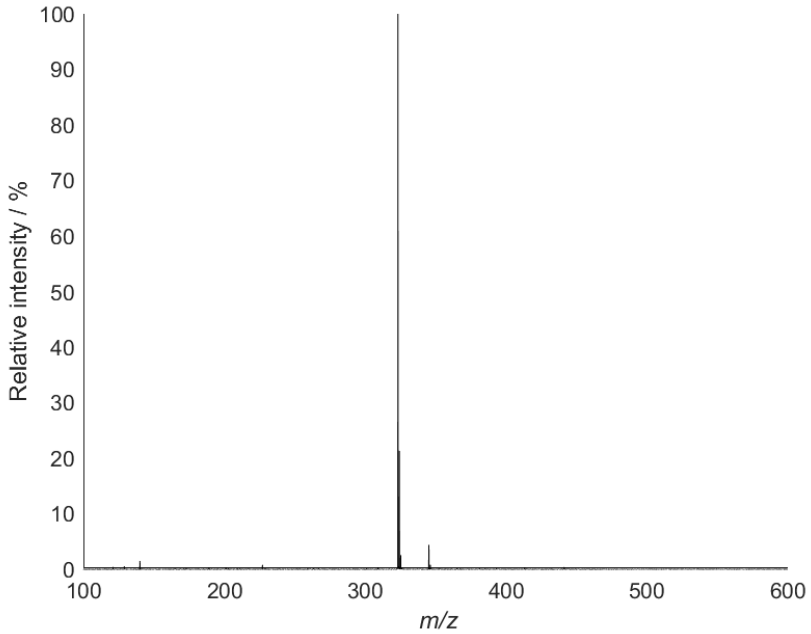


Figure SI37: CHANT mass spectrum (Pos ESI).

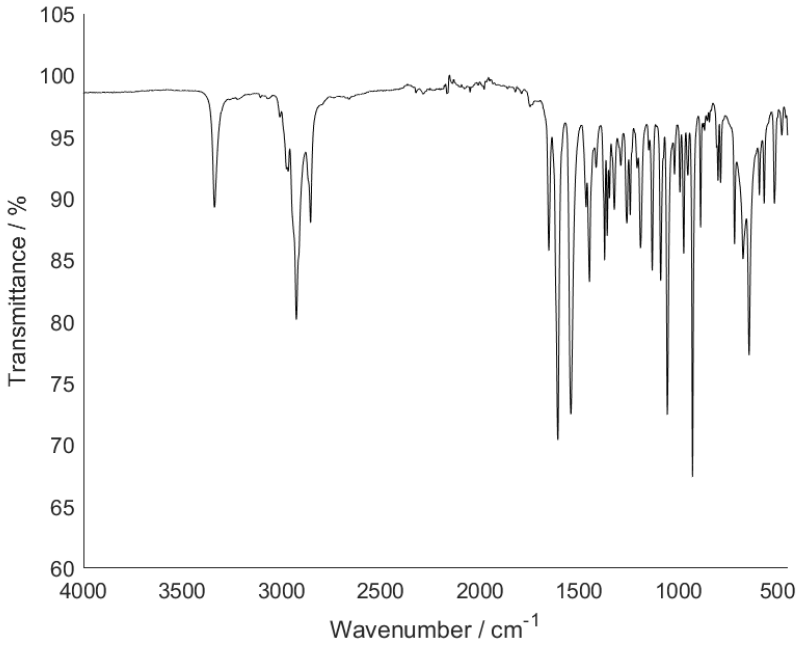


Figure SI38: CHANT IR spectrum.

## SI2.8. COANT

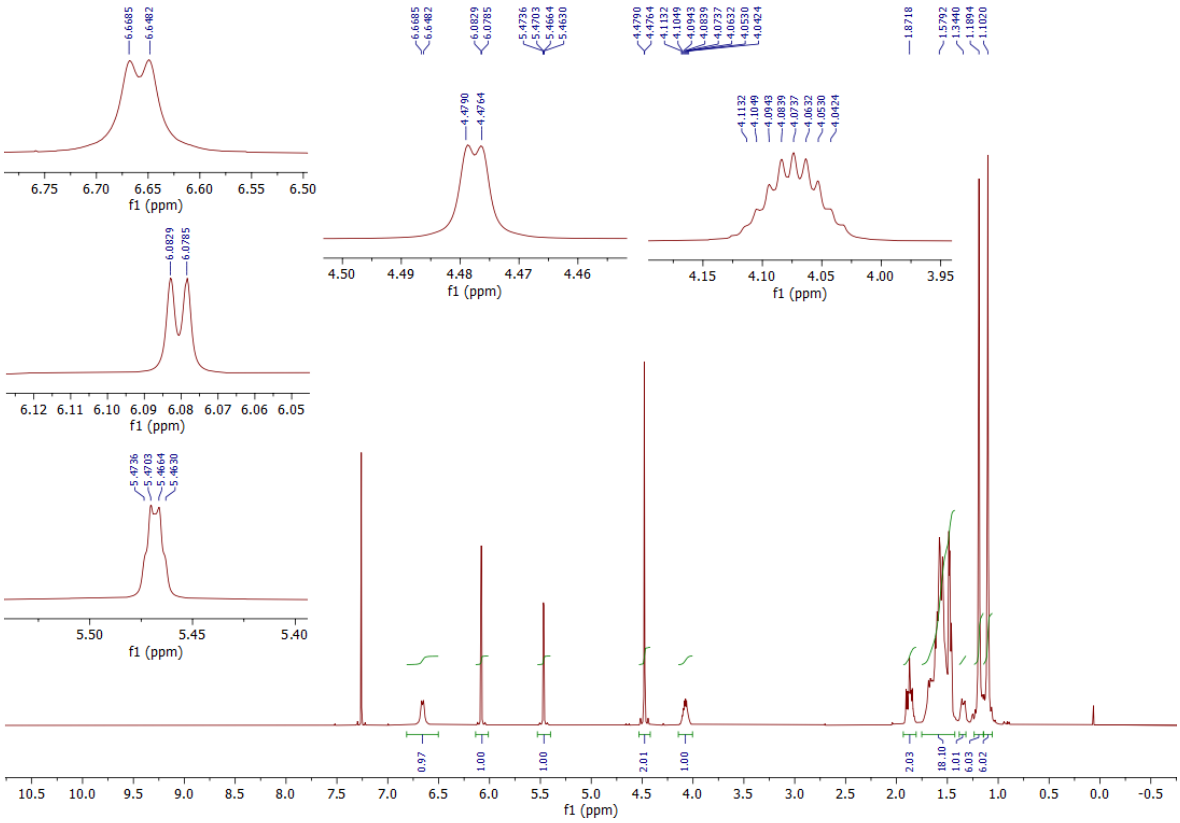


Figure SI39: COANT $^{1}$H NMR spectrum ($CDCl_3$, 400 MHz, 298 K).

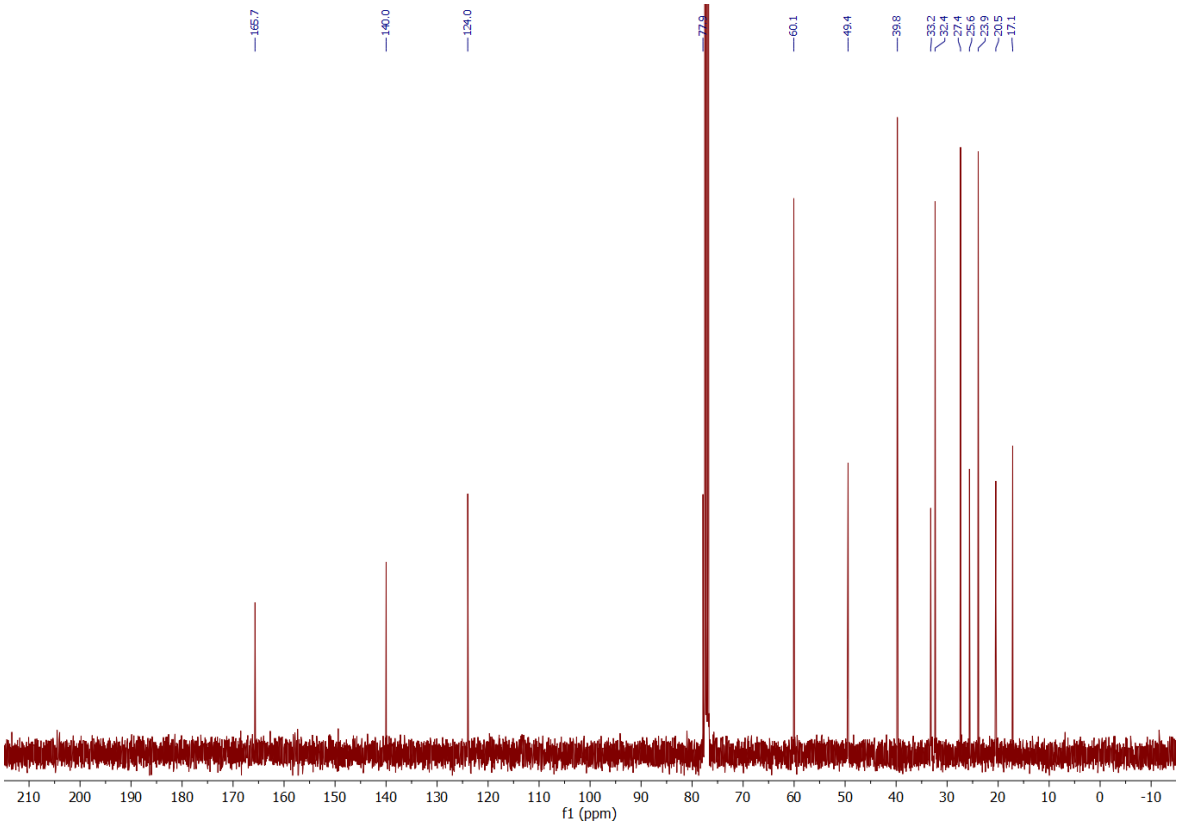


Figure SI40: COANT $^{13}C$ NMR spectrum ($CDCl_3$, 100 MHz, 298 K).

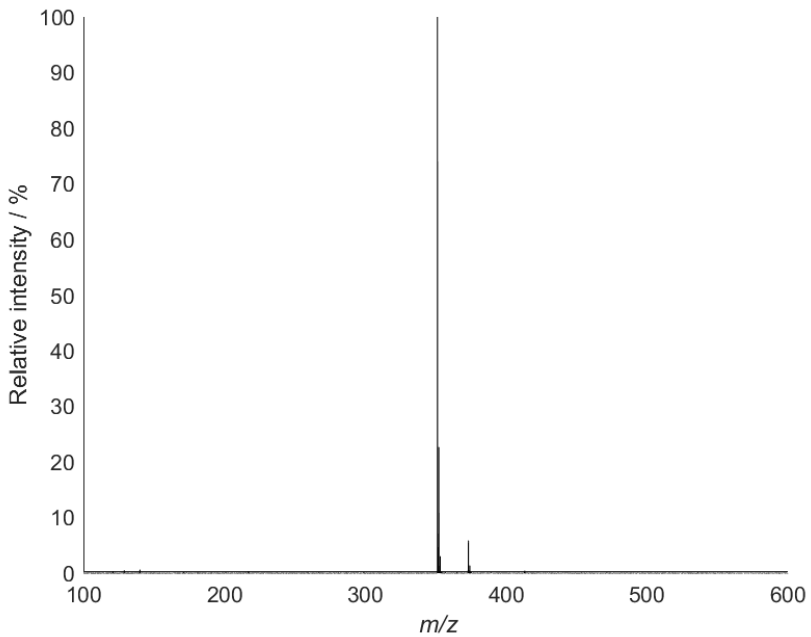


Figure SI41: COANT mass spectrum (Pos ESI).

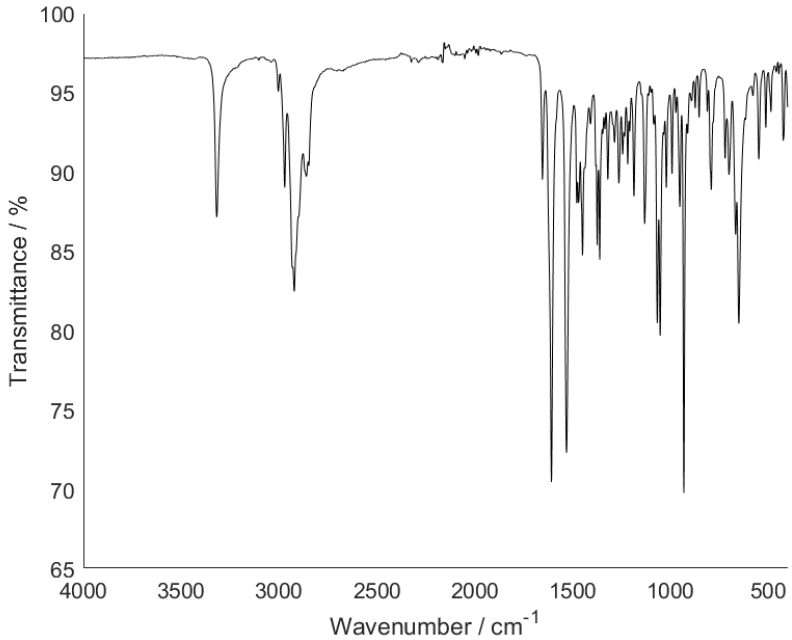


Figure SI42: COANT IR spectrum.

## SI2.9. DECANT

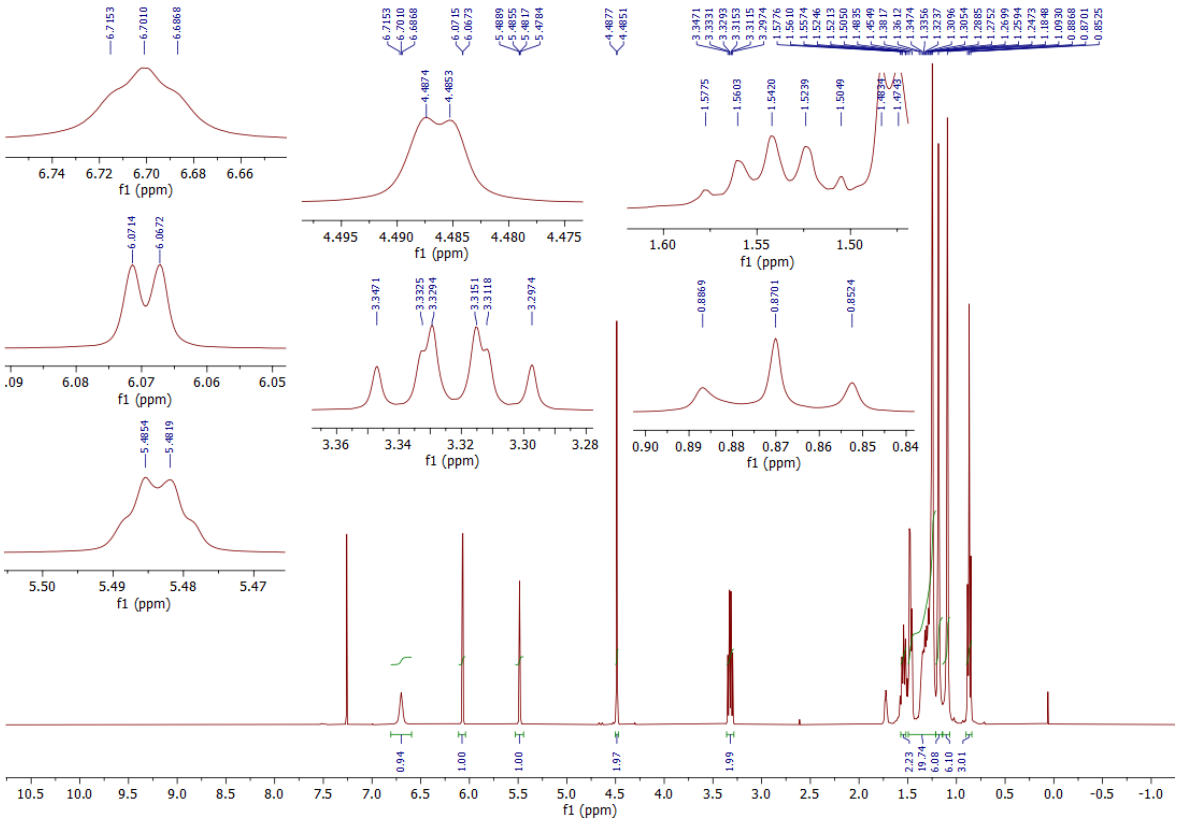


Figure SI43: DECANT $^{1}$H NMR spectrum ($CDCl_3$, 400 MHz, 298 K).

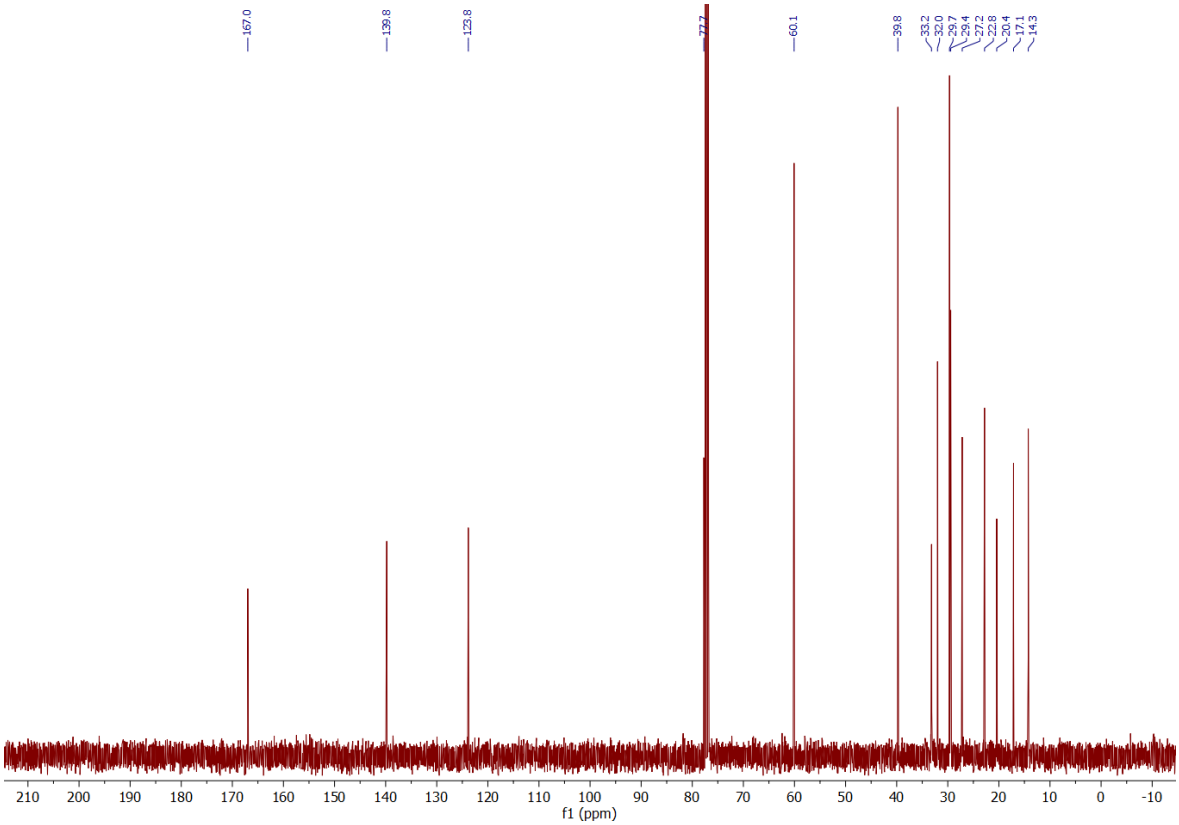


Figure SI44: DECANT $^{13}C$ NMR spectrum ($CDCl_3$, 100 MHz, 298 K).

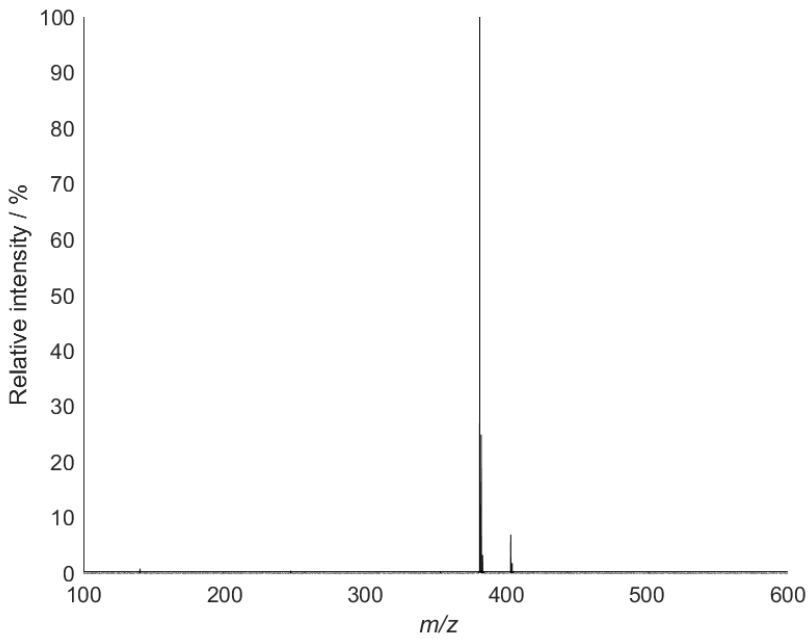


Figure SI45: DECANT mass spectrum (Pos ESI).

## SI2.10. DANT

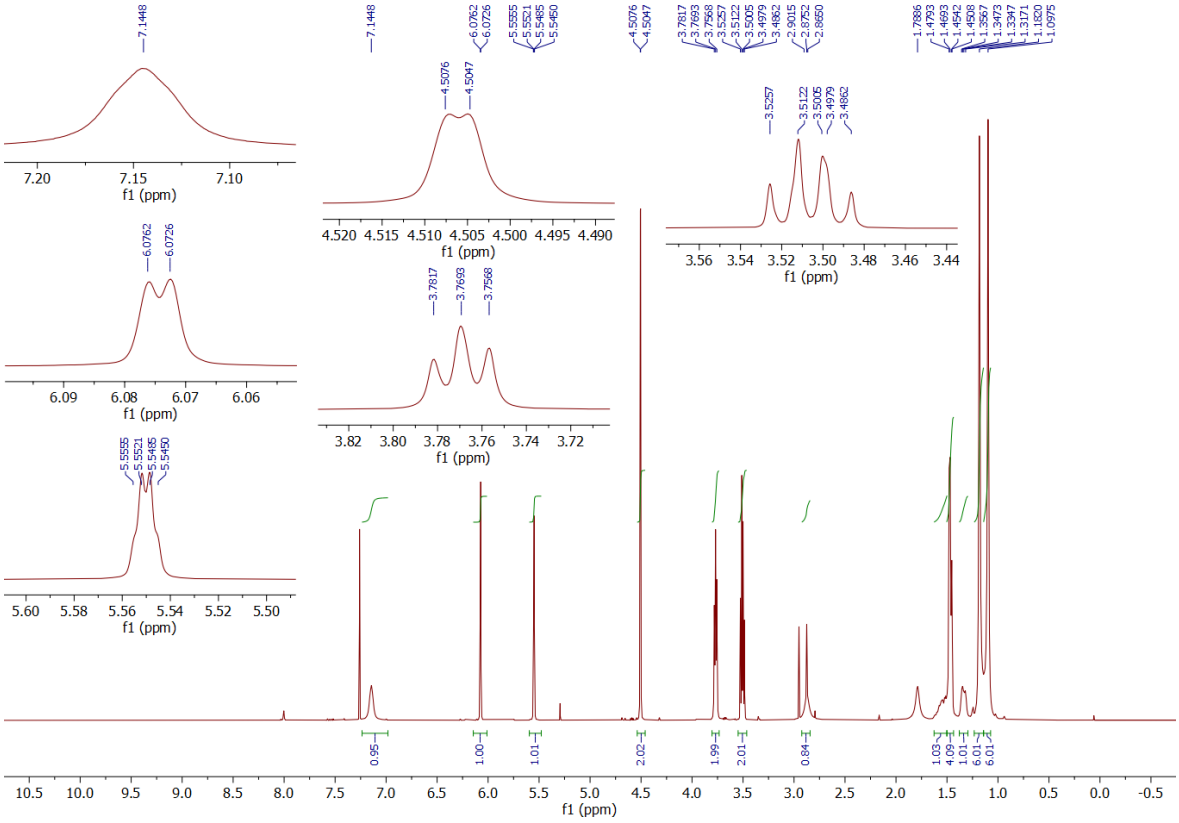


Figure SI46: DANT $^{1}$H NMR spectrum ($CDCl_3$, 400 MHz, 298 K).

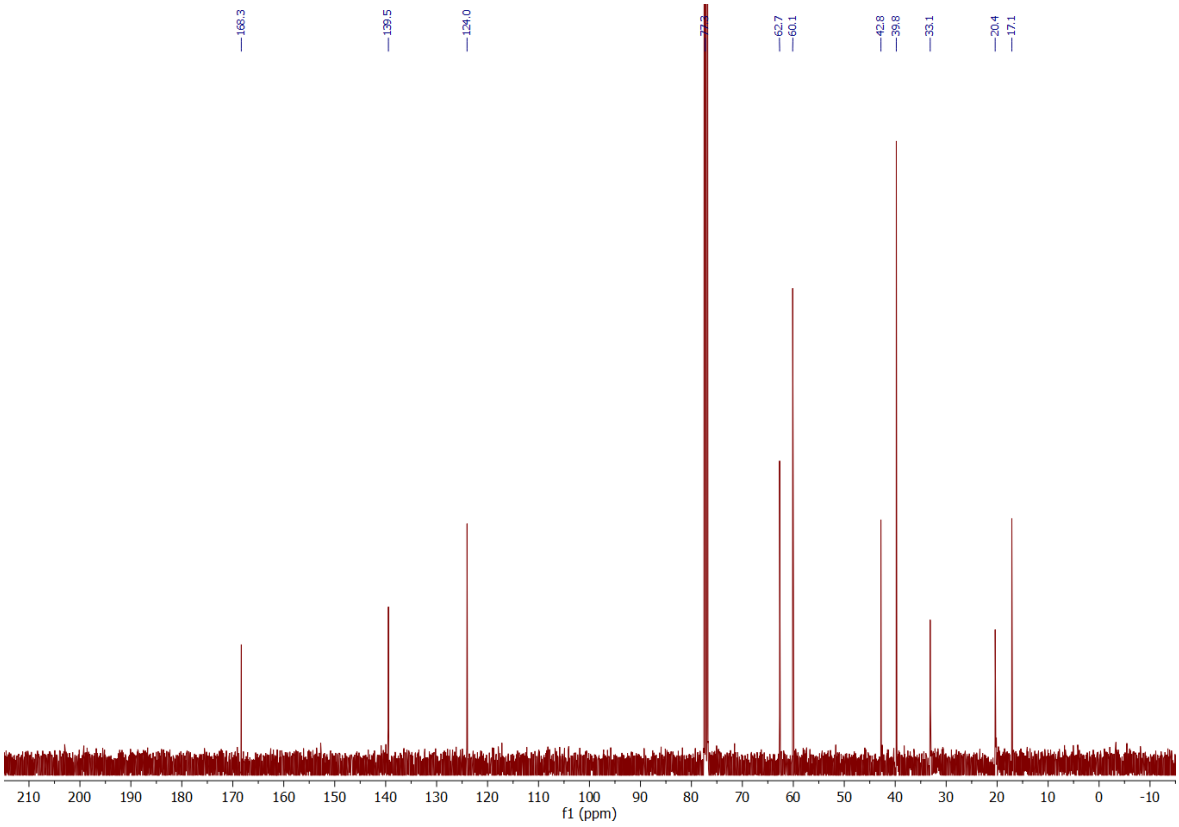


Figure SI47: DANT $^{13}$C NMR spectrum ($CDCl_3$, 100 MHz, 298 K).

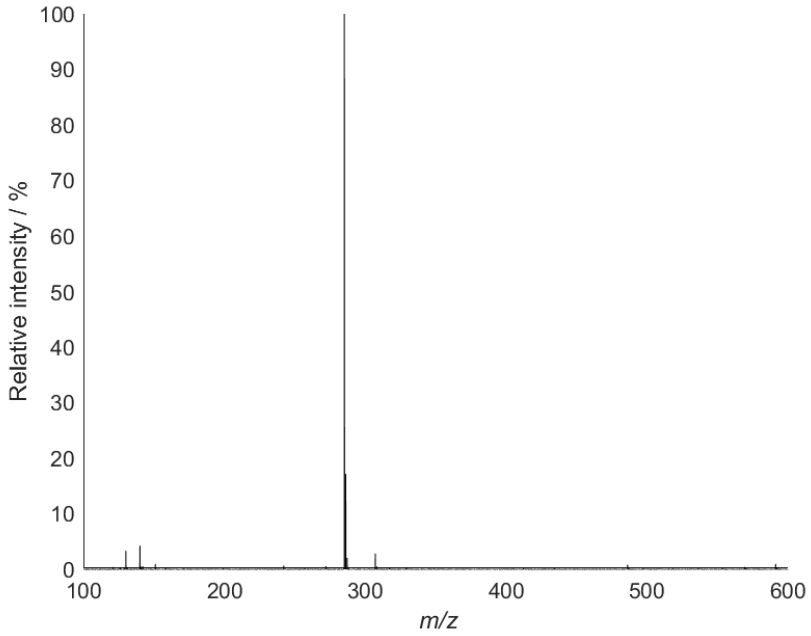


Figure SI48: DANT mass spectrum (Pos ESI).

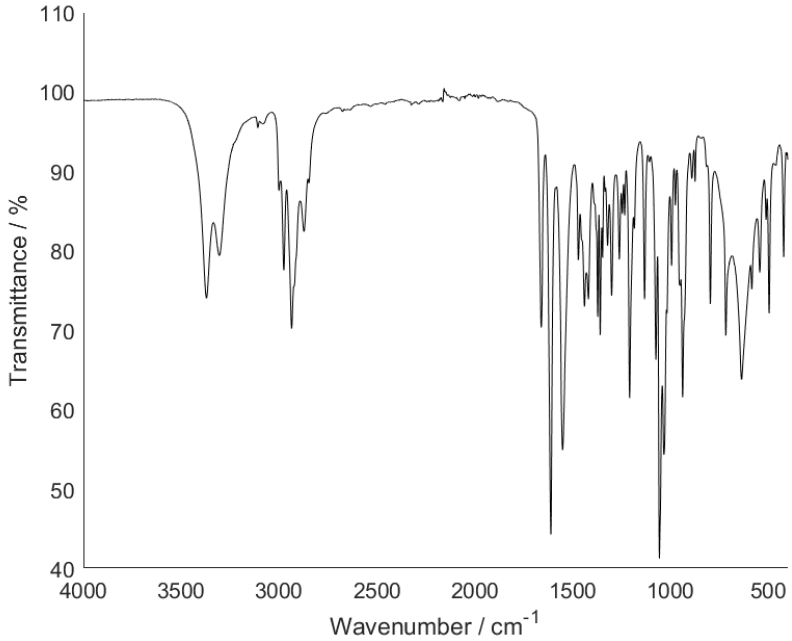


Figure SI49: DANT IR spectrum.

## SI2.11. AGLANT

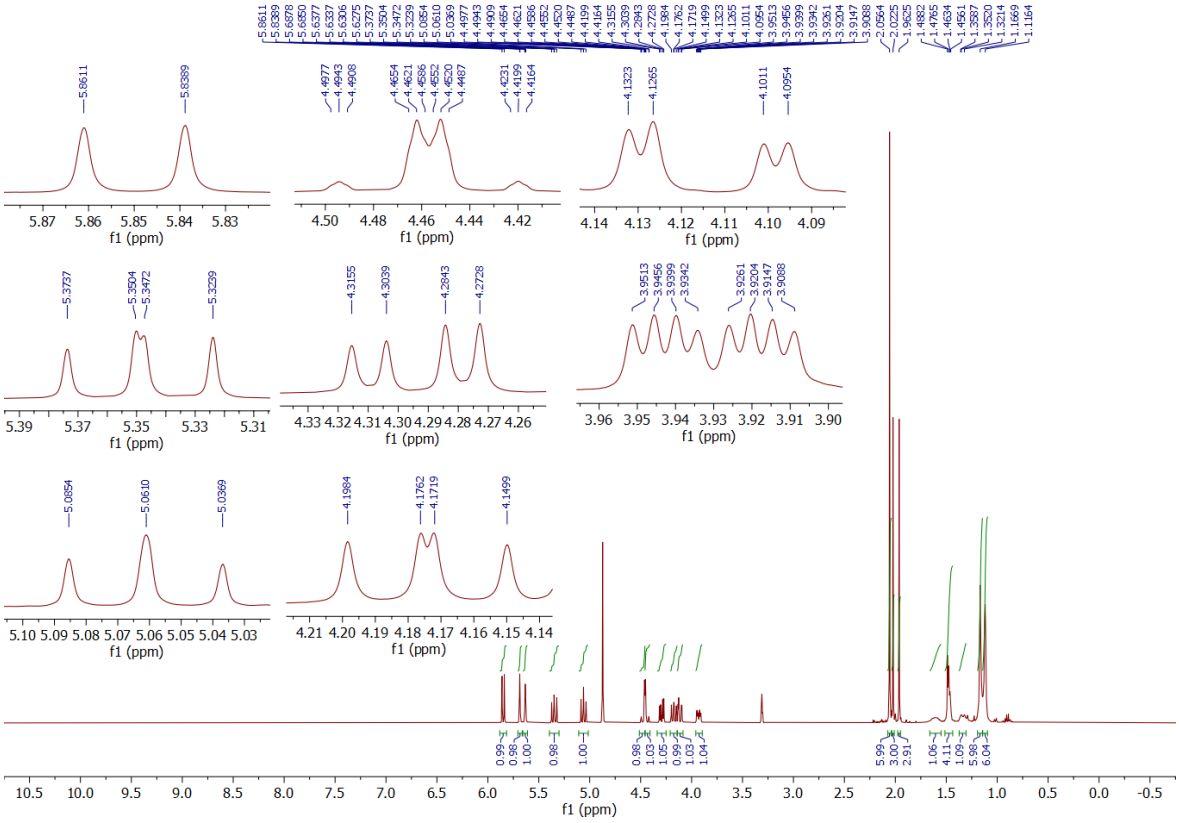


Figure SI50: AGLANT $^{1}$H NMR spectrum ($CD_3OD$, 400 MHz, 298 K).

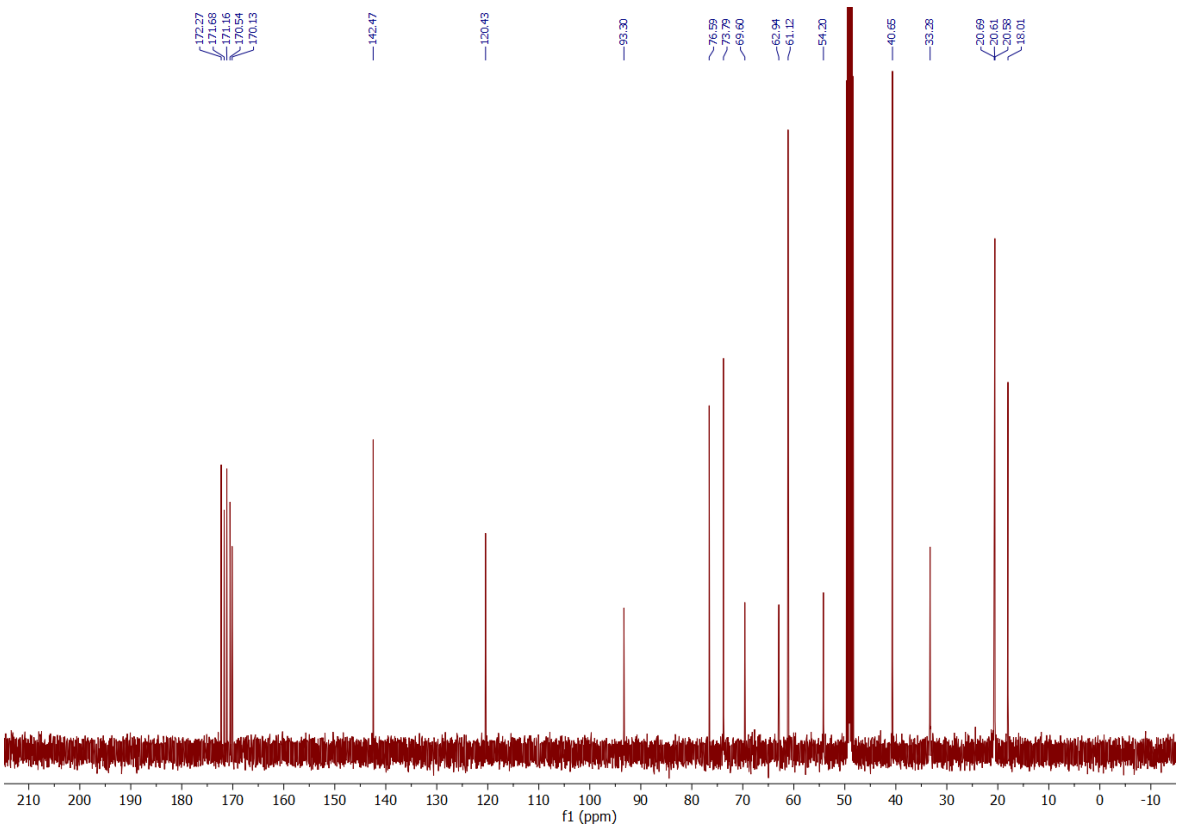


Figure SI51: AGLANT $^{13}$C NMR spectrum ($CD_3OD$, 100 MHz, 298 K).

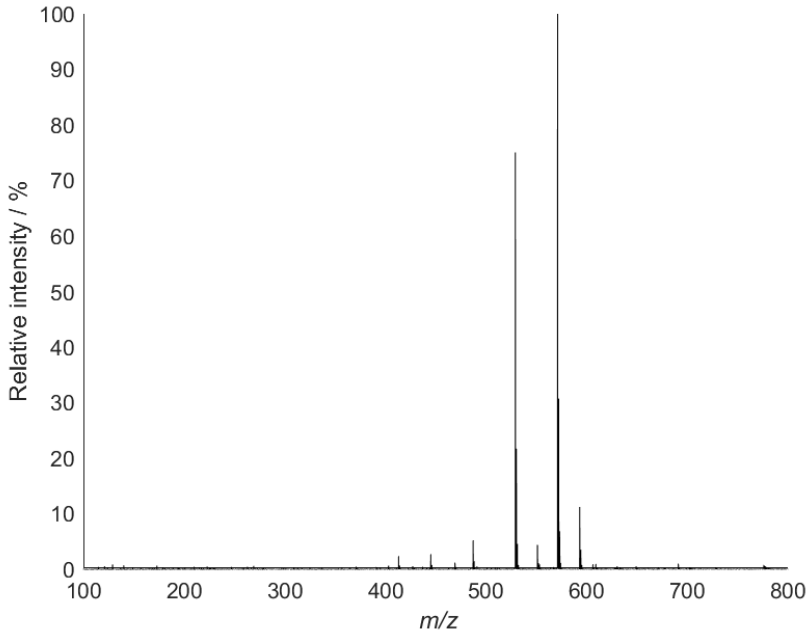


Figure SI52: AGLANT mass spectrum (Pos ESI).

## SI2.12. GLANT

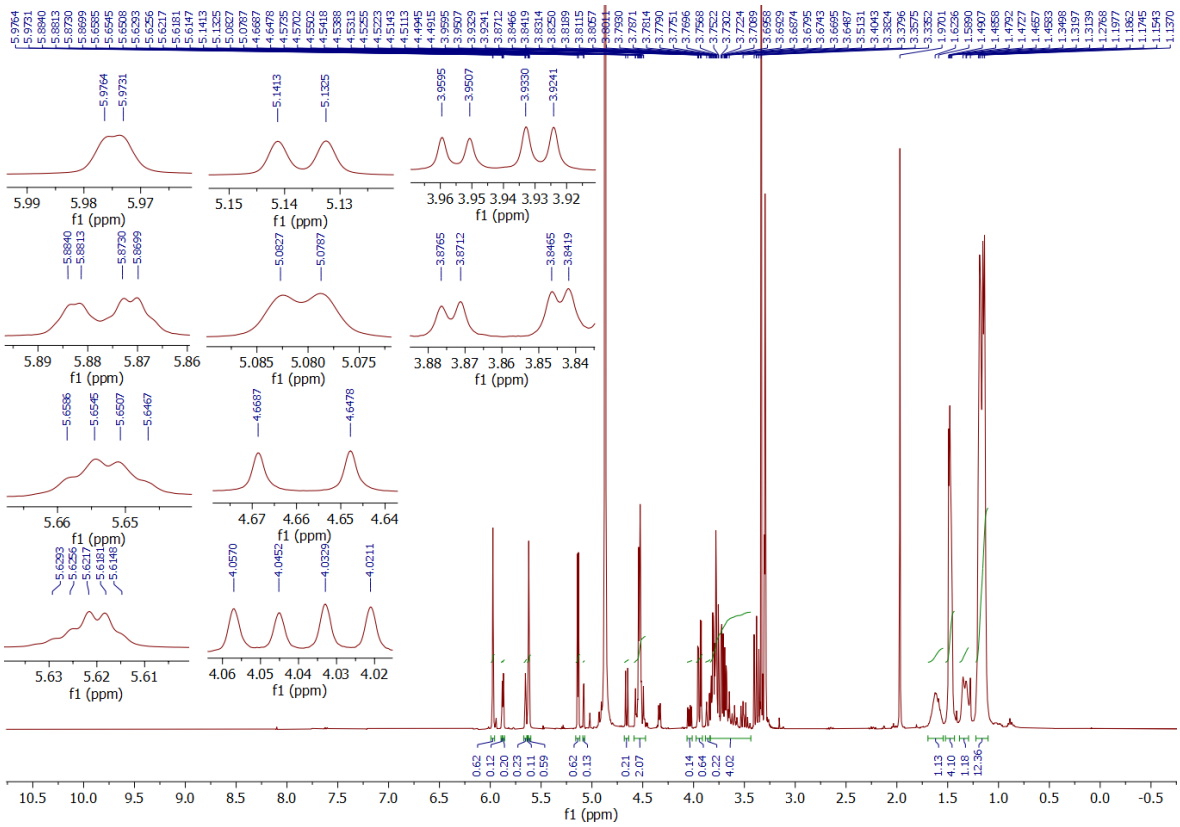


Figure SI53: GLANT $^{1}$H NMR spectrum ($CD_3OD$, 400 MHz, 298 K).

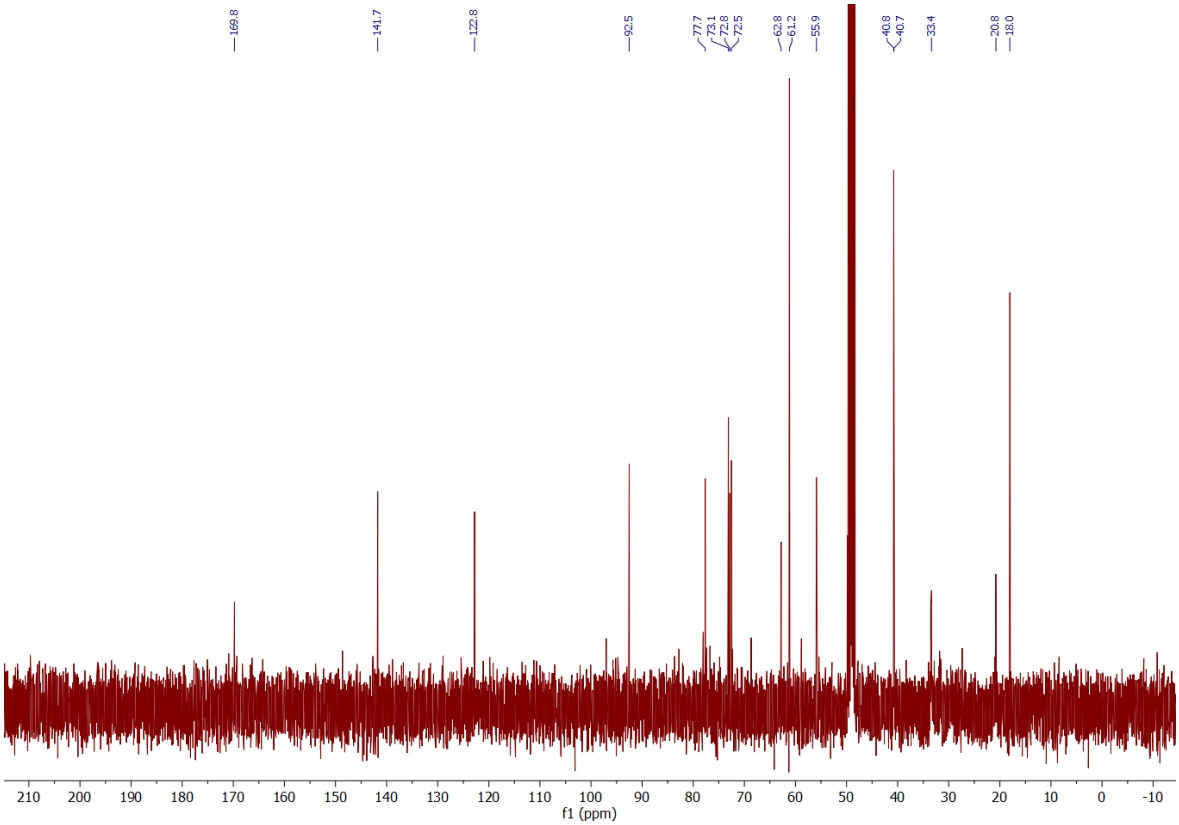


Figure SI54: GLANT $^{13}C$ NMR spectrum ($CD_3OD$, 100 MHz, 298 K).

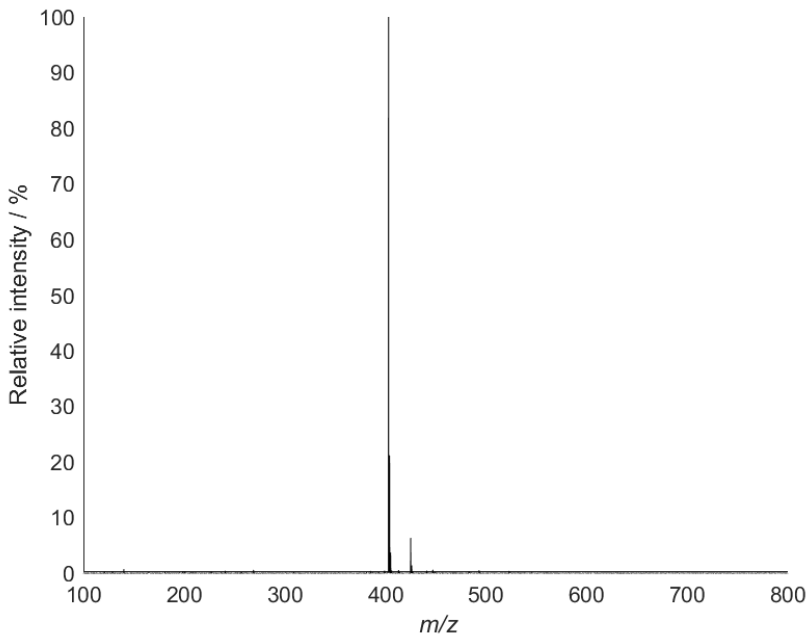


Figure SI55: GLANT mass spectrum (Pos ESI).

## SI2.13. Tabaqui-1

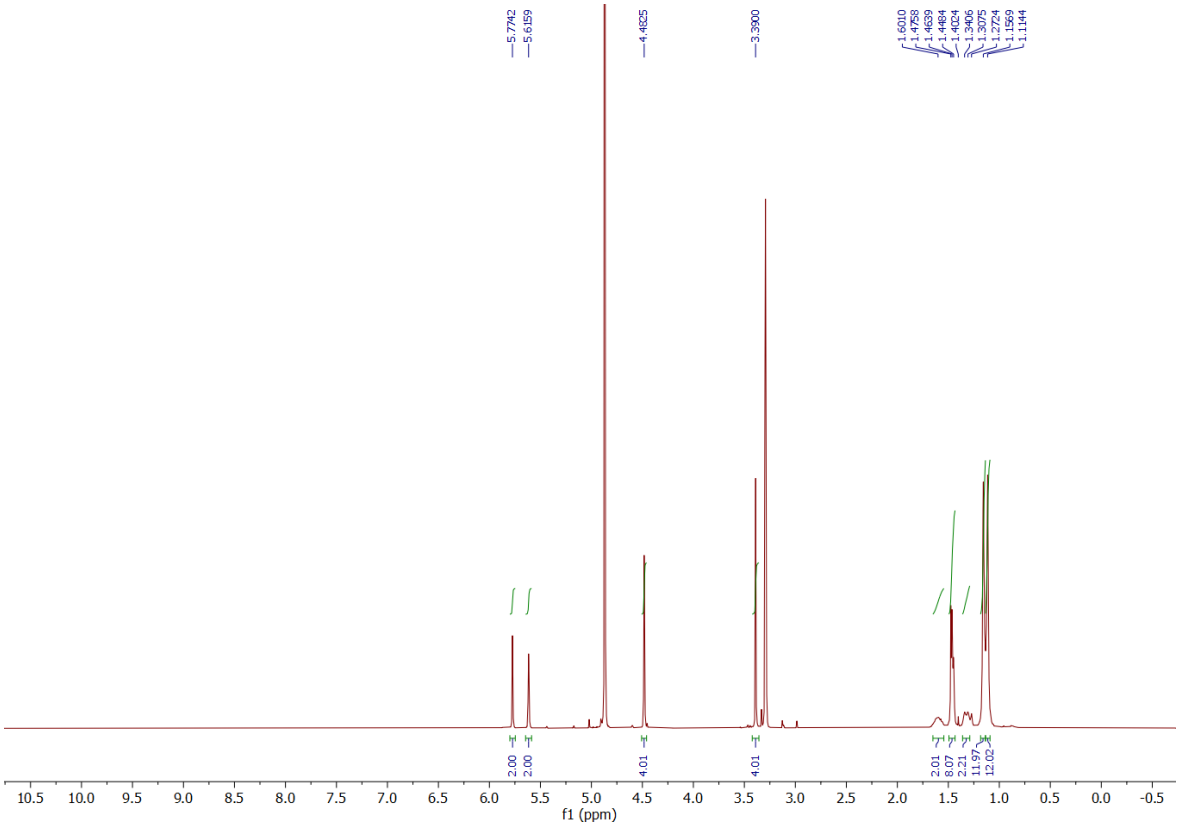


Figure SI56: Tabaqui-1 $^{1}H$ NMR spectrum ($CD_3OD$, 400 MHz, 298 K).

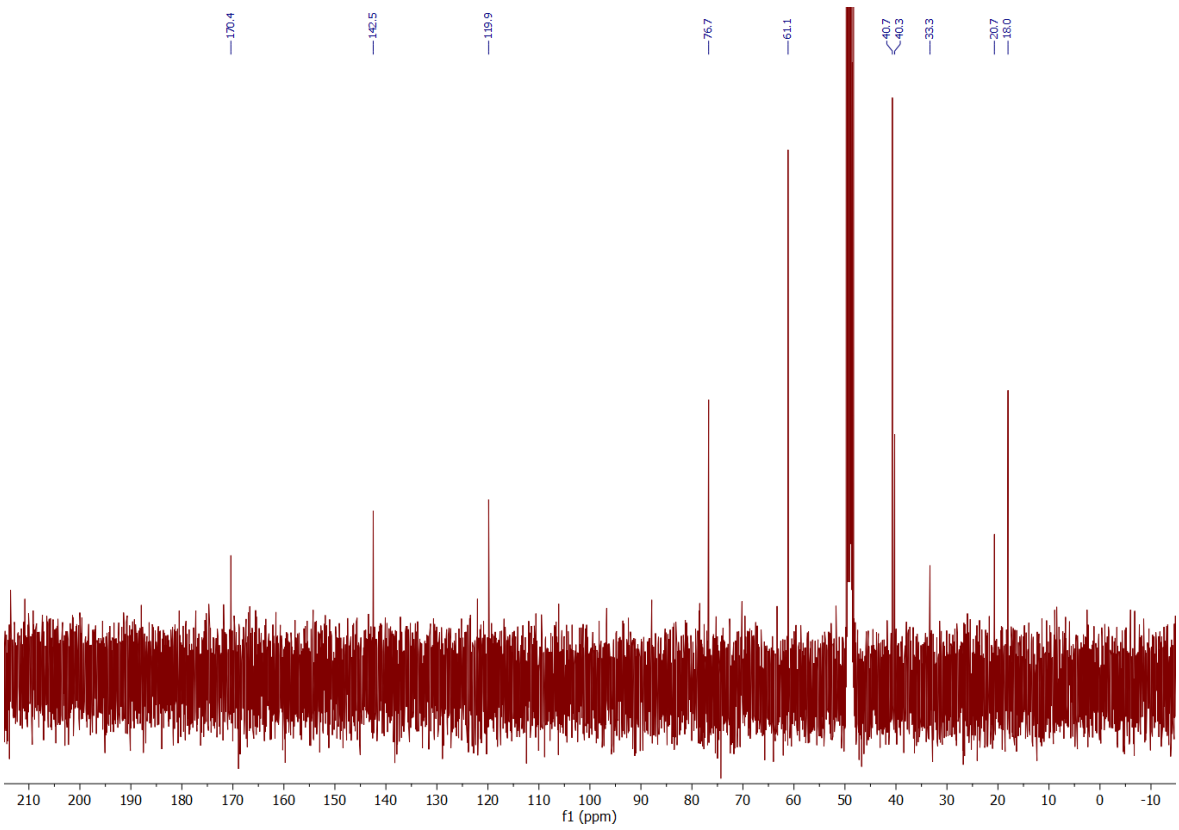


Figure SI57: Tabaqui-1 $^{13}C$ NMR spectrum ($CD_3OD$, 100 MHz, 298 K).

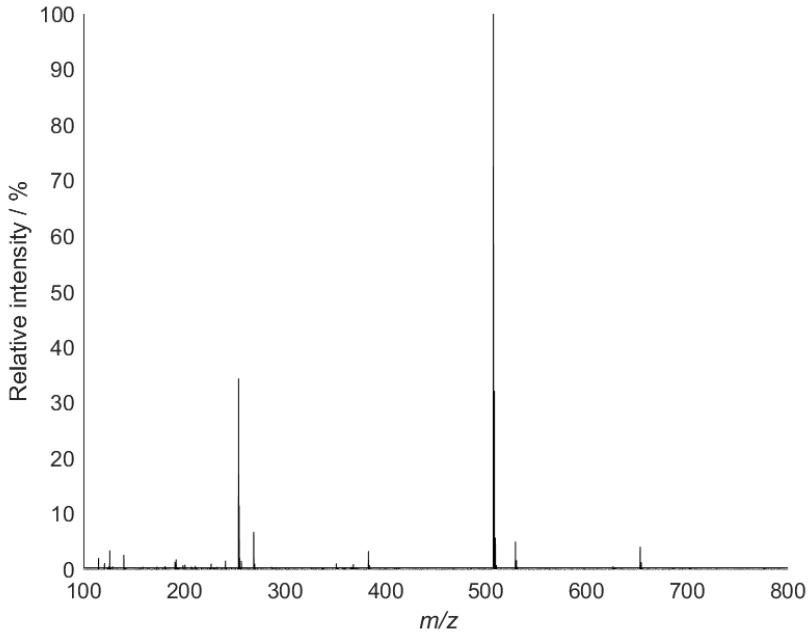


Figure SI58: Tabaqui-1 mass spectrum (Pos ESI).

## SI2.14. Tabaqui-2

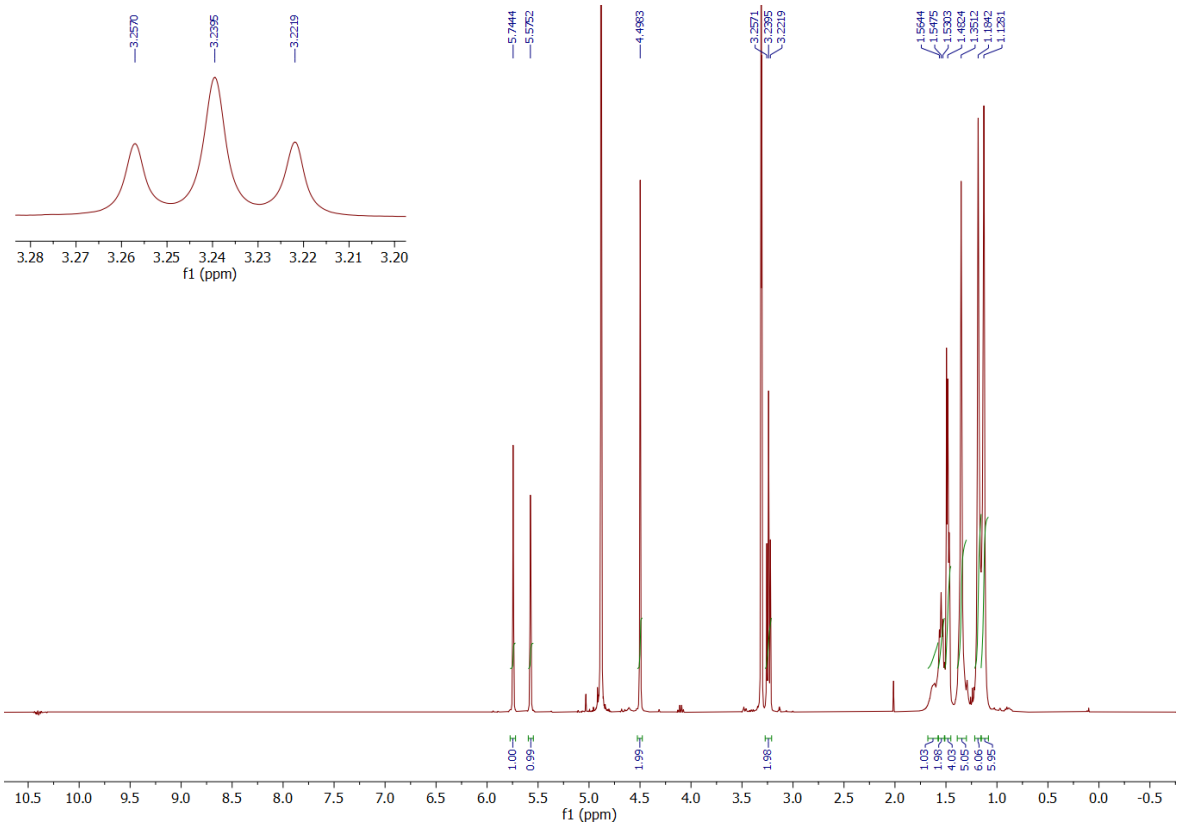


Figure SI59: Tabaqui-2 $^{1}$H NMR spectrum ($CD_3OD$, 400 MHz, 298 K).

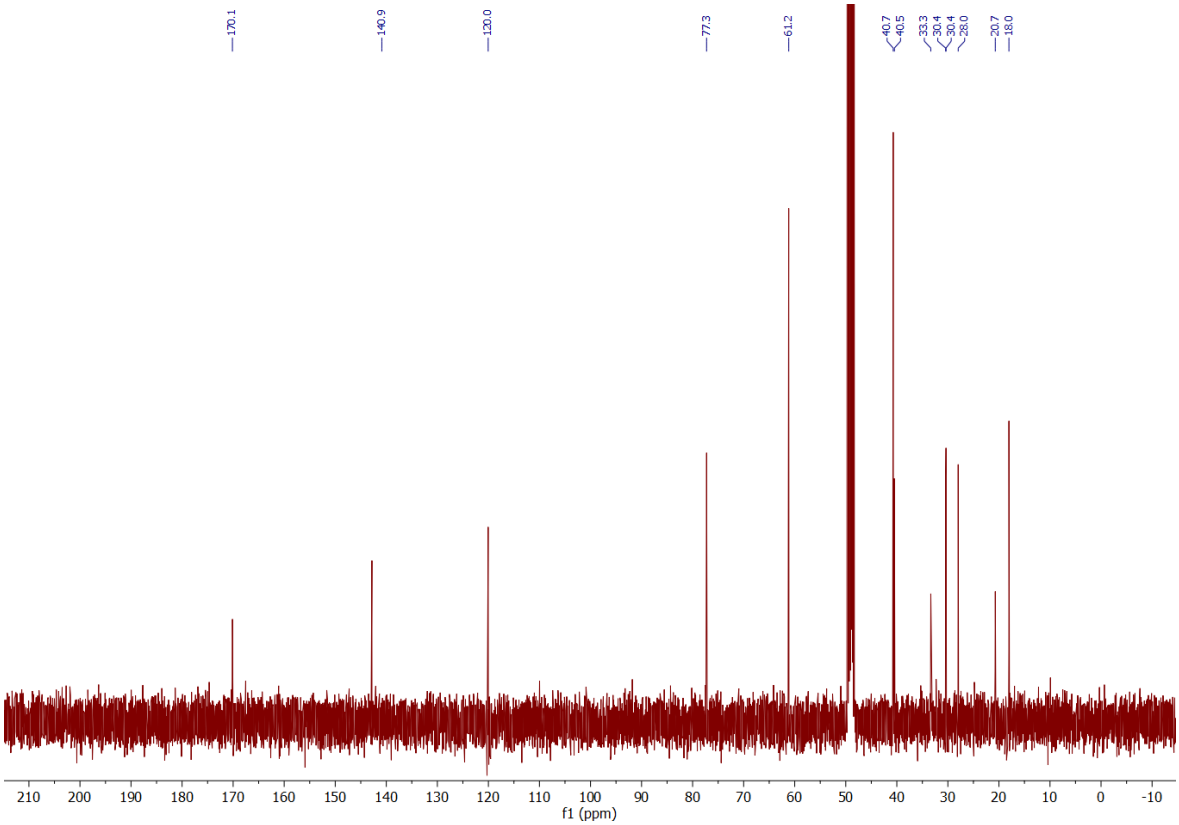


Figure SI60: Tabaqui-2 $^{13}C$ NMR spectrum ($CD_3OD$, 100 MHz, 298 K).

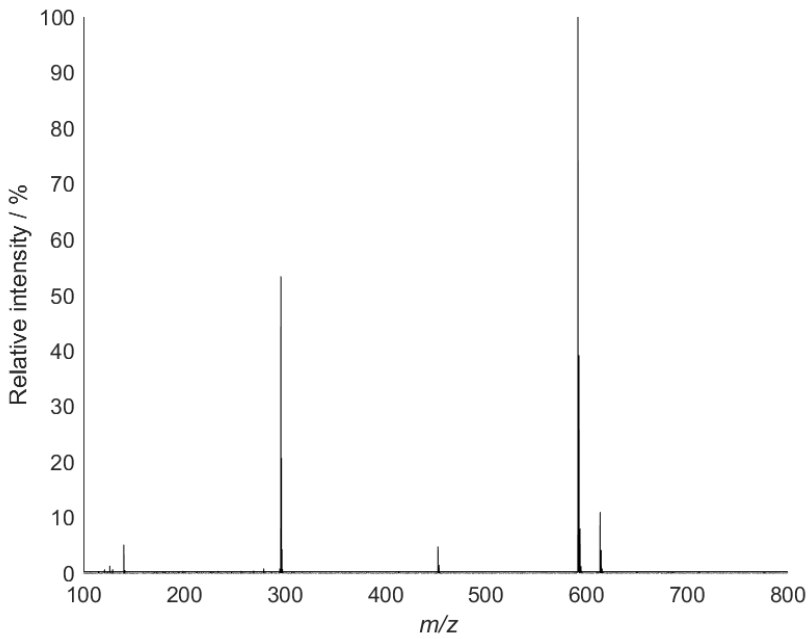


Figure SI61: Tabaqui-2 mass spectrum (Pos ESI).

## SI2.15. BIOANT

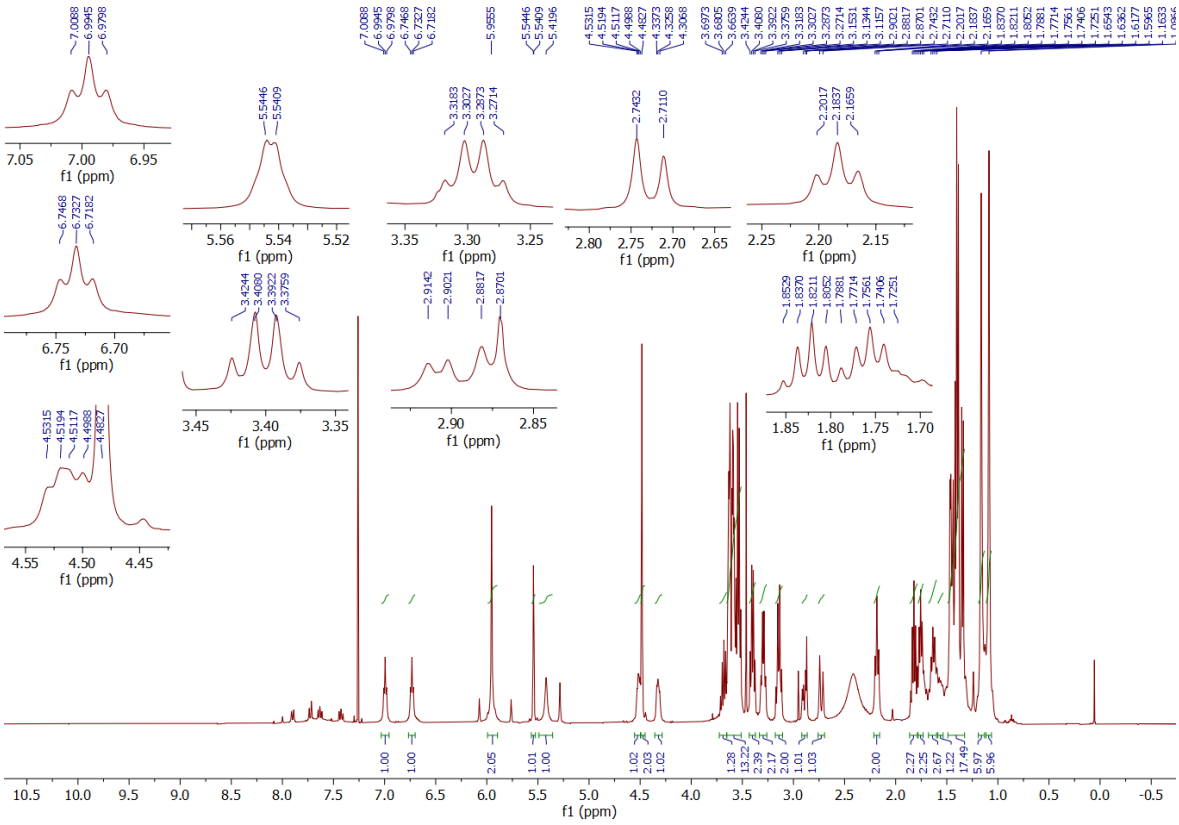

Figure SI62: BIOANT $^{1}H$ NMR spectrum ($CDCl_3$, 400 MHz, 298 K).

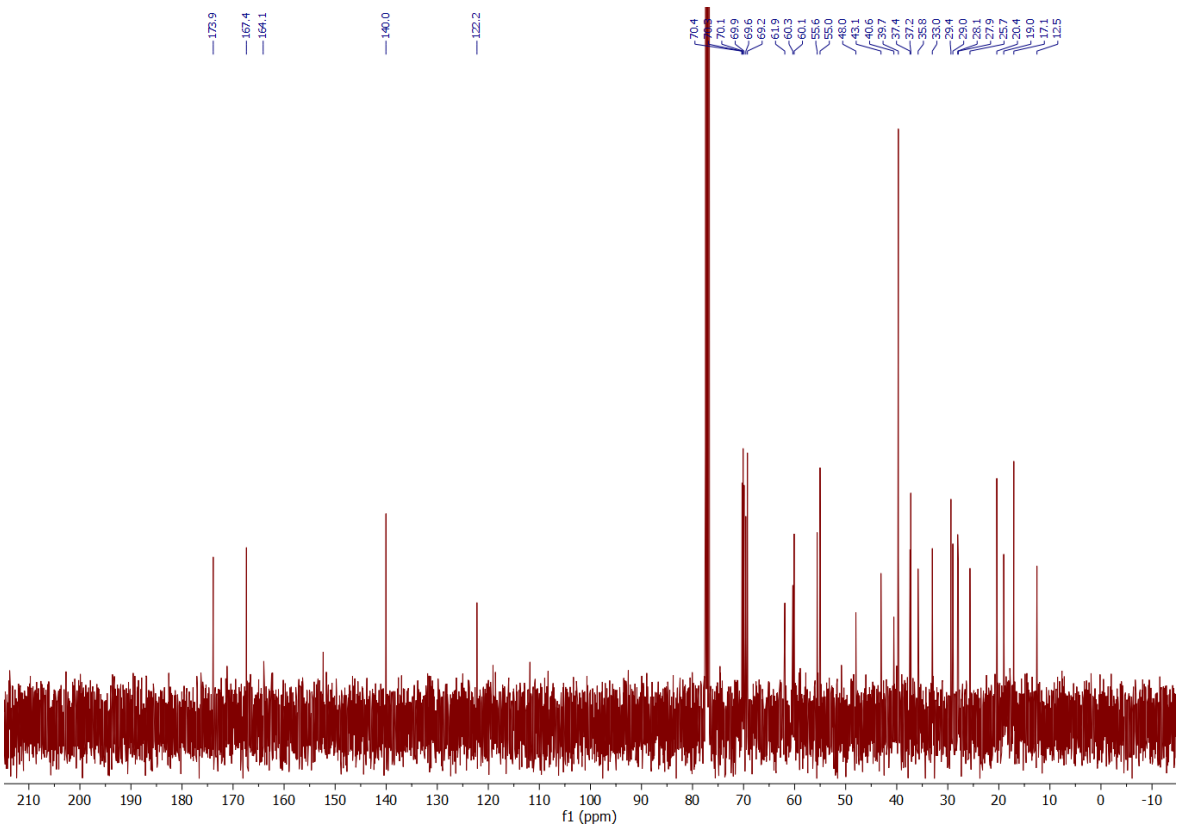

Figure SI63: BIOANT $^{13}C$ NMR spectrum ($CDCl_3$, 100 MHz, 298 K).

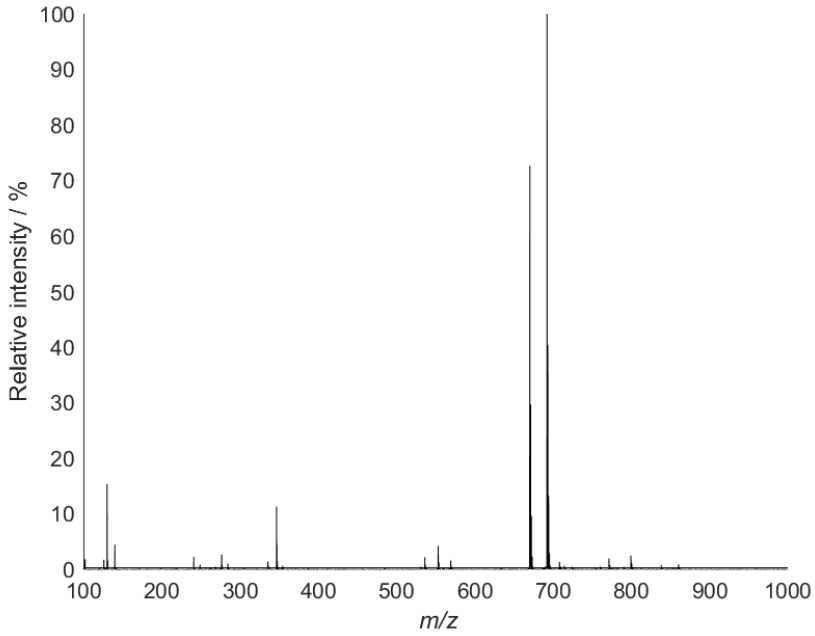


Figure SI64: BIOANT mass spectrum (Pos ESI).

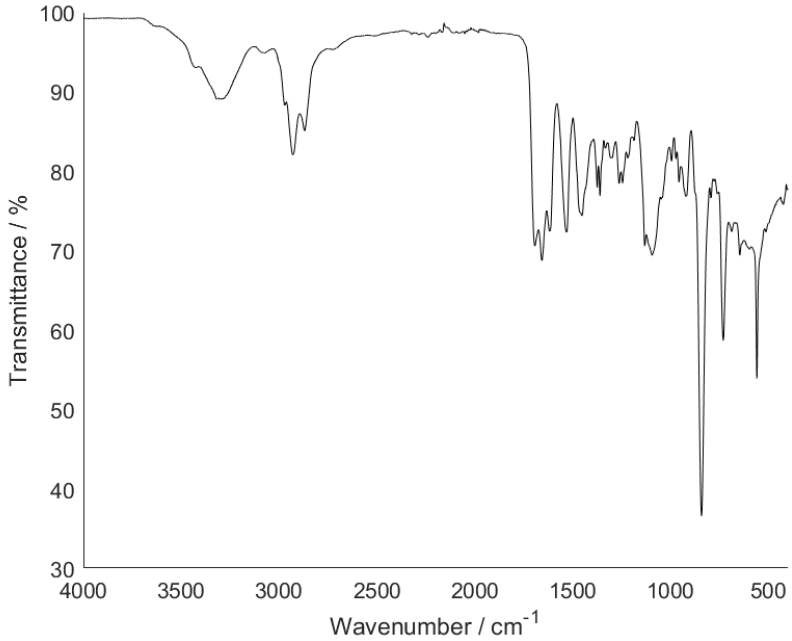


Figure SI65: BIOANT IR spectrum.

## SI2.16. DEADANT

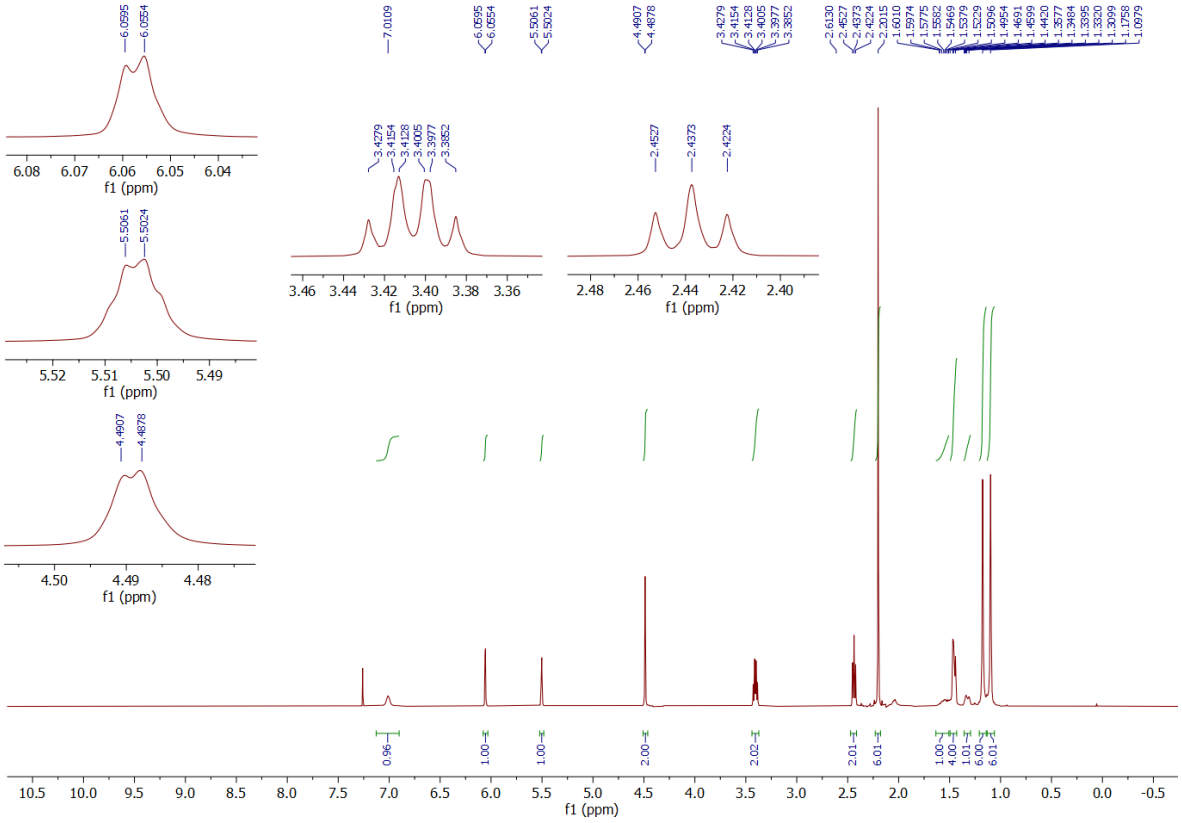

Figure SI66: DEADANT $^{1}$H NMR spectrum ($CDCl_3$, 400 MHz, 298 K).

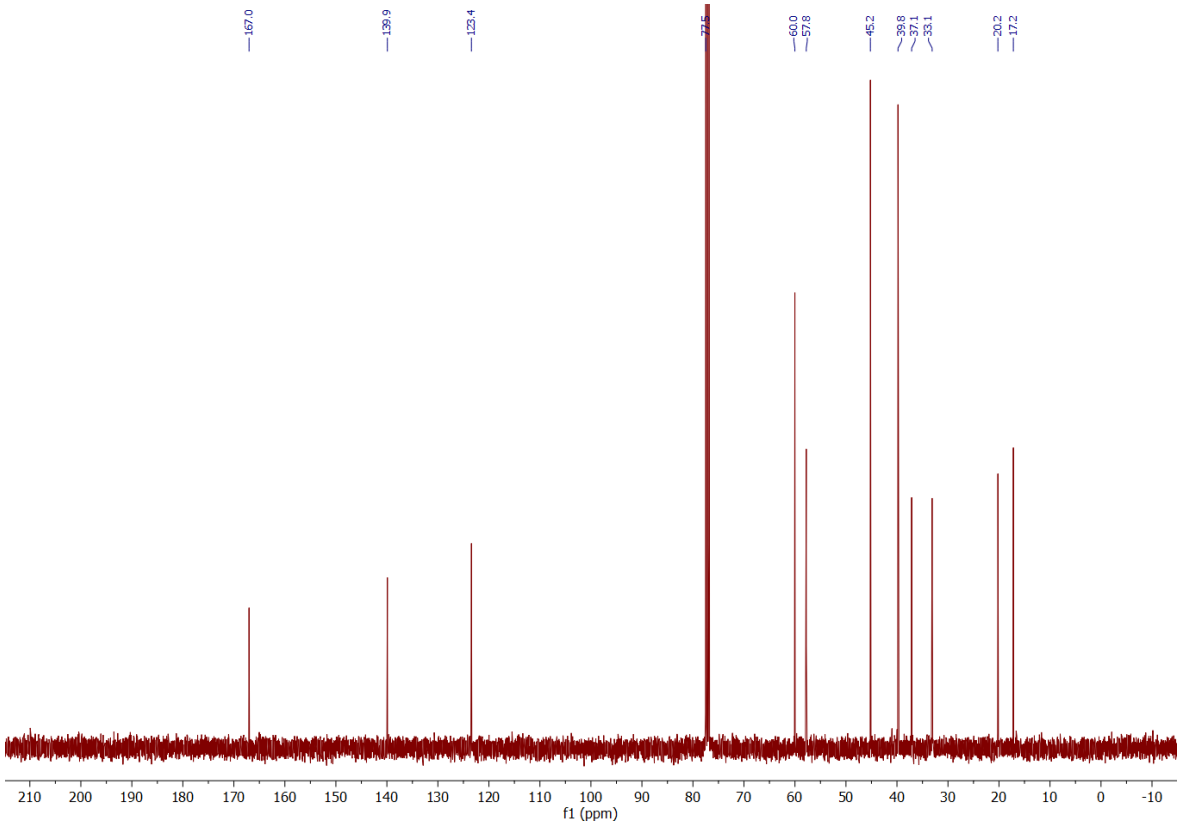

Figure SI67: DEADANT $^{13}$C NMR spectrum ($CDCl_3$, 100 MHz, 298 K).

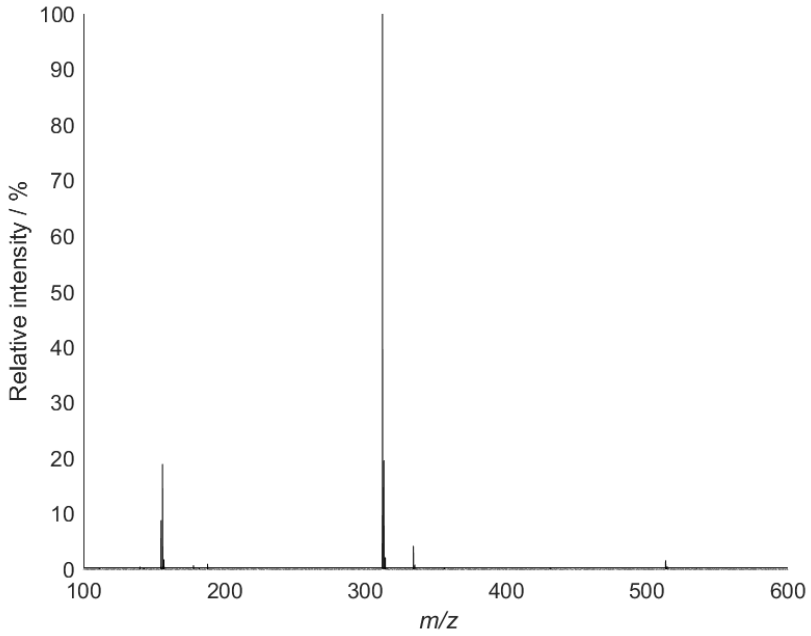


Figure SI68: DEADANT mass spectrum (Pos ESI).

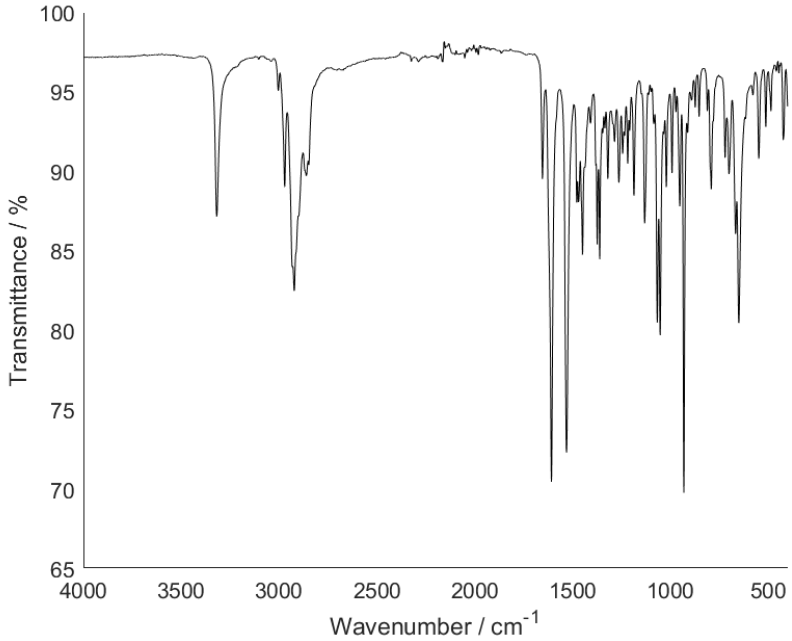


Figure SI69: DEADANT IR spectrum.

## SI2.17. TREADANT

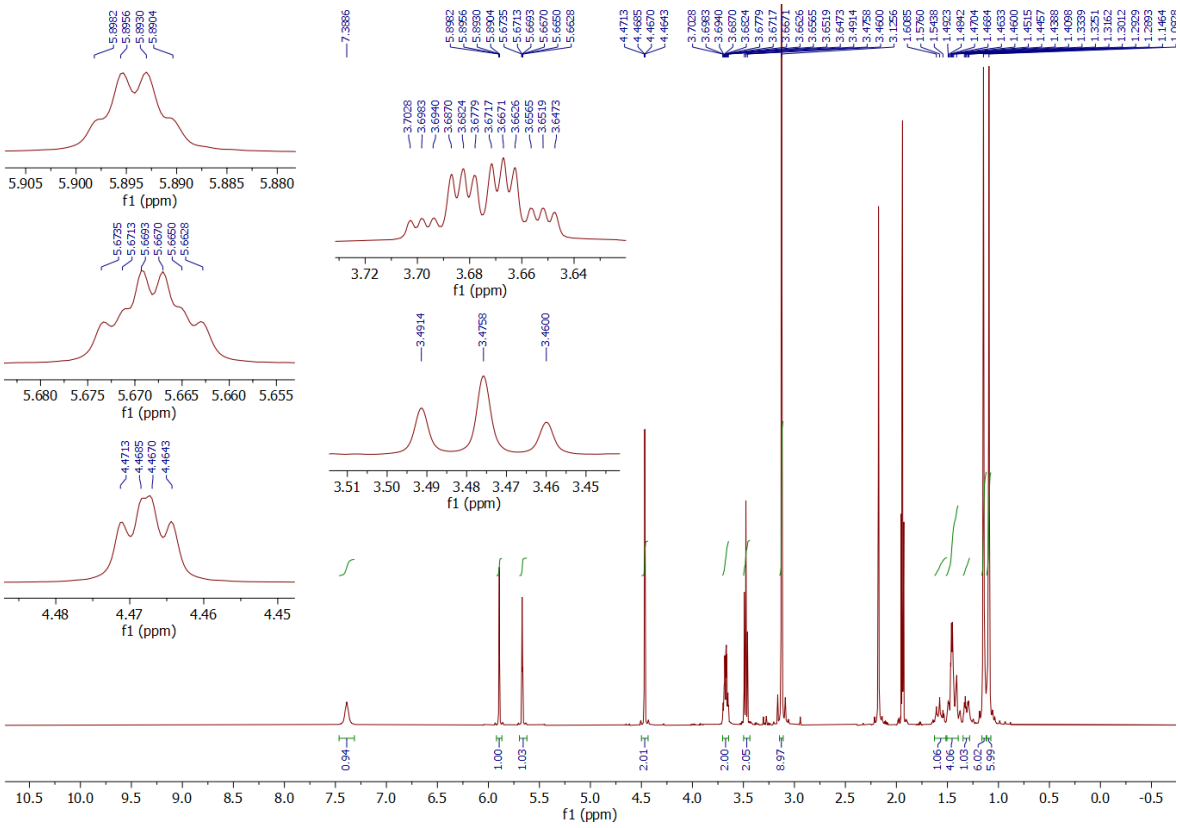

Figure SI70: TREADANT $^{1}$H NMR spectrum ($CDCl_3$, 400 MHz, 298 K).

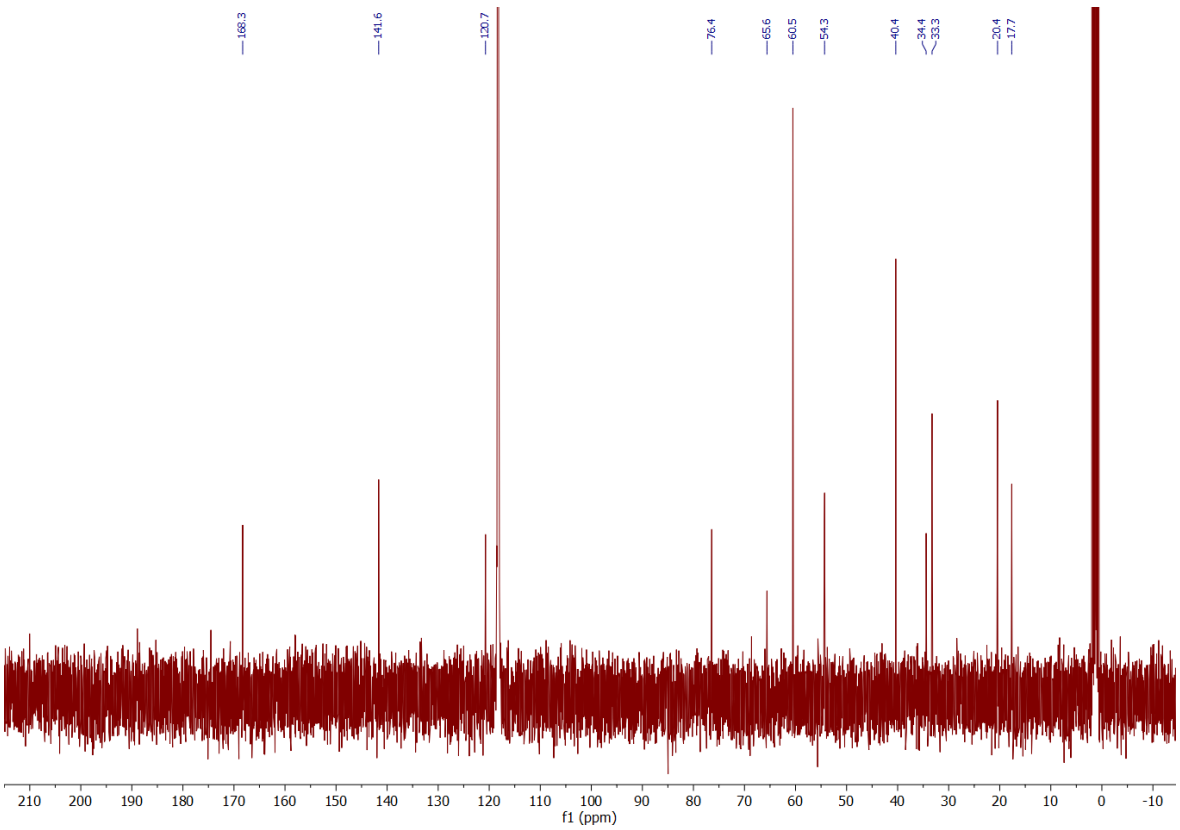

Figure SI71: TREADANT $^{13}$C NMR spectrum ($CDCl_3$, 100 MHz, 298 K).

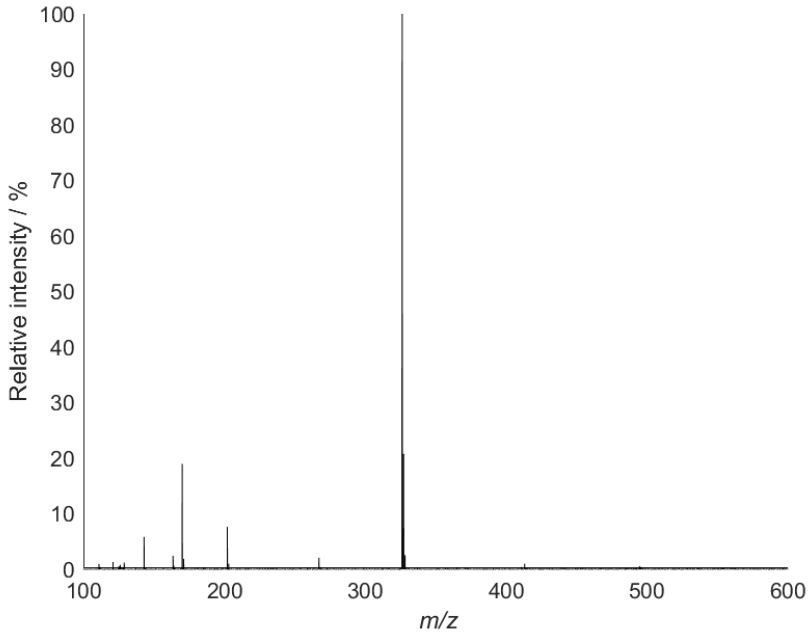


Figure SI72: TREADANT mass spectrum (Pos ESI).

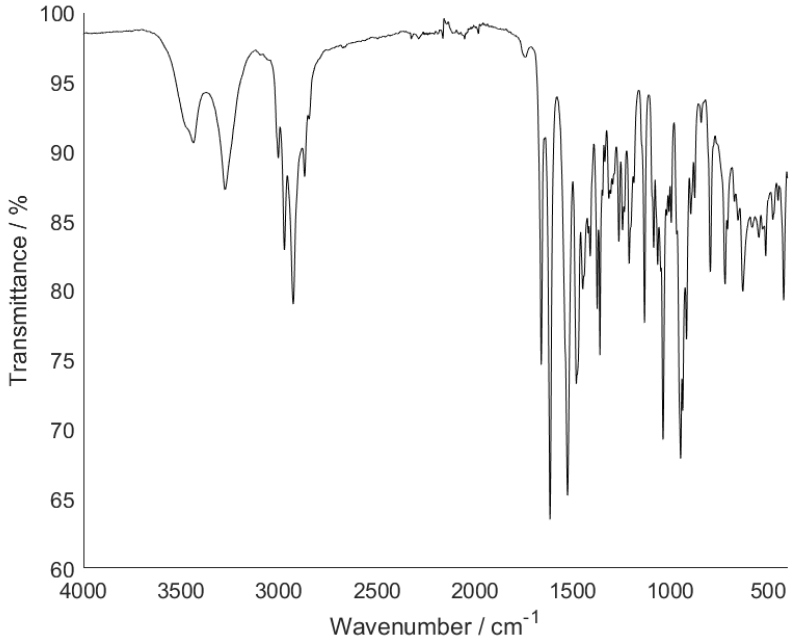


Figure SI73: TREADANT IR spectrum.

## SI2.18. SILANT

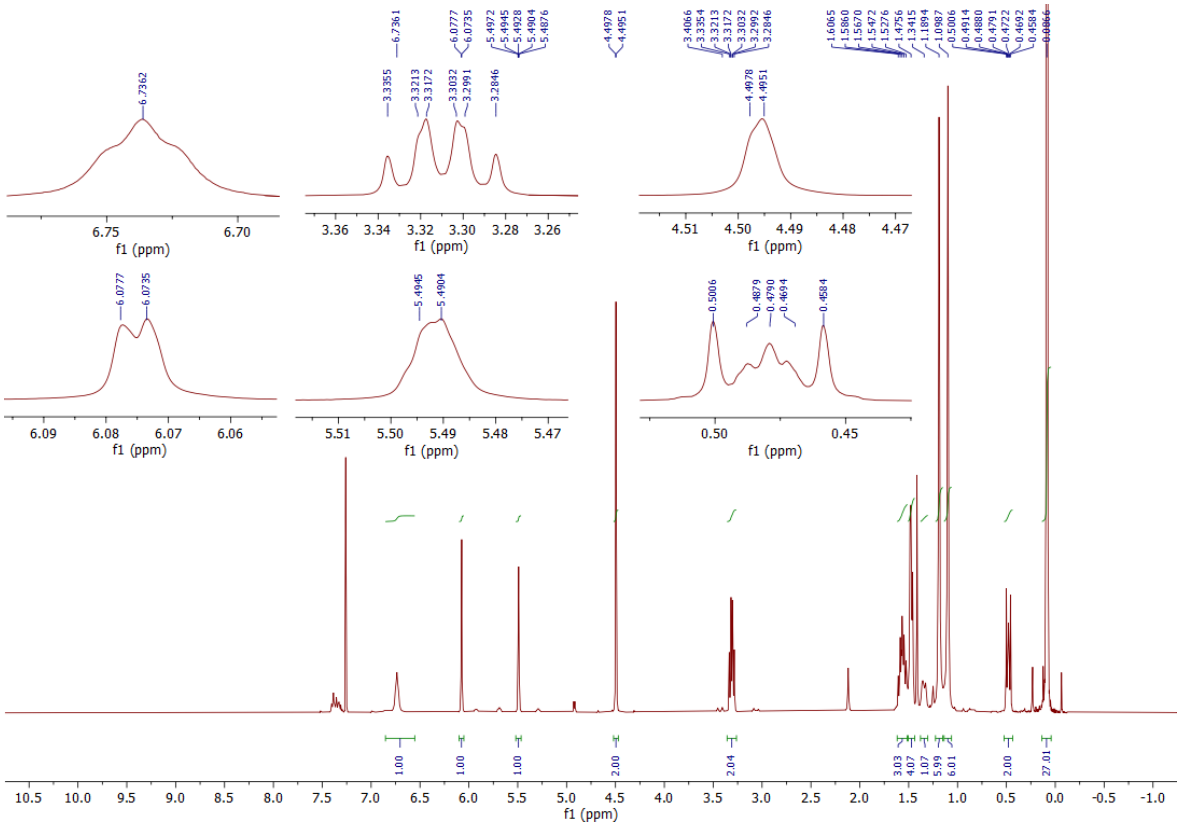


Figure SI74: SILANT $^{1}$H NMR spectrum ($CDCl_3$, 400 MHz, 298 K).

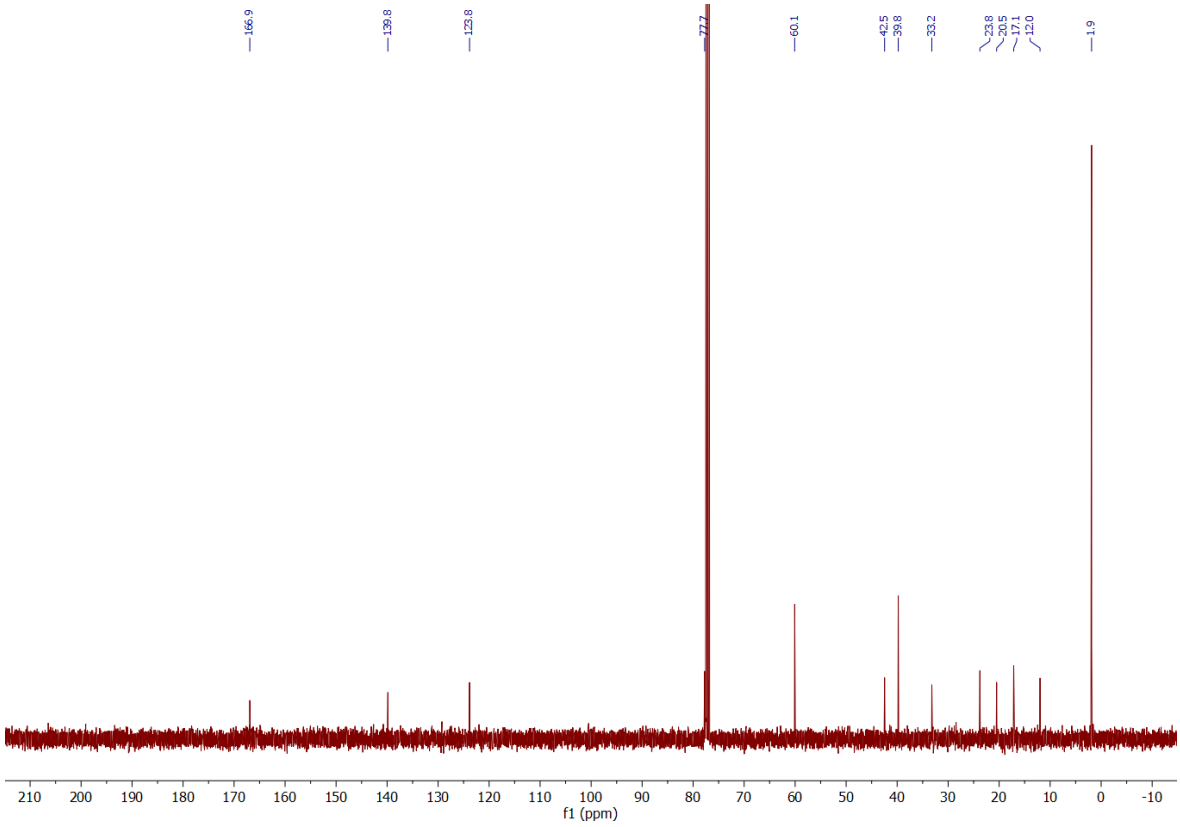


Figure SI75: SILANT $^{13}$C NMR spectrum ($CDCl_3$, 100 MHz, 298 K).

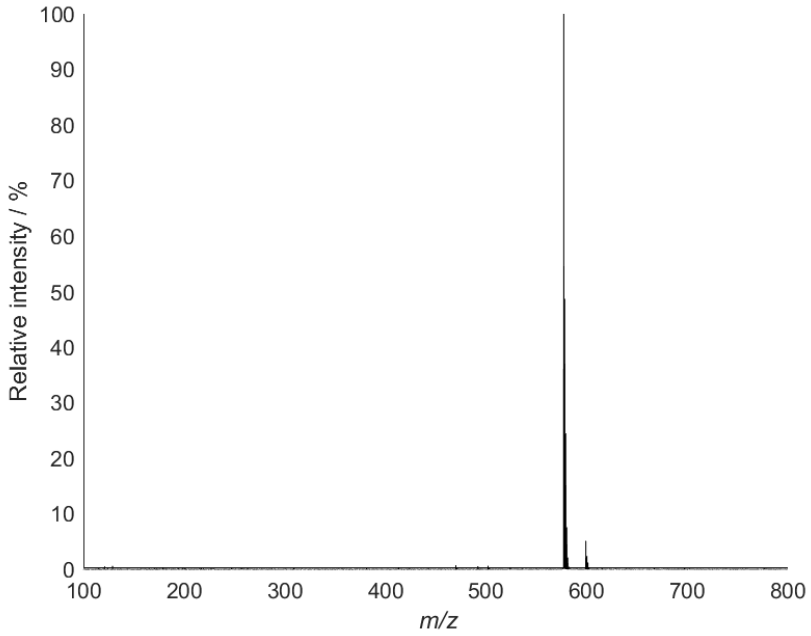


Figure SI76: SILANT mass spectrum (Pos ESI).

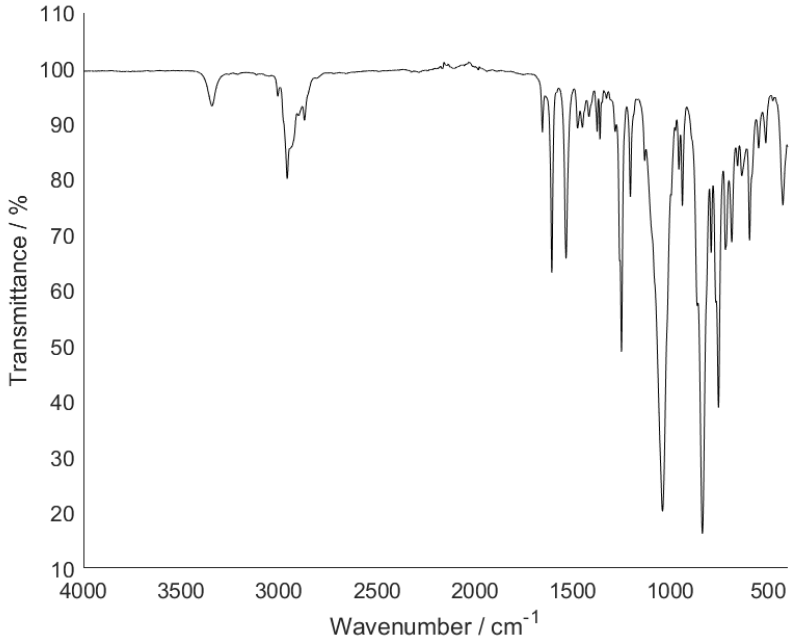


Figure SI77: SILANT IR spectrum.

# SI3. Synthetic radical reactions

## SI3.1. Barton reaction

Table SI1: Fragments identified from tandem MS of peak corresponding to [R2/R3−ART+H]$^+$ (*m/z* 254.212) from TART trapping of the Barton reaction, using isopentyl nitrite as substrate and CHANT as TART (11.4.2). Systematic *m/z* error = -0.0011; random *m/z* error = ±0.0007.

| Species | | Predicted *m/z* | Intensity relative to [R2/R3−ART+H]$^+$ | Implies radical |
|---|---|---|---|---|
| [R2−ART+H]$^+$ | 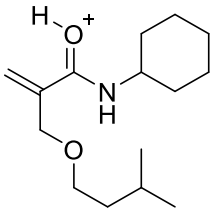 | 254.2120 | 100 | R2 |
| [R3−ART+H]$^+$ | 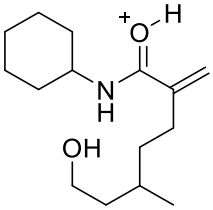 | 254.2120 | 100 | R3 |
| Fragments | 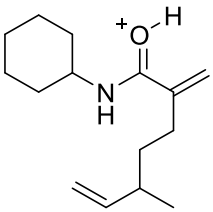 | 236.2014 | 1400 | R3 |
| | 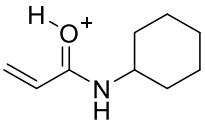 | 154.1232 | 130 | R2/R3 |
| | 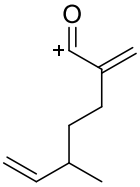 | 137.0966 | 90.6 | R3 |

## SI3.2. Hofmann-Löffler-Freytag (HLF) reaction

### SI3.2.1. Precursor synthesis

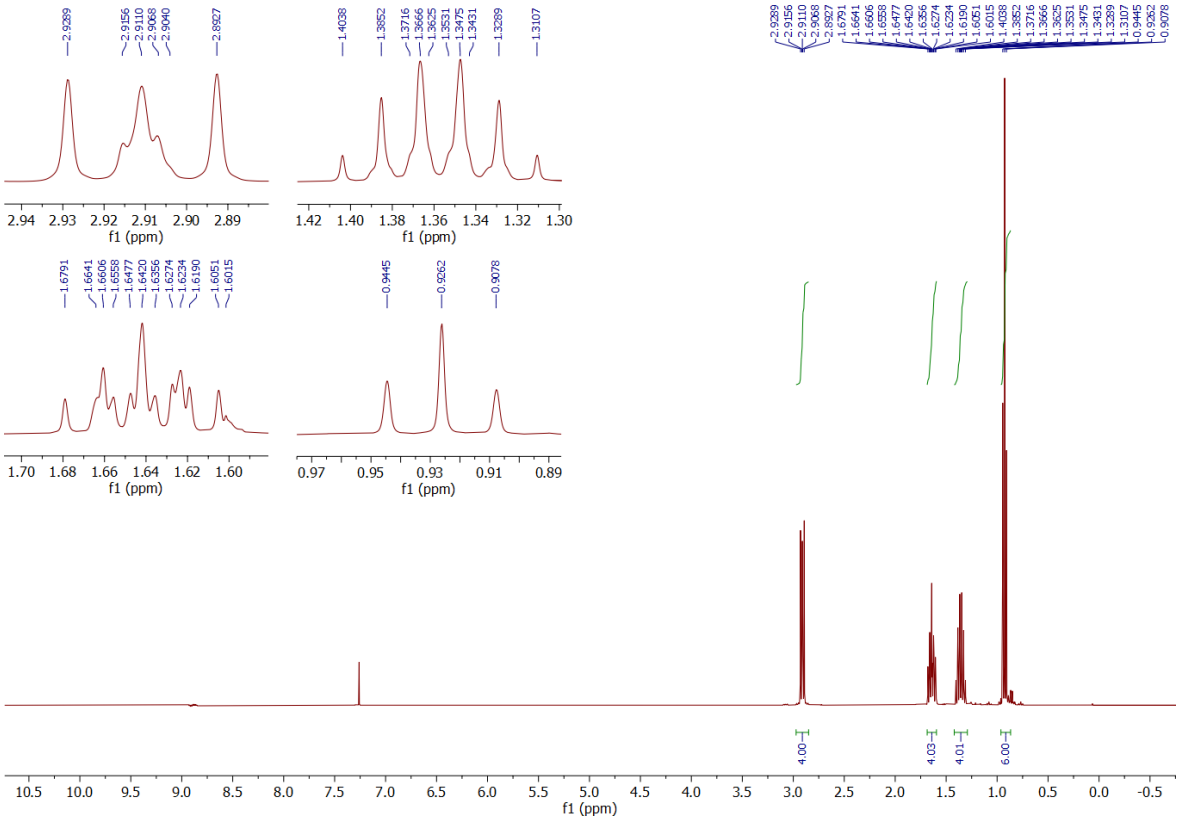


Figure SI78: *N*-Chlorodibutylamine $^{1}$H NMR spectrum ($CDCl_3$, 400 MHz, 298 K).

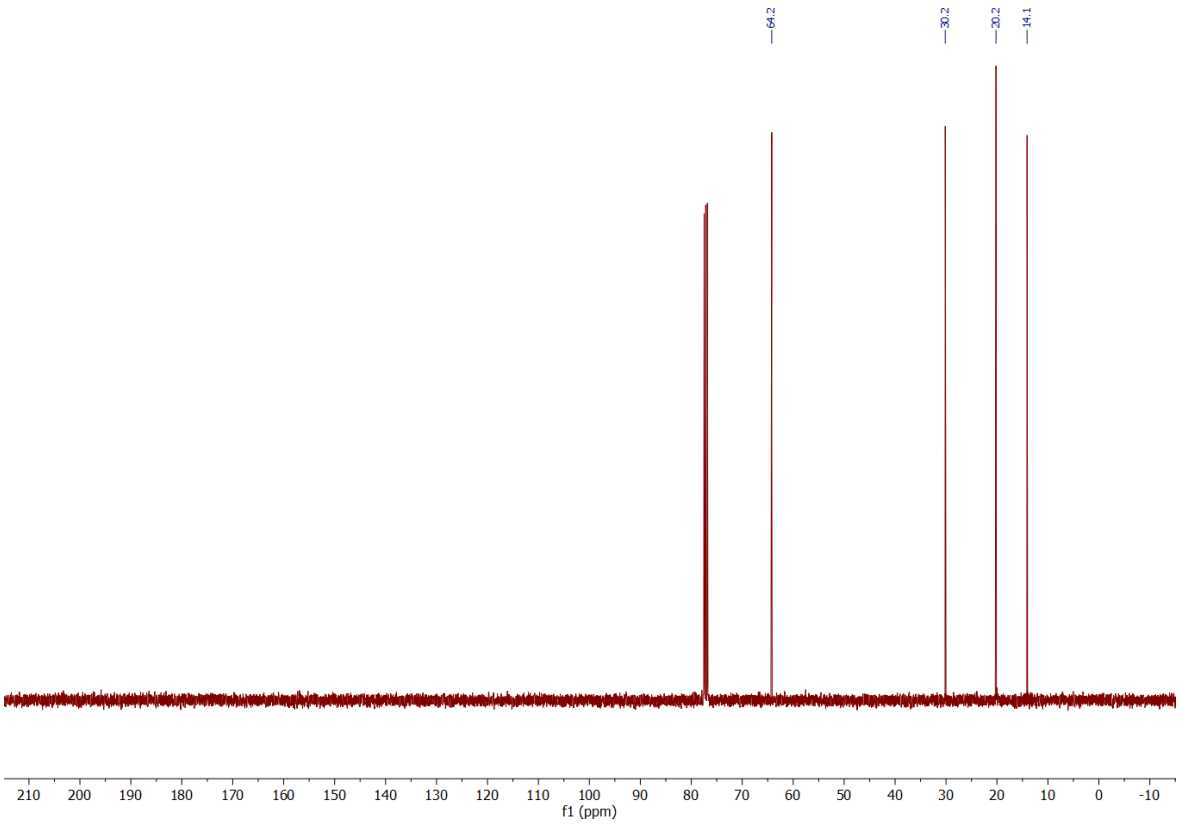


Figure SI79: *N*-Chlorodibutylamine $^{13}C$ NMR spectrum ($CDCl_3$, 100 MHz, 298 K).

## SI3.2.2. Trapping reaction

Table SI2: Fragments from tandem MS of peak corresponding to $[R2/R3-ART+H]^+$ (*m/z* 295.275) from TART trapping of the HLF reaction, using *N*-chlorodibutylamine as substrate and CHANT as TART (11.4.3.2). Systematic *m/z* error = -0.0007; random *m/z* error = ±0.0003.

| Species | | Predicted *m/z* | Intensity relative to $[R2/R3-ART+H]^+$ | Implies radical |
|---|---|---|---|---|
| $[R2-ART+H]^+$ | 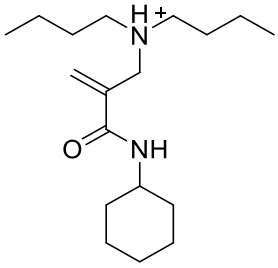 | 295.2749 | 100 | R2 |
| $[R3-ART+H]^+$ | 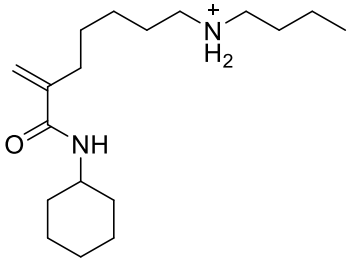 | 295.2749 | 100 | R3 |

| | | | | |
|---|---|---|---|---|
| | 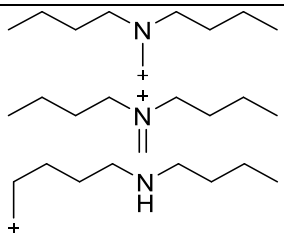 | 142.1596 | 20.4 | R2/R3 |
| | 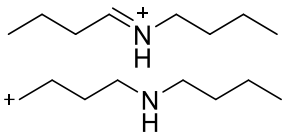 | 128.1439 | 6.70 | R2/R3 |
| | 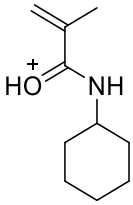 | 168.1388 | 4.31 | R2/R3 |
| Fragments | 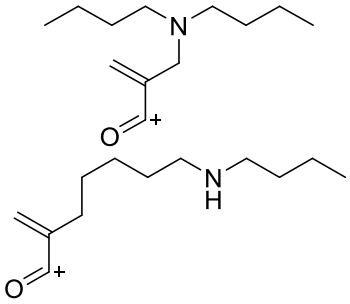 | 196.1701 | 0.882 | R2/R3 |
| | 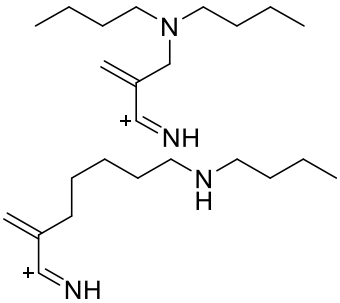 | 195.1861 | 0.864 | R2/R3 |
| | 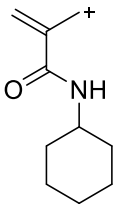 | 166.1232 | 0.836 | R2/R3 |
| | 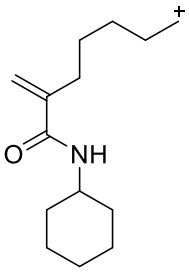 | 222.1858 | 0.709 | R3 |

| | | | | |
|---|---|---|---|---|
| Fragments | 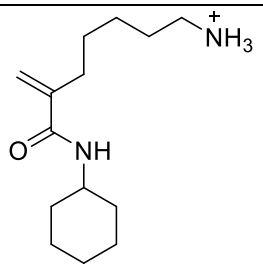 | 239.2123 | 0.537 | R2/R3 |
| | 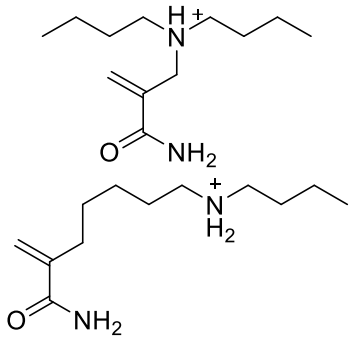 | 213.1967 | 0.419 | R2/R3 |
| | 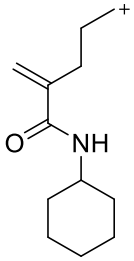 | 194.1545 | 0.257 | R3 |

Table SI3: Fragments from tandem MS of peak corresponding to $[R2-ART+D]^+$ (*m/z* 295.275) from TART trapping of the HLF reaction, using *N*-chlorodibutylamine as substrate and CHANT as TART (11.4.3.2). This was compared to previous tandem MS intensities obtained in protonated solvent. Systematic *m/z* error = -0.0007; random *m/z* error = ±0.0003.

| Species | | Predicted *m/z* | Intensity relative to $[R2/R3-ART+H]^+$ | | Implies radical |
|---|---|---|---|---|---|
| | | | $H_2O$ | $D_2O$ | |
| $[R2-ART+H]^+$ | 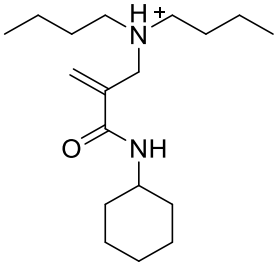 | 295.2749 | 100 | 100 | R2 |
| $[R3-ART+H]^+$ | 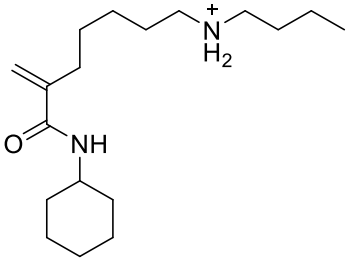 | 295.2749 | 100 | 100 | R3 |

| | | | | | |
|---|---|---|---|---|---|
| Fragments | 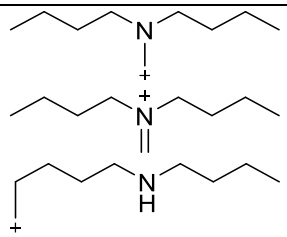 | 142.1596 | 20.4 | 13.6 | R2/R3 |
| | 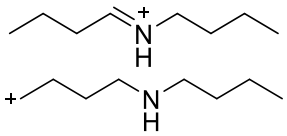 | 128.1439 | 6.70 | 5.67 | R2/R3 |
| | 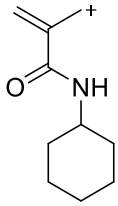 | 166.1232 | 0.836 | 0.554 | R2/R3 |
| | 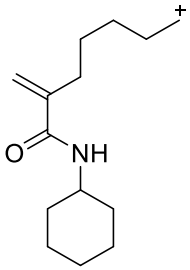 | 222.1858 | 0.709 | 0.046 | R3 |
| | 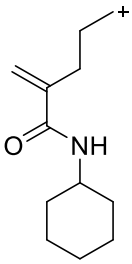 | 194.1545 | 0.257 | 0.086 | R3 |

Table SI4: Fragments from tandem HPLC-MS of the peak corresponding to $[R2/R3-ART+H]^+$ (*m/z* 295.275) from TART trapping of the HLF reaction, using *N*-chlorodibutylamine as substrate and CHANT as TART (11.4.3.2), observed during the first peak (13.49 min) and second peak (13.62 min). Systematic *m/z* error = -0.0007; random *m/z* error = ±0.0005.

| Species | | Predicted *m/z* | Intensity relative to $[R2/R3-ART+H]^+$ 1st peak | 2nd peak | Implies radical |
|---|---|---|---|---|---|
| $[R2-ART+H]^+$ | 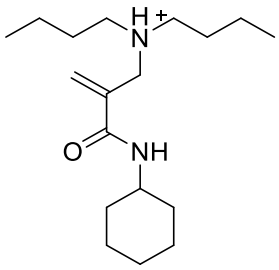 | 295.2749 | 100 | 100 | R2 |

| | | | | | |
|---|---|---|---|---|---|
| [R3−ART+H]$^+$ | 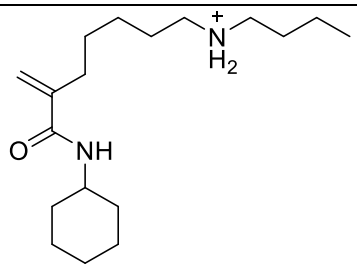 | 295.2749 | 100 | 100 | R3 |
| Fragments | 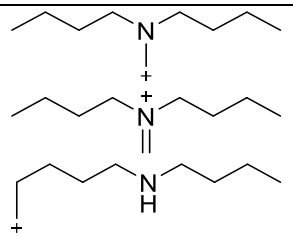 | 142.1596 | 39.7 | 39.6 | R2/R3 |
| | 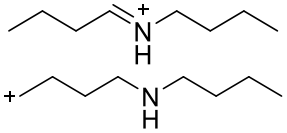 | 128.1439 | 11.8 | 11.3 | R2/R3 |
| | 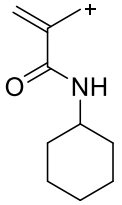 | 166.1232 | 1.09 | 1.15 | R2/R3 |
| | 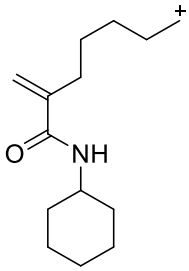 | 222.1858 | 0.912 | 0.402 | R3 |
| | 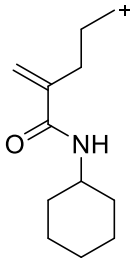 | 194.1545 | 0.653 | 0.531 | R3 |

## SI3.3. Radical aromatic aminophosphinoylation

Table SI5: Fragments identified from tandem MS of peak corresponding to $[R2-ART+H]^+$ (*m/z* 243.094) from TART trapping of radical aromatic aminophosphinoylation, using 4-methylstyrene, 4-chloroalanine, and DPPO as substrates and allyl-TEMPO as TART (11.4.5). Systematic *m/z* error = -0.0009; random *m/z* error = ±0.0002.

| Species | | Predicted *m/z* | Intensity relative to parent ion / % |
|---|---|---|---|
| $[R2-ART+H]^+$ | 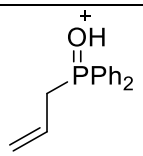 | 243.0939 | 100 |
| Fragments | 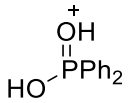 | 219.0575 | 490 |
| |  | 201.0469 | 62.7 |

Table SI6: Fragments identified from tandem MS of peak corresponding to $[R3-ART+H]^+$ (*m/z* 361.172) from TART trapping of radical aromatic aminophosphinoylation, using 4-methylstyrene, 4-chloroalanine, and DPPO as substrates and allyl-TEMPO as TART (11.4.5). Systematic *m/z* error = -0.0009; random *m/z* error = ±0.0004.

| Species | | Predicted *m/z* | Intensity relative to parent ion / % |
|---|---|---|---|
| $[R3-ART+H]^+$ | 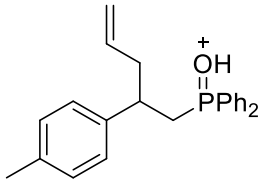 | 361.1721 | 100 |
| Fragments |  | 201.0469 | 212 |
| | 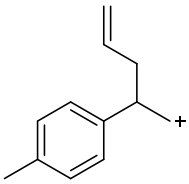 | 159.1174 | 57.2 |

## SI3.4. Radical decarboxylative aromatic iodination

Table SI7: Fragments identified from tandem MS of peak corresponding to $[R1-ART+H]^+$ (*m/z* 318.171) from TART trapping of radical decarboxylative aromatic iodination, using *p*-anisic acid as substrate and CHANT as TART (11.4.6). Systematic *m/z* error = -0.0011; random *m/z* error = ±0.0006.

| Species | | Predicted *m/z* | Intensity relative to parent ion / % |
|---|---|---|---|
| $[R1-ART+H]^+$ | 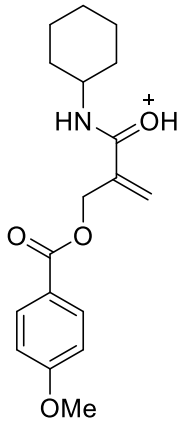 | 318.1705 | 100 |
| Fragments | 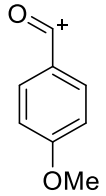 | 135.0446 | 829 |
| | 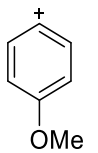 | 107.0497 | 46.8 |
| | 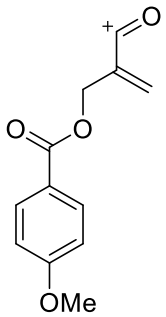 | 219.0657 | 14.0 |
| | 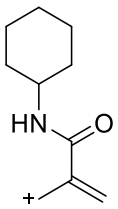 | 166.1232 | 1.46 |

Table SI8: Fragments identified from tandem MS of peak corresponding to [R3−ART+H]$^+$ (*m/z* 274.181) from TART trapping of radical decarboxylative aromatic iodination, using *p*-anisic acid as substrate and CHANT as TART (11.4.6). Systematic *m/z* error = -0.0010; random *m/z* error = ±0.0004.

| Species | | Predicted *m/z* | Intensity relative to parent ion / % |
|---|---|---|---|
| [R3−ART+H]$^+$ | 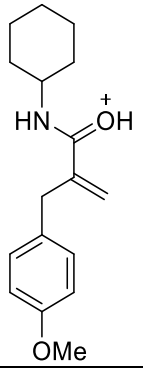 | 274.1807 | 100 |
| Fragments | 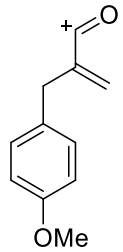 | 175.0759 | 52.0 |
| | 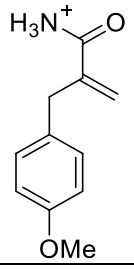 | 192.1024 | 24.9 |

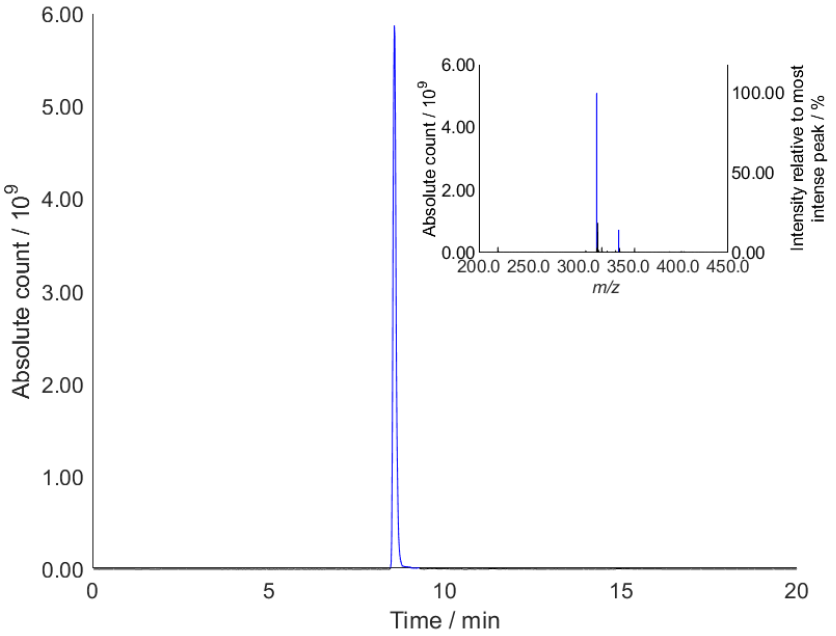


Figure SI80: HPLC-MS chromatogram of peak corresponding to [R1−ART+H/Na]$^+$ (*m/z* 318.171±0.002 and *m/z* 340.152±0.002), detected from TART trapping of radical decarboxylative aromatic iodination, using *p*-anisic acid as substrate and CHANT as TART (11.4.6). Mass spectrum (inset) recorded at time of maximum chromatogram intensity (8.57 min, blue) shows *m/z* 318.171 cleanly isolated (blue).

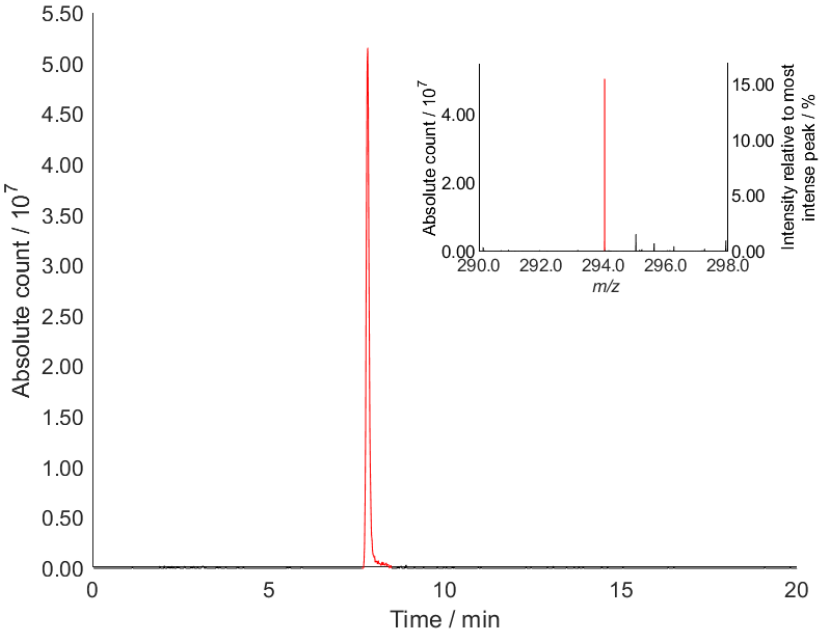


Figure SI81: HPLC-MS chromatogram of peak corresponding to [R2−ART+H/Na]$^+$ (*m/z* 294.035±0.002 and *m/z* 316.017±0.002), detected from TART trapping of radical decarboxylative aromatic iodination, using *p*-anisic acid as substrate and CHANT as TART (11.4.6). Mass spectrum (inset) recorded at time of maximum chromatogram intensity (7.82 min, red) shows *m/z* 294.035 cleanly isolated (red).

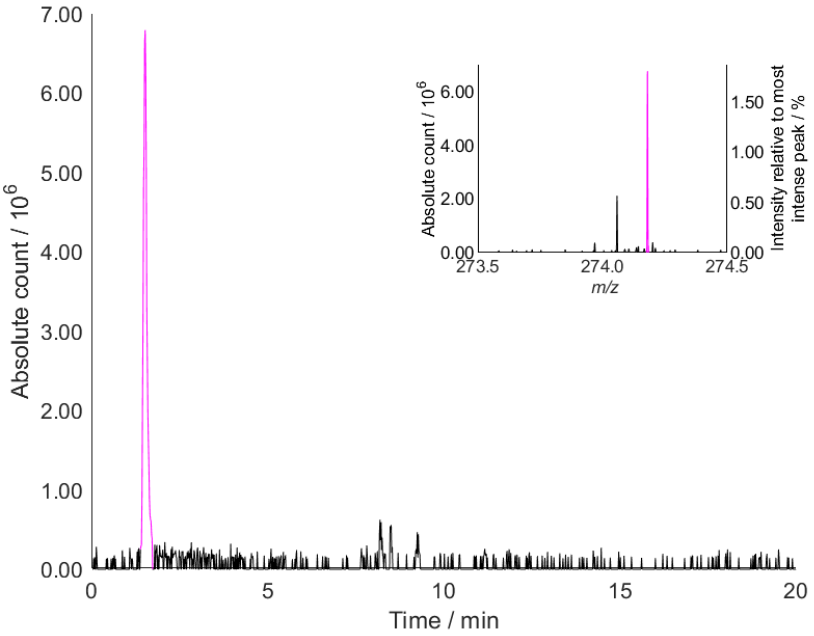


Figure SI82: HPLC-MS chromatogram of peak corresponding to [R3−ART+H/Na]$^+$ (*m/z* 274.181±0.002 and *m/z* 296.163±0.002), detected from TART trapping of radical decarboxylative aromatic iodination, using *p*-anisic acid as substrate and CHANT as TART (11.4.6). Mass spectrum (inset) recorded at time of maximum chromatogram intensity (1.53 min, pink) shows *m/z* 274.181 cleanly isolated (pink).

# SI4. Photochemistry

## SI4.1. Radical cyanomethylation

Table SI9: Fragments identified from tandem MS of peak corresponding to [R1−ART+H]$^+$ (*m/z* 286.181) from TART trapping of Ru-photocatalysed radical cyanomethylation (11.5.1). Systematic *m/z* error = -0.0008; random *m/z* error = ±0.0002.

| Species | | Predicted *m/z* | Intensity relative to parent ion / % |
|---|---|---|---|
| [R1−ART+H]$^+$ | 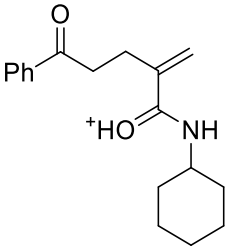 | 286.1807 | 100 |
| Fragments | 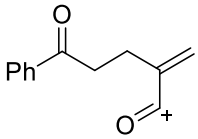 | 187.0759 | 777 |
| | 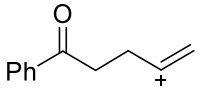 | 159.0810 | 139 |

Table SI10: Fragments identified from tandem MS of peak corresponding to [R4−ART+H]$^+$ (*m/z* 248.163) from TART trapping of Ru-photocatalysed radical cyanomethylation (11.5.1). Systematic *m/z* error = -0.0007; random *m/z* error = ±0.0002.

| Species | | Predicted *m/z* | Intensity relative to most intense fragment / % |
|---|---|---|---|
| [R4−ART+H]$^+$ | 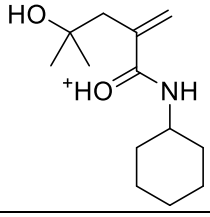 | 248.1626 | 0[a] |
| Fragments | 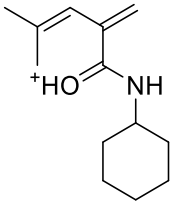 | 208.1701 | 100 |
| | 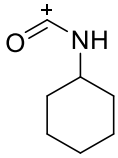 | 126.0919 | 13.6 |
| | 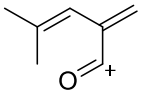 | 109.0653 | 6.95 |

[a]Parent ion cleanly isolated prior to CID, but CID caused total peak fragmentation.

## SI4.2. Radical thiol-ene addition

### SI4.2.1. Literature replication

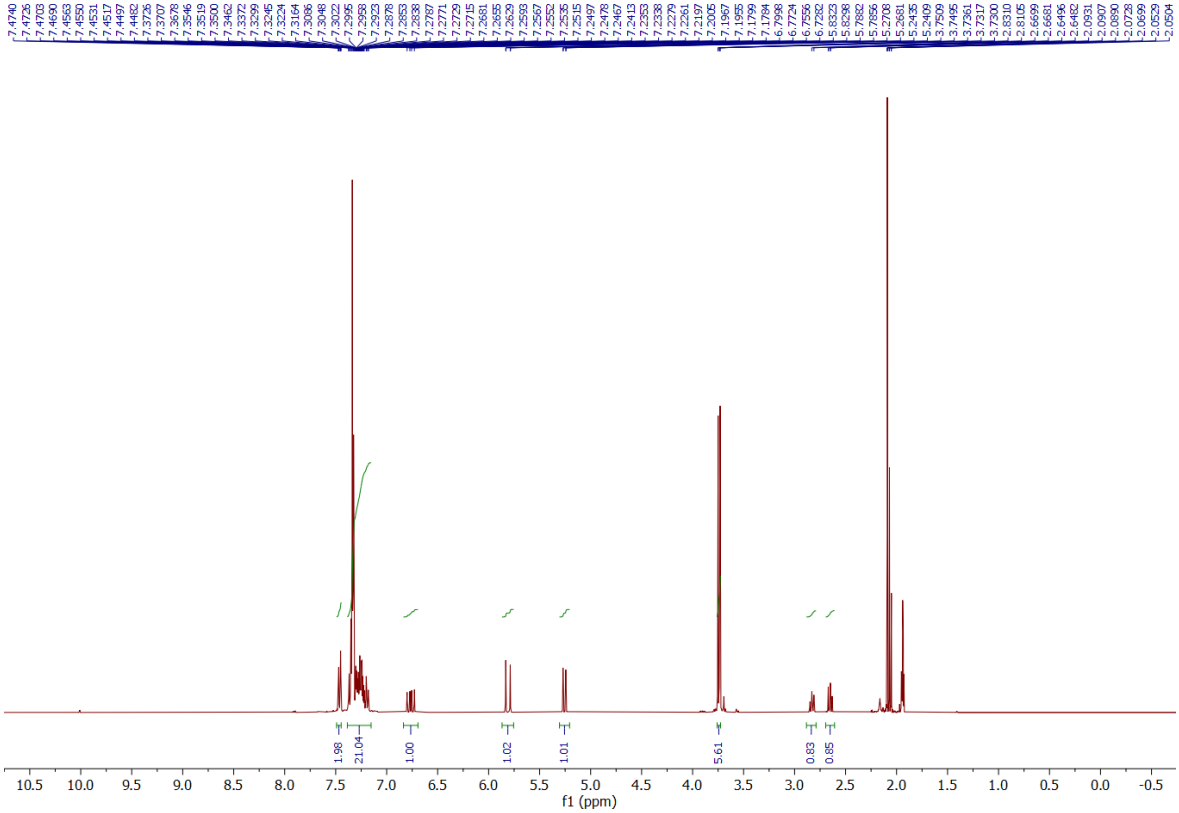


Figure SI83: $^{1}$H NMR spectrum of radical thiol-ene addition literature replication (11.5.2.1, $CD_3CN$, 400 MHz, 298 K).

## SI4.2.2. Controls

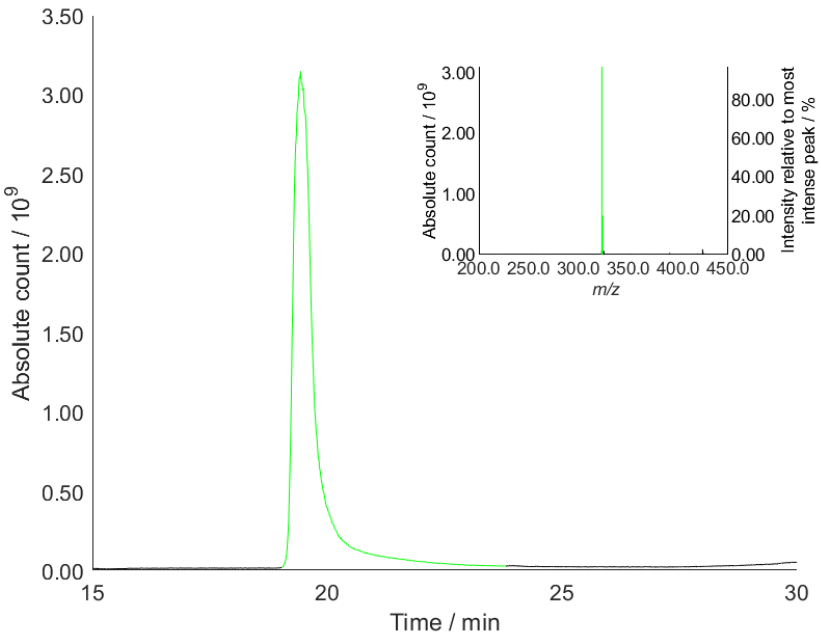


Figure SI84: HPLC-MS chromatogram of peak corresponding to $[CHANT+H]^+$ (*m/z* 323.270±0.002), detected from TART trapping of radical thiol-ene addition, using benzyl mercaptan and styrene as substrates (11.5.2.3). Mass spectrum (inset) recorded at time of maximum chromatogram intensity (19.4 min, green) shows *m/z* 323.270 cleanly isolated (green).

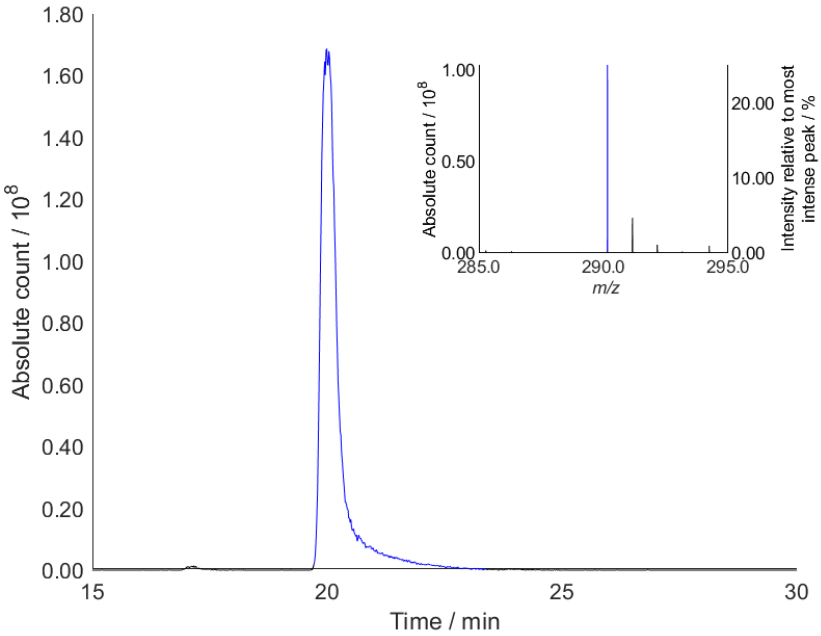


Figure SI85: HPLC-MS chromatogram of peaks corresponding to $[R1-ART+H/Na]^+$ (*m/z* 290.158±0.002 and *m/z* 312.140±0.002), detected TART trapping of radical thiol-ene addition, using benzyl mercaptan and styrene as substrates (11.5.2.3). Mass spectrum (inset) recorded at time of maximum chromatogram intensity (20.0 min, blue) shows *m/z* 290.158 cleanly isolated (blue).

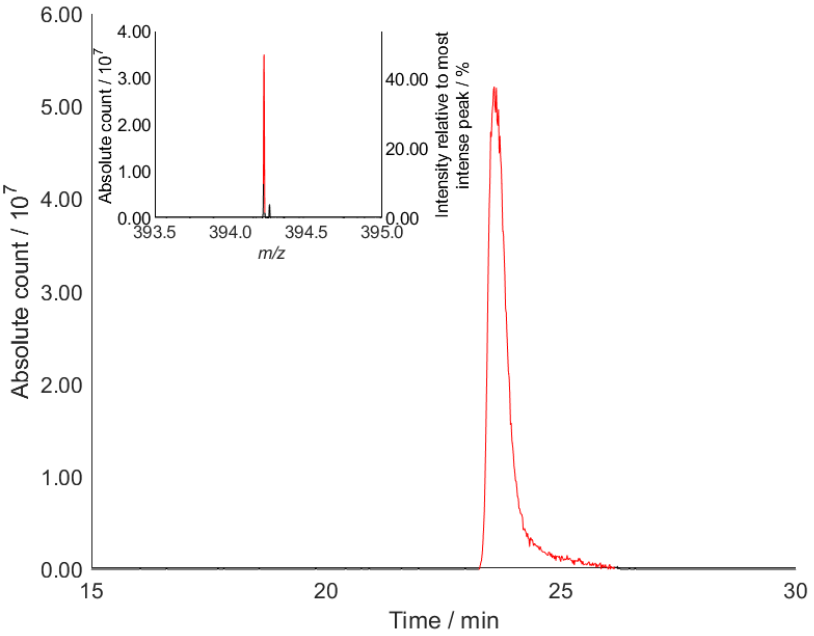


Figure SI86: HPLC-MS chromatogram of peaks corresponding to [R2−ART+H/Na]$^+$ (*m/z* 394.220±0.002 and *m/z* 416.202±0.002), detected TART trapping of radical thiol-ene addition, using benzyl mercaptan and styrene as substrates (11.5.2.3). Mass spectrum (inset) recorded at time of maximum chromatogram intensity (24.0 min, red) shows *m/z* 394.220 cleanly isolated (red).

## SI4.2.3. TART-trapped radical isolation

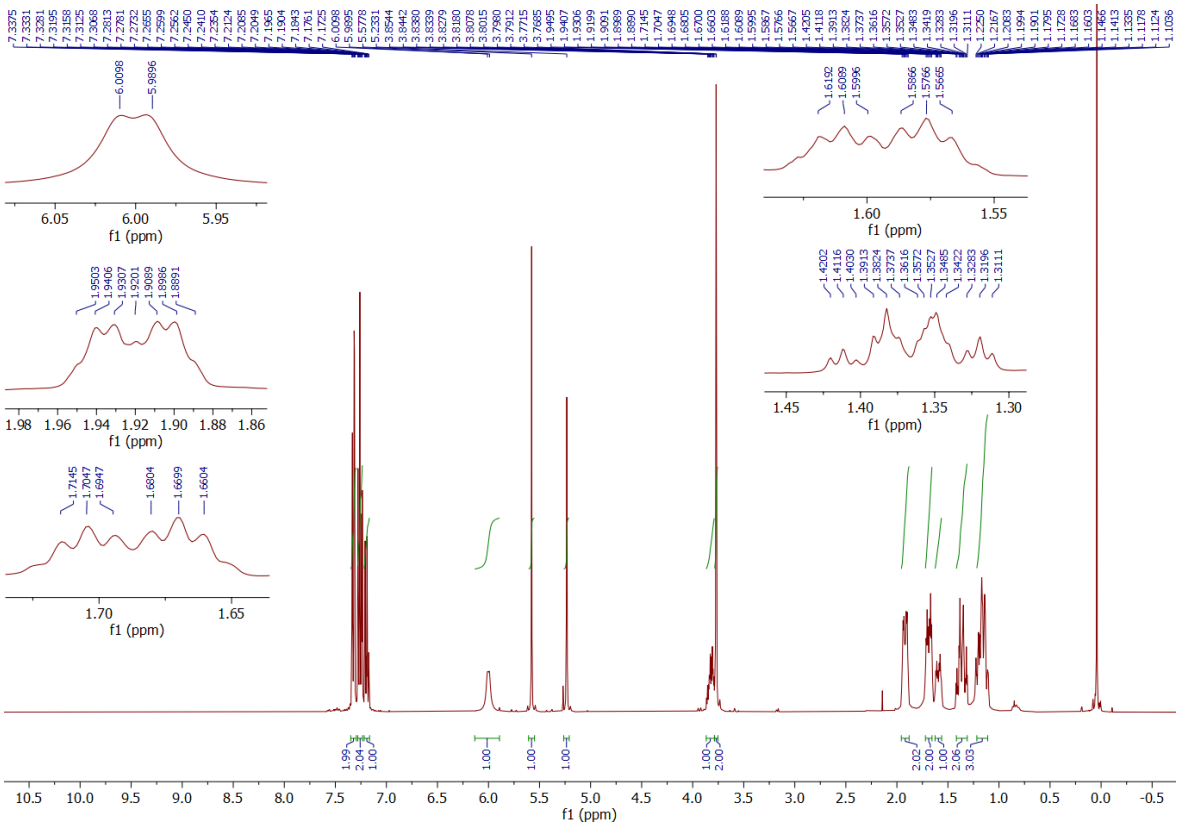


Figure SI87: *N*-Cyclohexyl-2-[(phenylsulfanyl)methyl]acrylamide $^1$H NMR spectrum ($CDCl_3$, 400 MHz, 298 K).

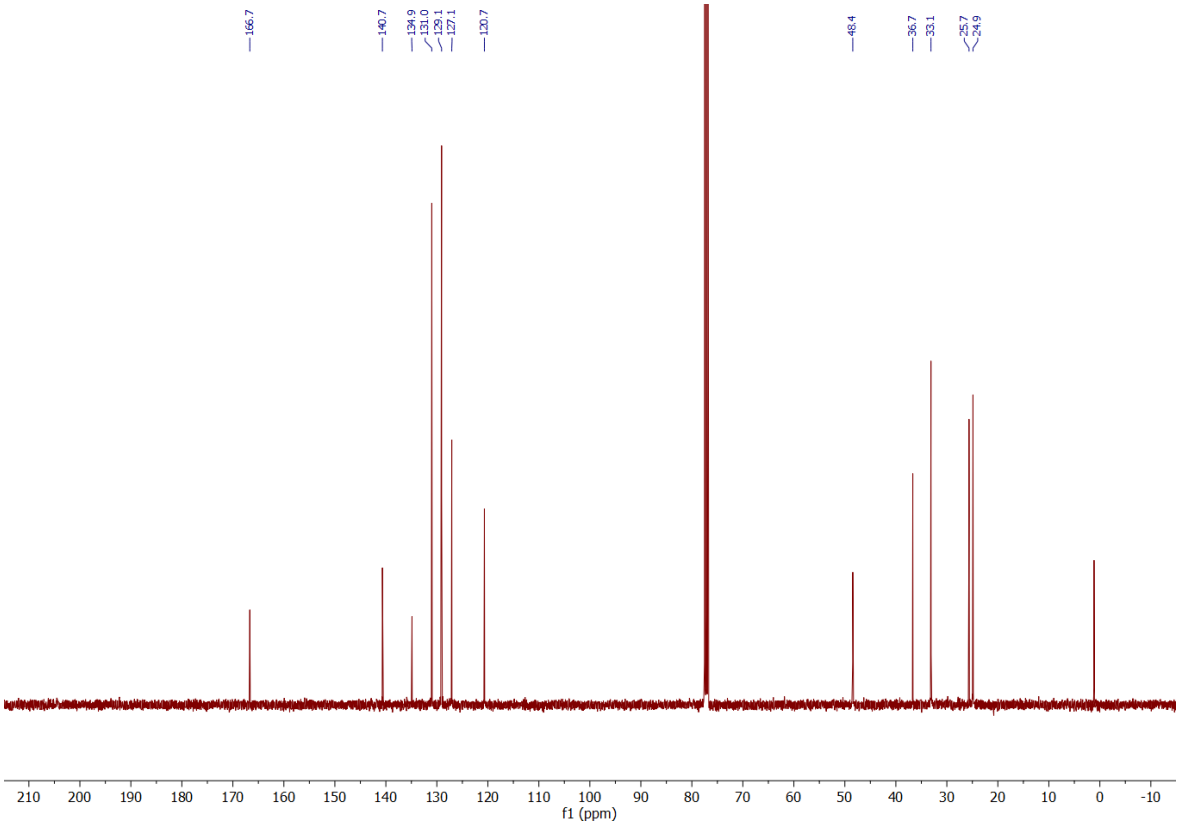


Figure SI88: *N*-Cyclohexyl-2-[(phenylsulfanyl)methyl]acrylamide $^{13}C$ NMR spectrum ($CDCl_3$, 100 MHz, 298 K).

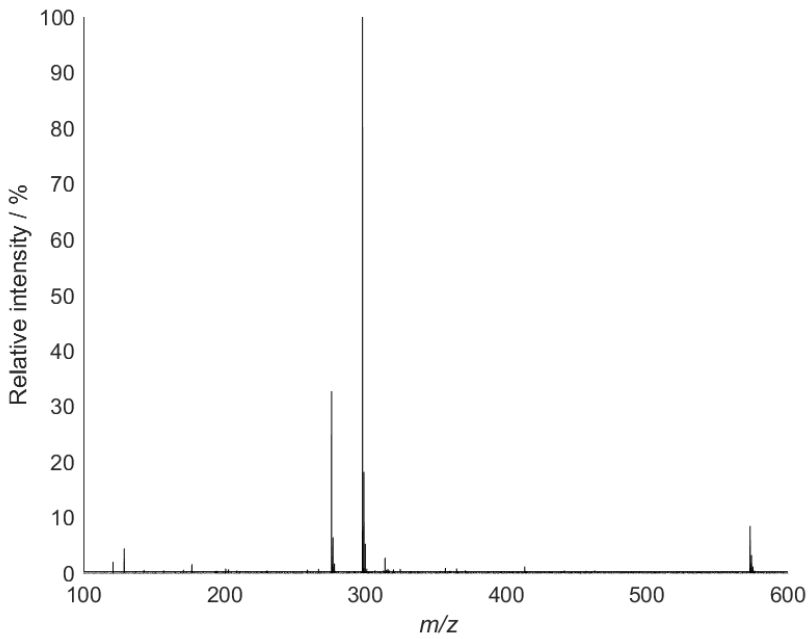


Figure SI89: *N*-Cyclohexyl-2-[(phenylsulfanyl)methyl]acrylamide mass spectrum (Pos ESI).

## SI4.2.4. Kinetics experiments and kinetic modelling

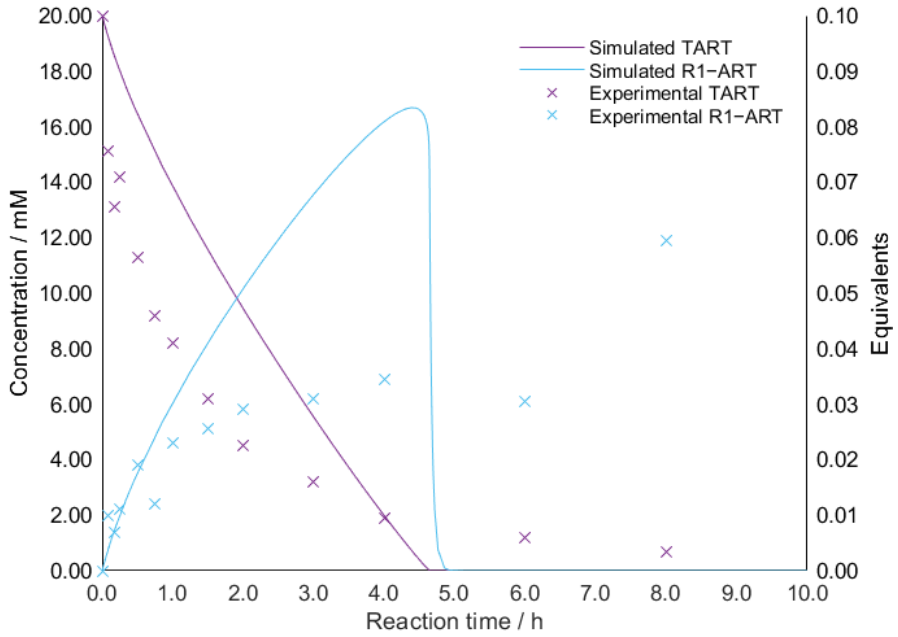


Figure SI90: Experimental data (scatter, 11.5.2.7) and fitted simulation (lines, 11.10.2) of TART trapping of radical thiol-ene addition, using thiophenol and styrene as substrates and TART (purple) and R1−ART (sky blue). Initiation rate constant used in the simulation was informed from experimental data.

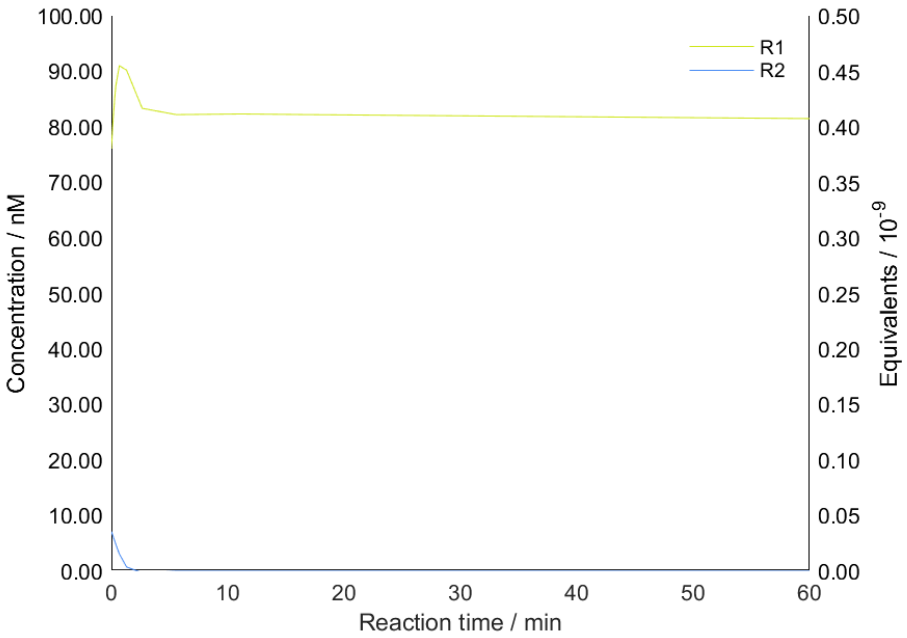


Figure SI91: Kinetical model produced for radical thiol-ene addition, replicating conditions of TART trapping of thiol-ene addition (11.5.2.8) but in absence of TART, using thiophenol and styrene as substrates, showing [R1] and [R2], indicating R1 was the radical resting state.

## SI4.2.5. Effect of different thiols on reaction kinetics

Table SI11: Fragments identified from tandem MS of peak corresponding to $[R1-ART+H]^+$ (*m/z* 290.158) from TART trapping of radical thiol-ene addition, using benzyl mercaptan (S2.1) and styrene (S3.1) as substrates after 72 h (11.5.2.8). Systematic *m/z* error = -0.0010; random *m/z* error = ±0.0004.

| Species | | Predicted *m/z* | Intensity relative to parent ion / % |
|---|---|---|---|
| $[R1-ART+H]^+$ | 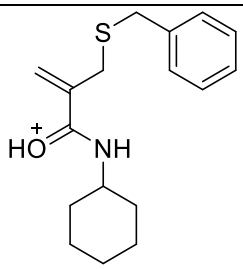 | 290.1578 | 100 |
| Fragments | 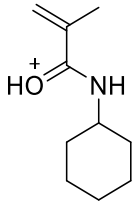 | 168.1388 | 16.6 |
| | 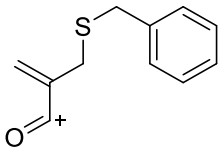 | 191.0531 | 11.9 |

Table SI12: Fragments identified from tandem MS of peak corresponding to $[R2-ART+H]^+$ (*m/z* 394.220) from TART trapping of radical thiol-ene addition, benzyl mercaptan (S2.1) and styrene (S3.1) as substrates after 72 h (11.5.2.8). Systematic *m/z* error = -0.0013; random *m/z* error = ±0.0004.

| Species | | Predicted *m/z* | Intensity relative to parent ion / % |
|---|---|---|---|
| $[R2-ART+H]^+$ | 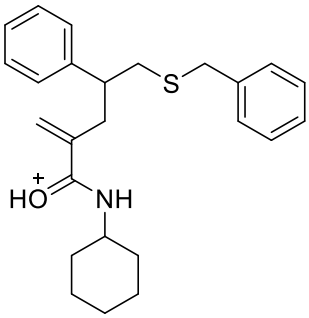 | 394.2204 | 100 |
| Fragments | 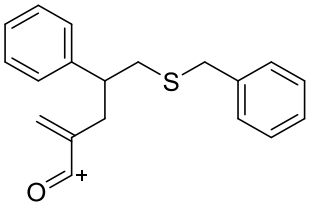 | 295.1157 | 28.8 |

Table SI13: Fragments identified from tandem MS of peak corresponding to $[R1-ART+H]^+$ (*m/z* 276.142) from TART trapping of radical thiol-ene addition, using thiophenol (S2.2) and styrene (S3.1) as substrates after 24 h (11.5.2.8). Systematic *m/z* error = -0.0007; random *m/z* error = ±0.0002.

| Species | | Predicted *m/z* | Intensity relative to parent ion / % |
|---|---|---|---|
| $[R1-ART+H]^+$ | 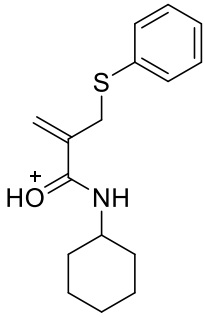 | 276.1422 | 100 |
| Fragments | 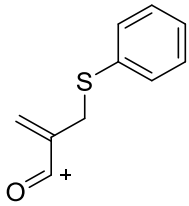 | 177.0374 | 78.0 |
| | 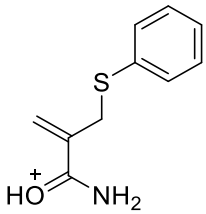 | 194.0640 | 15.6 |
| | 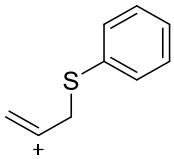 | 149.0425 | 11.5 |

Table SI14: Fragments identified from tandem MS of peak corresponding to $[R2-ART+H]^+$ (*m/z* 380.205) from TART trapping of radical thiol-ene addition, using thiophenol (S2.2) and styrene (S3.1) as substrates after 24 h (11.5.2.8). Systematic *m/z* error = -0.0009; random *m/z* error = ±0.0003.

| Species | | Predicted *m/z* | Intensity relative to parent ion / % |
|---|---|---|---|
| $[R2-ART+H]^+$ | 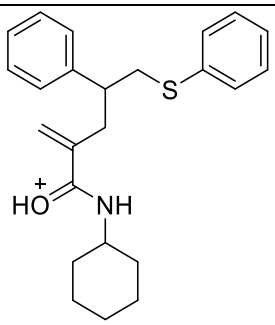 | 380.2048 | 100 |
| Fragments | 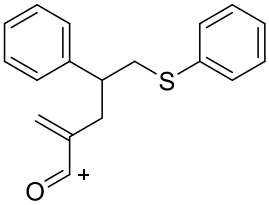 | 281.1000 | 158 |

| | | | |
|---|---|---|---|
| Fragments | 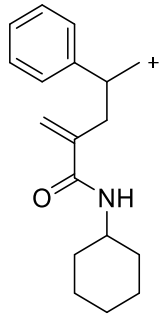 | 270.1858 | 80.5 |

Table SI15: Fragments identified from tandem MS of peak corresponding to $[R1-ART+H]^+$ (*m/z* 306.153) from TART trapping of radical thiol-ene addition, using 3-methoxythiophenol (S2.3) and styrene (S3.1) as substrates after 24 h (11.5.2.8). Systematic *m/z* error = -0.0007; random *m/z* error = ±0.0002.

| Species | | Predicted *m/z* | Intensity relative to parent ion / % |
|---|---|---|---|
| $[R1-ART+H]^+$ | 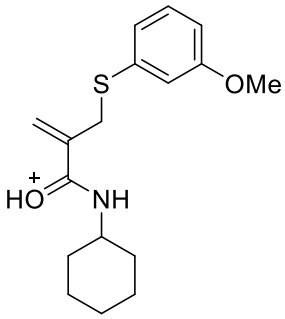 | 306.1528 | 100 |
| Fragments | 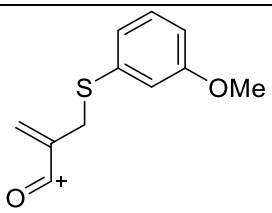 | 207.0480 | 84.0 |
| | 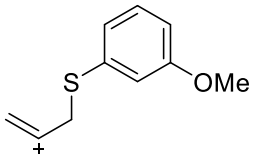 | 179.0531 | 13.7 |
| | 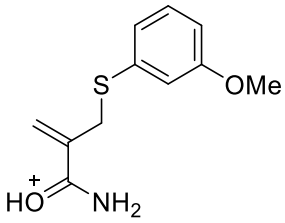 | 224.0745 | 5.42 |

Table SI16: Fragments identified from tandem MS of peak corresponding to [R1−ART+H]$^+$ (*m/z* 282.189) from TART trapping of radical thiol-ene addition, using cyclohexanethiol (S2.4) and styrene (S3.1) as substrates after 72 h (11.5.2.8). Systematic *m/z* error = -0.0010; random *m/z* error = ±0.0004.

| Species | | Predicted *m/z* | Intensity relative to parent ion / % |
|---|---|---|---|
| [R1−ART+H]$^+$ | 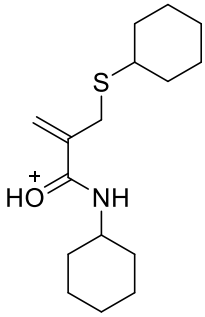 | 282.1891 | 100 |
| Fragments | 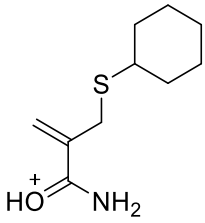 | 200.1109 | 74.7 |
| | 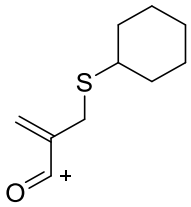 | 183.0844 | 15.9 |
| | 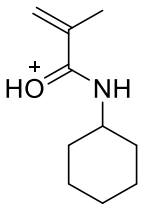 | 168.1388 | 14.4 |

Table SI17: Fragments identified from tandem MS of peak corresponding to [R2−ART+H]$^+$ (*m/z* 386.252) from TART trapping of radical thiol-ene addition, using cyclohexanethiol (S2.4) and styrene (S3.1) as substrates after 72 h (11.5.2.8). Systematic *m/z* error = -0.0010; random *m/z* error = ±0.0002.

| Species | | Predicted *m/z* | Intensity relative to parent ion / % |
|---|---|---|---|
| [R2−ART+H]$^+$ | 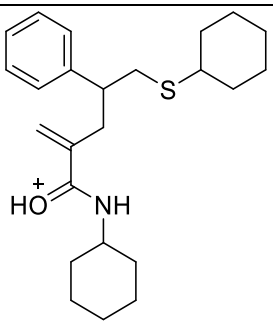 | 386.2517 | 100 |

| | | | |
|---|---|---|---|
| Fragments | 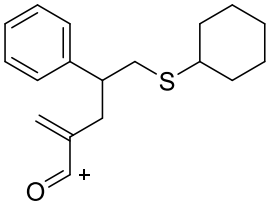 | 287.1470 | 61.9 |
| | 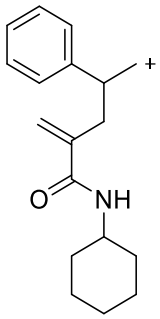 | 270.1858 | 29.7 |

Table SI18: Fragments identified from tandem MS of peak corresponding to $[R1-ART+H]^+$ (*m/z* 334.148) from TART trapping of radical thiol-ene addition, using methyl thiosalicylate (S2.5) and styrene (S3.1) as substrates after 24 h (11.5.2.8). Systematic *m/z* error = -0.0007; random *m/z* error = ±0.0002.

| Species | | Predicted *m/z* | Intensity relative to parent ion / % |
|---|---|---|---|
| $[R1-ART+H]^+$ | 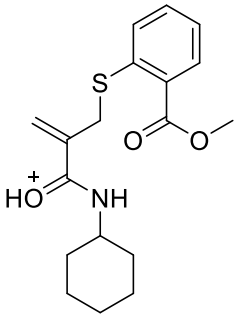 | 334.1477 | 100 |
| Fragments | 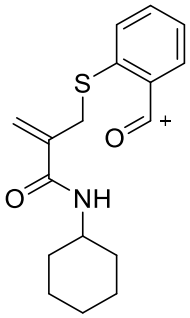 | 302.1215 | 242 |
| | 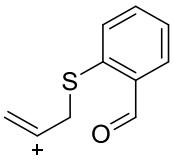 | 177.0374 | 29.5 |
| | 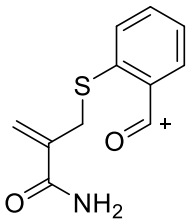 | 220.0432 | 20.4 |

Table SI19: Fragments identified from tandem MS of peak corresponding to $[R1-ART+H]^+$ (*m/z* 256.173) from TART trapping of radical thiol-ene addition, using $^t$BuSH (S2.6) and styrene (S3.1) as substrates after 72 h (11.5.2.8). Systematic *m/z* error = -0.0009; random *m/z* error = ±0.0003.

| Species | | Predicted *m/z* | Intensity relative to parent ion / % |
|---|---|---|---|
| $[R1-ART+H]^+$ | 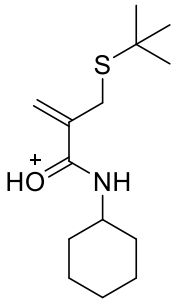 | 256.1735 | 100 |
| Fragments | 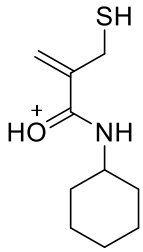 | 200.1109 | 124 |

Table SI20: Fragments identified from tandem MS of peak corresponding to $[R2-ART+H]^+$ (*m/z* 360.236) from TART trapping of radical thiol-ene addition, using $^t$BuSH (S2.6) and styrene (S3.1) as substrates after 72 h (11.5.2.8). Systematic *m/z* error = -0.0011; random *m/z* error = ±0.0004.

| Species | | Predicted *m/z* | Intensity relative to parent ion / % |
|---|---|---|---|
| $[R2-ART+H]^+$ | 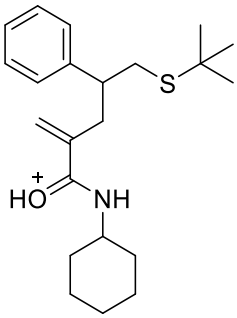 | 360.2361 | 100 |
| Fragments | 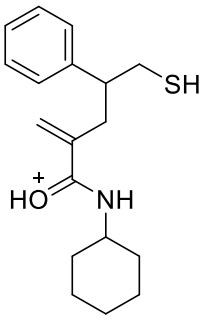 | 304.1735 | 77.5 |

| | | | |
|---|---|---|---|
| Fragments | 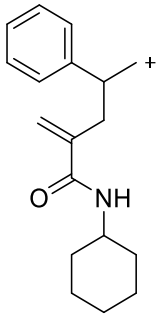 | 270.1858 | 6.26 |
| | 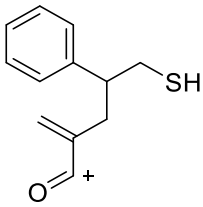 | 205.0687 | 4.73 |

## SI4.2.6. Effect of different alkenes on reaction kinetics

Table SI21: Species identified from TART trapping of Ru-photocatalysed radical thiol-ene addition under standard conditions after 2 h, using benzyl mercaptan (S2.1) and different alkenes as substrates, CHANT as TART and MS for characterisation (11.5.2.9). Cl containing species are shown with $^{35}$Cl only. Systematic *m/z* error = -0.0005; random error *m/z* = ±0.0008; 100% intensity = 2.11×10$^{9}$ absolute count.

| Alkenes S3. | | 1 | 2 | 3 | 4 | 5 | 6 |
|---|---|---|---|---|---|---|---|
| Species | | Intensity relative to unreacted TART standard / % | | | | | |
| TART | [CHANT+H]$^+$ | 111 | 56.7 | 35.3 | 13.6 | 48.1 | 56.5 |
| Trapped radicals | [R1−ART+H]$^+$ | 0.018 | 0.309 | 0.210 | 0.913 | 0.072 | 0.178 |
| | [R1−ART+Na]$^+$ | 0.238 | 2.46 | 2.04 | 7.83 | 0.616 | 1.26 |
| | [R1−TEMPO+H]$^+$ | 0 | 0 | 0 | 0.005 | 0 | 0 |
| | [R2−ART+H]$^+$ | 0.091 | 0.003 | 0 | 0.040 | 0 | 0 |
| | [R2−ART+Na]$^+$ | 0 | 0 | 0 | 0 | 0 | 0 |
| | [R2−TEMPO+H]$^+$ | 1.45 | 0.017 | 0.013 | 0.112 | 0.057 | 0.043 |
| Other trapped radicals | [R1−ART+S2+H]$^+$ (thiol-ene addition) | 0 | 0.037 | 0.026 | 0 | 0.003 | 0.013 |
| | [R1−ART+S2+Na]$^+$ (thiol-ene addition) | 0 | 0.039 | 0.047 | 0.347 | 0.002 | 0.011 |
| Products | [P2+H]$^+$ | 0.016 | 0.007 | 0.001 | 0.011 | 0 | 0.019 |
| | [P2+Na]$^+$ | 0.018 | 0 | 0 | 0.038 | 0 | 0.191 |
| Other products | [TART+S2+H]$^+$ (thiol-ene addition) | 0.426 | 5.58 | 3.57 | 13.3 | 0.979 | 2.53 |

Table SI22: Fragments identified from tandem MS of peak corresponding to [R1−ART+H]$^+$ (*m/z* 290.158) from TART trapping of radical thiol-ene addition, using benzyl mercaptan (S2.1) and different alkenes (S3.1-S3.6) as substrates after 24 h (11.5.2.9). Systematic *m/z* error = -0.0009; random *m/z* error = ±0.0004.

| Species | | Predicted *m/z* | Intensity relative to parent ion / % | | | | | |
|---|---|---|---|---|---|---|---|---|
| | | | S3.1 | S3.2 | S3.3 | S3.4 | S3.5 | S3.6 |
| [R1−ART+H]$^+$ | 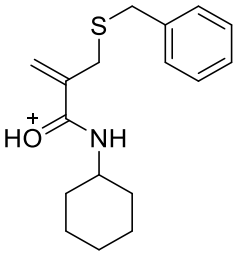 | 290.1578 | 100 | 100 | 100 | 100 | 100 | 100 |

| | | | | | | | | |
|---|---|---|---|---|---|---|---|---|
| Fragments | 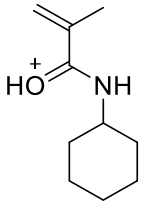 | 168.1388 | 18.0 | 19.3 | 21.4 | 19.3 | 15.7 | 21.3 |
| | 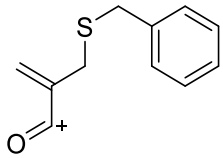 | 191.0531 | 11.5 | 15.5 | 19.3 | 14.2 | 14.6 | 11.8 |
| | 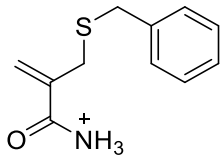 | 208.0796 | 0 | 0 | 6.17 | 0 | 0 | 0 |

## SI4.3. Radical dearomative spirocyclisation

Table SI23: Fragments identified from tandem MS of peak corresponding to $[R1-ART+H]^+$ (*m/z* 256.173) from TART trapping of radical dearomative spirocyclisation, using $^t$BuSH (S2.6) as substrate (11.5.3.2). Systematic *m/z* error = -0.0008; random *m/z* error = ±0.0003.

| Species | | Predicted *m/z* | Intensity relative to parent ion / % |
|---|---|---|---|
| $[R1-ART+H]^+$ | 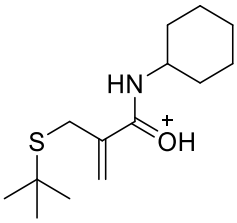 | 256.1735 | 100 |
| Fragments | 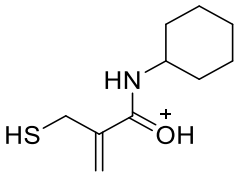 | 200.1109 | 1130 |
| | 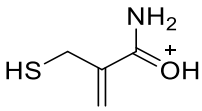 | 118.0327 | 37.1 |

Table SI24: Fragments identified from tandem MS of peak corresponding to $[R2/R3-ART+H]^+$ (*m/z* 529.289) from TART trapping of radical dearomative spirocyclisation, using $^t$BuSH (S2.6) as substrate (11.5.3.2). Systematic *m/z* error = -0.0012; random *m/z* error = ±0.0005.

| Species | | Predicted *m/z* | Intensity relative to parent ion / % |
|---|---|---|---|
| $[R3-ART+H]^{+a}$ | 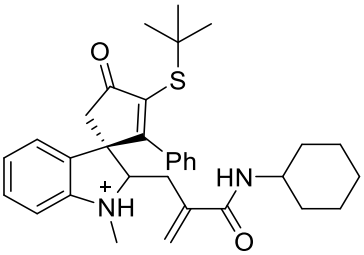 | 529.2889 | 100 |

| | | | |
|---|---|---|---|
| | 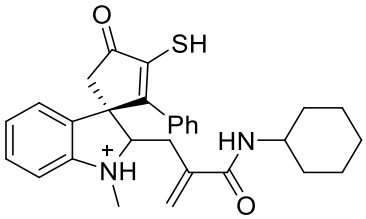 | 473.2263 | 50.7 |
| Fragments | 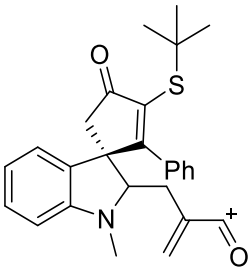 | 430.1841 | 34.5 |
| | 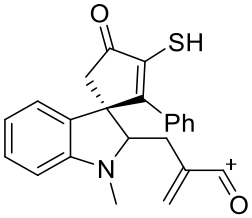 | 374.1215 | 30.2 |

[a]All peaks could equally be assigned to [R2−ART+H]$^+$ fragments.

# SI5. Biochemistry

## SI5.1. Alcohols

Table SI25: Fragments identified from tandem MS of peak corresponding to $[R1.1-ART+H]^+$ (*m/z* 219.134) from TART trapping of •OH-initiated methanol degradation, using DEADANT as TART (11.6.2). Systematic *m/z* error = -0.0008; random *m/z* error = ±0.0003.

| Species | | Predicted *m/z* | Intensity relative to parent ion / % |
|---|---|---|---|
| $[R1.1-ART+H]^+$ | 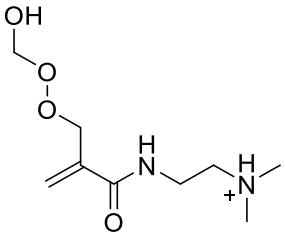 | 219.1345 | 100 |
| Fragments | 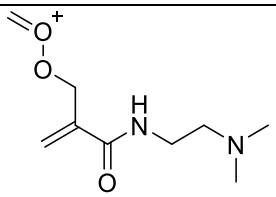 | 201.1239 | 121 |
| | 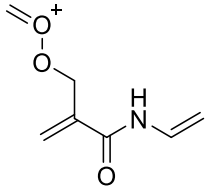 | 156.0661 | 85.0 |
| | 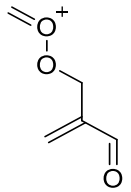 | 115.0871 | 53.1 |
| | 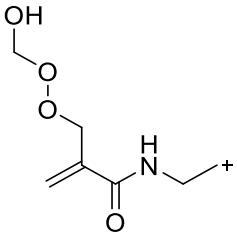 | 174.0766 | 26.6 |

Table SI26: Fragments identified from tandem MS of peak corresponding to [R1.1.1.1.1−ART+H]$^+$ (*m/z* 217.119) from TART trapping of •OH-initiated methanol degradation, using DEADANT as TART (11.6.2). Systematic *m/z* error = -0.0007; random *m/z* error = ±0.0002.

| Species | | Predicted *m/z* | Intensity relative to parent ion / % |
|---|---|---|---|
| [R1.1.1.1.1−ART+H]$^+$ | 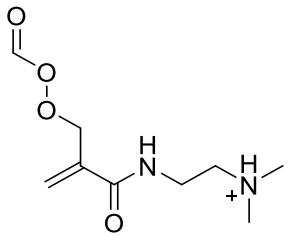 | 217.1188 | 100 |
| Fragments | 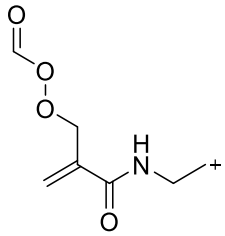 | 172.061 | 240 |
| | 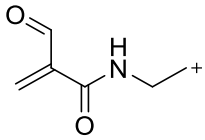 | 126.0555 | 99.2 |

Table SI27: Fragments identified from tandem MS of peak corresponding to [R1−ART+H]$^+$ (*m/z* 229.192) from TART trapping of •OH-initiated $^t$BuOH degradation, using DEADANT as TART (11.6.2). Systematic *m/z* error = -0.0007; random *m/z* error = ±0.0002.

| Species | | Predicted *m/z* | Intensity relative to parent ion / % |
|---|---|---|---|
| [R1−ART+H]$^+$ | 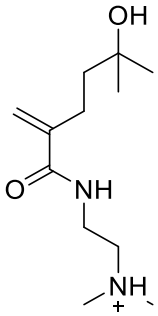 | 229.1916 | 100 |
| Fragments | 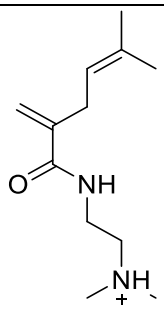 | 211.1810 | 48.9 |

| | | | |
|---|---|---|---|
| Fragments | 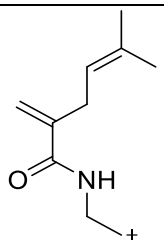 | 166.1232 | 11.9 |

Table SI28: Fragments identified from tandem MS of peak corresponding to $[R1.1-ART+H]^+$ (*m/z* 261.181) from TART trapping of •OH-initiated $^t$BuOH degradation, using DEADANT as TART (11.6.2). Systematic *m/z* error = -0.0008; random *m/z* error = ±0.0003.

| Species | | Predicted *m/z* | Intensity relative to parent ion / % |
|---|---|---|---|
| $[R1.1.1-ART+H]^+$ | 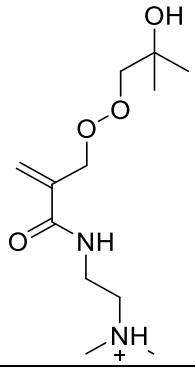 | 261.1814 | 100 |
| Fragments | 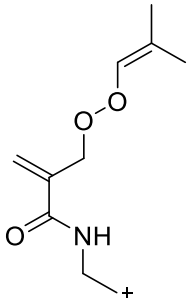 | 198.1130 | 55.3 |
| | 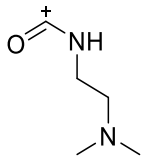 | 115.0871 | 40.4 |
| | 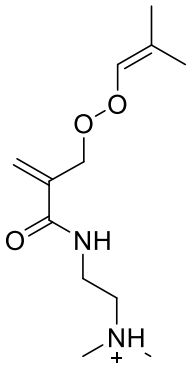 | 243.1709 | 37.8 |

Table SI29: Fragments identified from tandem MS of peak corresponding to $[R1.1.1-ART+H]^+$ (*m/z* 241.187) from TART trapping of •OH-initiated $^t$BuOH degradation, using DEADANT as TART (11.6.2). Systematic *m/z* error = -0.0006; random *m/z* error = ±0.0003.

| Species | | Predicted *m/z* | Intensity relative to most intense fragment / % |
|---|---|---|---|
| $[R1.1.1-ART+H]^+$ | 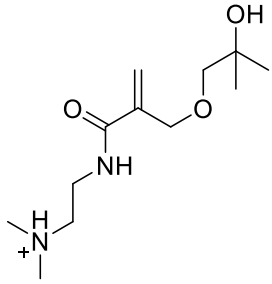 | 241.1865 | 0[a] |
| Fragments | 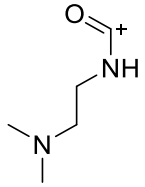 | 115.0871 | 100 |
| | 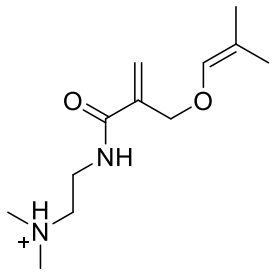 | 227.1759 | 86.7 |
| | 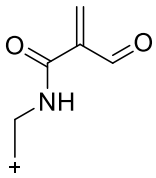 | 126.0555 | 44.5 |
| | 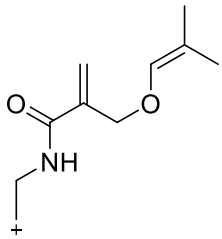 | 182.1181 | 41.4 |

[a]Parent ion cleanly isolated prior to CID, but CID caused total peak fragmentation.

## SI5.2. Nucleobases

Table SI30: Fragments identified from tandem MS of peak corresponding to $[R1.1-ART+H]^+$ (*m/z* 331.162) from TART trapping of •OH-initiated thymine degradation, using DEADANT as TART (11.6.4). Systematic *m/z* error = -0.0008; random *m/z* error = ±0.0003.

| Species | | Predicted *m/z* | Intensity relative to parent ion / % |
|---|---|---|---|
| $[R1.1-ART+H]^+$ | 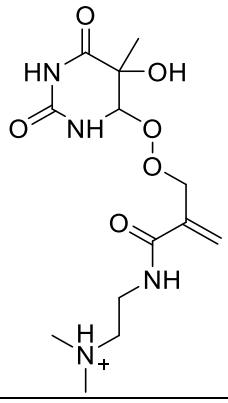 | 331.1618 | 100 |
| Fragments | 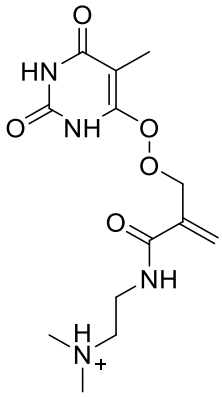 | 313.1512 | 78.8 |
| | 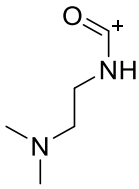 | 115.0871 | 57.3 |
| | 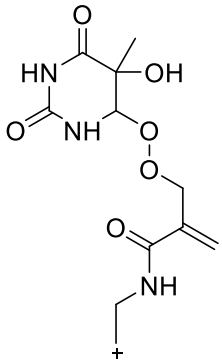 | 286.1039 | 43.9 |

| | | | |
|---|---|---|---|
| Fragments | 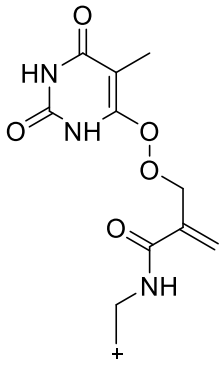 | 268.0933 | 20.5 |
| | 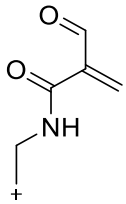 | 126.0555 | 11.1 |

[a]All peaks could equally be assigned to [R2.1−ART+H]$^+$, [hydroxylated R1.1.1−ART+H]$^+$ and [hydroxylated R2.1.1−ART+H]$^+$ fragments.

## SI5.3. Dipeptides

Table SI31: D exchanges observed for MS peaks corresponding to TART-trapped radicals from $D_2O$ exchange of •OH-initiated Ac-Gly-Gly-OH degradation, using DEADANT as TART and MS for characterisation (Pos ESI-MS, 4.2.2.2). Systematic *m/z* error = 0.0000; random *m/z* error = ±0.0008.

| Species | Predicted D shift | Proportion of total intensity of all D-shifted species / % | | | | |
|---|---|---|---|---|---|---|
| | | 3D | 4D | 5D | 6D | 7D |
| R1:R3−ART | **5D** | 0 | 9.7 | **90.3** | 0 | 0 |
| R1.1:R3.1−ART | **5D** | 0 | 1.3 | 17.6 | **81.1** | 0 |
| R1.1.1:R3.1.1−ART | **5D** | 0 | 14.6 | **85.4** | 0 | 0 |

# SI6. Alkene ozonolysis

## SI6.1. α-Pinene

### SI6.1.1. Optimisation

#### SI6.1.1.1. TART phase

Additives dodecamethylpentasiloxane (A.1), Galden™ HT270 (A.2), $[C_4mim]^+[Tf_2N]^-$ (A.3) and $[C_4pyrr]^+[Tf_2N]^-$ (A.4) were used for TART trapping of α-pinene ozonolysis using solid supported TART (Table SI32).

Table SI32: Species identified from TART trapping of α-pinene ozonolysis, using CHANT solution or solid supported CHANT with different additives and MS for characterisation (11.7.3.2). Systematic *m/z* error = -0.0006; random *m/z* error = ±0.0003; 100% intensity = $5.08\times10^9$ absolute count.

| Species | | Intensity relative to unreacted TART standard / % | | | | | |
|---|---|---|---|---|---|---|---|
| | | Solution | Functionalised celite/ | | | | |
| | | | - | A.1 | A.2 | A.3 | A.4 |
| TART | [CHANT+H]$^+$ | 19.7 | 11.2 | 20.0 | 7.14 | 17.4 | 18.0 |
| Trapped radicals | [R1.1/R1.2−ART+Na]$^+$ | 0.047 | 0.016 | 0 | 0.026 | 0.002 | 0.003 |
| | [R1.1.1/R1.2.1−ART+Na]$^+$ | 0.040 | 0.050 | 0 | 0.119 | 0.005 | 0.005 |
| | [R2.1−ART+Na]$^+$ | 0.053 | 0.005 | 0 | 0.009 | 0 | 0 |
| | [R2.1.1−ART+Na]$^+$ | 0.029 | 0.008 | 0 | 0.014 | 0 | 0 |
| Products | [Pinaldehyde+Na]$^+$ | 2.81 | 0.202 | 0.001 | 0.278 | 0.055 | 0.058 |
| | [Pinonic acid+Na]$^{+a}$ | 0.676 | 0.286 | 0 | 0.381 | 0.074 | 0.071 |
| | [P1.1.3/P1.2.3+Na]$^{+a}$ | 0.676 | 0.286 | 0 | 0.381 | 0.074 | 0.071 |
| | [P1.2.4+Na]$^+$ | 0.005 | 0.017 | 0 | 0.022 | 0.003 | 0.003 |
| | [P2.1.3+Na]$^+$ | 0.105 | 0.010 | 0 | 0.013 | 0.001 | 0.001 |
| | [P2.1.4+Na]$^+$ | 0.071 | 0.019 | 0 | 0.026 | 0.006 | 0.004 |

[a]Other table entries have predicted species with same *m/z*.

#### SI6.1.1.2. Functionality of TART, solvent and additives

Table SI33: Species identified from TART trapping of α-pinene ozonolysis, conducted using different TARTs and MS for characterisation (11.7.3). Systematic *m/z* error = -0.0006; random *m/z* error = ±0.0012; 100% intensity = $5.08\times10^9$ absolute count.

| Species | | Intensity relative to unreacted CHANT standard / % | | | |
|---|---|---|---|---|---|
| | | Grantham TART[a] | CHANT[a] | DEADANT[b] | TREADANT[c] |
| TART | [CHANT+H]$^+$ | 0.055 | 11.9 | 0.034 | 1.066 |
| Trapped radicals | [R1.1/R1.2−ART+Na/H/0]$^+$ | 0.738 | 0.024 | 0.007 | 0 |
| | [R1.1.1/R1.2.1−ART+Na/H/0]$^+$ | 0.759 | 0.053 | 0.011 | 0 |
| | [R2.1−ART+Na/H/0] | 1.10 | 0.055 | 0 | 0 |
| | [R2.1.1−ART+Na+Na/H/0]$^+$ | 0.558 | 0.100 | 0.005 | 0.005 |
| Products | [Pinaldehyde+Na]$^+$ | 1.93 | 2.04 | 1.58 | 1.48 |
| | [Pinonic acid+Na]$^{+d}$ | 2.59 | 1.91 | 4.82 | 1.07 |
| | [P1.1.3/P1.2.3+Na]$^{+d}$ | 2.59 | 1.91 | 4.82 | 1.07 |
| | [P1.2.4+Na]$^+$ | 0.020 | 0.017 | 0.010 | 0.007 |
| | [P2.1.3+Na]$^+$ | 0.117 | 0.091 | 0.122 | 0.053 |
| | [P2.1.4+Na]$^+$ | 0.194 | 0.140 | 0.024 | 0.032 |

[a]TART-trapped radicals shown as sodiated MS adducts. [b]TART-trapped radicals shown as protonated MS adducts. [c]TART-trapped radicals pre-charged and hence have no (0) cation. [d]Other table entries have predicted species with same *m/z*.

Table SI34: Species identified from TART trapping of α-pinene ozonolysis, using different TARTs dissolved in different solvents and MS for characterisation (11.7.3). Systematic *m/z* error = -0.0006; random *m/z* error = ±0.0006; 100% intensity = $5.08\times10^9$ absolute count.

| Species | | Intensity relative to unreacted CHANT standard / % | | | | |
|---|---|---|---|---|---|---|
| | | CHANT[a]/ | | DEADANT[b]/ | | |
| | | MeCN | DMF | MeCN | DMF | $H_2O$ |
| TART | [CHANT+H]$^+$ | 19.7 | 13.4 | 0 | 0 | 0.069 |
| Trapped radicals | [R1.1/R1.2−ART+Na/H]$^+$ | 0.047 | 0 | 0.002 | 0.001 | 0.001 |
| | [R1.1.1/R1.2.1−ART+Na/H]$^+$ | 0.040 | 0.001 | 0 | 0 | 0.002 |
| | [R2.1−ART+Na/H]$^+$ | 0.053 | 0 | 0 | 0 | 0 |
| | [R2.1.1−ART+Na/H]$^+$ | 0.029 | 0.004 | 0 | 0 | 0 |
| Products | [Pinaldehyde+Na]$^+$ | 2.81 | 0.107 | 1.12 | 0.669 | 0.078 |
| | [Pinonic acid+Na]$^{+c}$ | 0.676 | 0.024 | 0.291 | 0.321 | 0.022 |
| | [P1.1.3/P1.2.3+Na]$^{+c}$ | 0.676 | 0.024 | 0.291 | 0.321 | 0.022 |
| | [P1.2.4+Na]$^+$ | 0.005 | 0 | 0.002 | 0.003 | 0 |
| | [P2.1.3+Na]$^+$ | 0.105 | 0 | 0.007 | 0.037 | 0 |
| | [P2.1.4+Na]$^+$ | 0.071 | 0.002 | 0.025 | 0.027 | 0.002 |

[a]TART-trapped radicals shown as sodiated MS adducts. [b]TART-trapped radicals shown as protonated MS adducts. [c]Other table entries have predicted species with same *m/z*.

Table SI35: Species identified from TART trapping of α-pinene ozonolysis, using DEADANT as TART dissolved in different solvents and MS for characterisation (11.7.3). Systematic *m/z* error = -0.0006; random *m/z* error = ±0.0008; 100% intensity = $5.08\times10^9$ absolute count.

| Species | | Intensity relative to unreacted CHANT standard / % | | | | |
|---|---|---|---|---|---|---|
| | | MeCN/ | | $H_2O$/ | | |
| | | - | TFA | - | TFA | AcOH/ NaOAc |
| TART | [CHANT+H]$^+$ | 0.028 | 1.28 | 0.069 | 19.7 | 18.8 |
| Trapped radicals | [R1.1/R1.2−ART+Na]$^+$ | 0.014 | 0.004 | 0.001 | 0.001 | 0.003 |
| | [R1.1.1/R1.2.1−ART+Na]$^+$ | 0.006 | 0.014 | 0.002 | 0.002 | 0.005 |
| | [R2.1−ART+Na]$^+$ | 0.000 | 0.003 | 0 | 0.004 | 0.006 |
| | [R2.1.1−ART+Na]$^+$ | 0.001 | 0.004 | 0 | 0.001 | 0.001 |
| Products | [Pinaldehyde+Na]$^+$ | 0.466 | 0.755 | 0.078 | 1.65 | 2.16 |
| | [Pinonic acid+Na]$^{+a}$ | 0.251 | 1.30 | 0.022 | 0.461 | 0.744 |
| | [P1.1.3/P1.2.3+Na]$^{+a}$ | 0.251 | 1.30 | 0.022 | 0.461 | 0.744 |
| | [P1.2.4+Na]$^+$ | 0.002 | 0.008 | 0 | 0.016 | 0.009 |
| | [P2.1.3+Na]$^+$ | 0.006 | 0.070 | 0 | 0.017 | 0.022 |
| | [P2.1.4+Na]$^+$ | 0.010 | 0.017 | 0.002 | 0.104 | 0.126 |

[a]Other table entries have predicted species with same *m/z*.

Table SI36: Species identified from TART trapping of α-pinene ozonolysis, conducted using Grantham TART and MS for characterisation (11.7.3). Systematic *m/z* error = -0.0006; random *m/z* error = ±0.0005; 100% intensity = $5.08\times10^9$ absolute count.

| Species | | Predicted *m/z* | Intensity relative to unreacted CHANT standard / % | |
|---|---|---|---|---|
| | | | Trapless control | Grantham TART |
| TART | $[CHANT+H]^+$ | 266.2484 | 0 | 0.055 |
| Trapped radicals | $[R1.1/R1.2-ART+Na]^+$ | 331.1885 | 0.686 | 0.738 |
| | $[R1.1.1/R1.2.1-ART+Na]^+$ | 315.1936 | 1.068 | 0.759 |
| | $[R2.1-ART+Na]$ | 303.1936 | 0.951 | 1.10 |
| | $[R2.1.1-ART+Na+Na]^+$ | 287.1987 | 0.267 | 0.558 |
| Products | $[Pinaldehyde+Na]^+$ | 191.1048 | 2.229 | 1.93 |
| | $[Pinonic\ acid+Na]^{+a}$ | 207.0997 | 2.549 | 2.59 |
| | $[P1.1.3/P1.2.3+Na]^{+a}$ | 207.0997 | 2.549 | 2.59 |
| | $[P1.2.4+Na]^+$ | 205.0841 | 0.022 | 0.020 |
| | $[P2.1.3+Na]^+$ | 179.1048 | 0.094 | 0.117 |
| | $[P2.1.4+Na]^+$ | 177.0891 | 0.234 | 0.194 |

[a]Other table entries have predicted species with same *m/z*.

### SI6.1.1.3. TART concentration

Table SI37: Species identified from TART trapping of α-pinene ozonolysis, using CHANT at different concentrations and MS for characterisation (11.7.3). Systematic *m/z* error = -0.0006; random *m/z* error = ±0.0009; 100% intensity = $5.08\times10^9$ absolute count.

| Species | | Predicted *m/z* | Intensity relative to unreacted TART standard / % | | |
|---|---|---|---|---|---|
| | | | 50 μM | 500 μM | 5000 μM |
| TART | $[CHANT+H]^+$ | 323.2698 | 40.7 | 21.8 | 56.6 |
| Trapped radicals | $[R1.1/R1.2-ART+Na]^+$ | 388.2100 | 0.012 | 0.013 | 0.012 |
| | $[R1.1.1/R1.2.1-ART+Na]^+$ | 372.2151 | 0.030 | 0.037 | 0.006 |
| | $[R2.1-ART+Na]^+$ | 360.2151 | 0.011 | 0.061 | 0.005 |
| | $[R2.1.1-ART+Na]^+$ | 344.2202 | 0.001 | 0.017 | 0 |
| Products | $[Pinaldehyde+Na]^+$ | 191.1048 | 0.529 | 1.45 | 0.217 |
| | $[Pinonic\ acid+Na]^{+a}$ | 207.0997[a] | 0.169 | 1.51 | 0.040 |
| | $[P1.1.3/P1.2.3+Na]^{+a}$ | 207.0997[a] | 0.169 | 1.51 | 0.040 |
| | $[P1.2.4+Na]^+$ | 205.0841 | 0.003 | 0.010 | 0 |
| | $[P2.1.3+Na]^+$ | 179.1048 | 0.007 | 0.059 | 0 |
| | $[P2.1.4+Na]^+$ | 177.0891 | 0.014 | 0.034 | 0.001 |

[a]Other table entries have predicted species with same *m/z*.

## SI6.1.2. Detailed results

### SI6.1.2.1. Formula Find

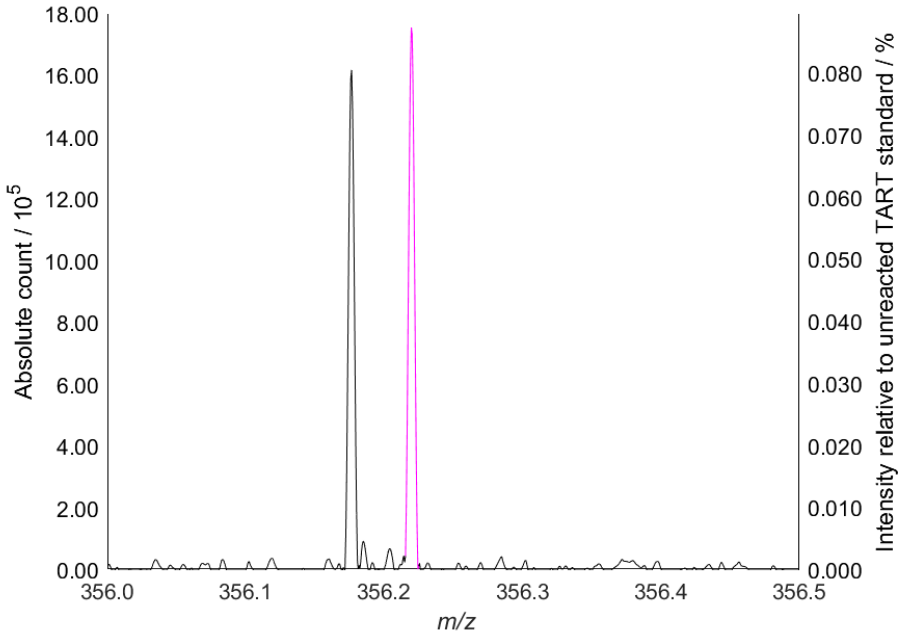


Figure SI92: Background corrected mass spectrum from TART trapping of α-pinene ozonolysis (11.7.2), showing the peak corresponding to $[R6/R7-ART+Na]^+$ (*m/z* 356.220, pink). 100% intensity = $2.01\times10^9$ absolute count.

### SI6.1.2.2. HPLC-MS

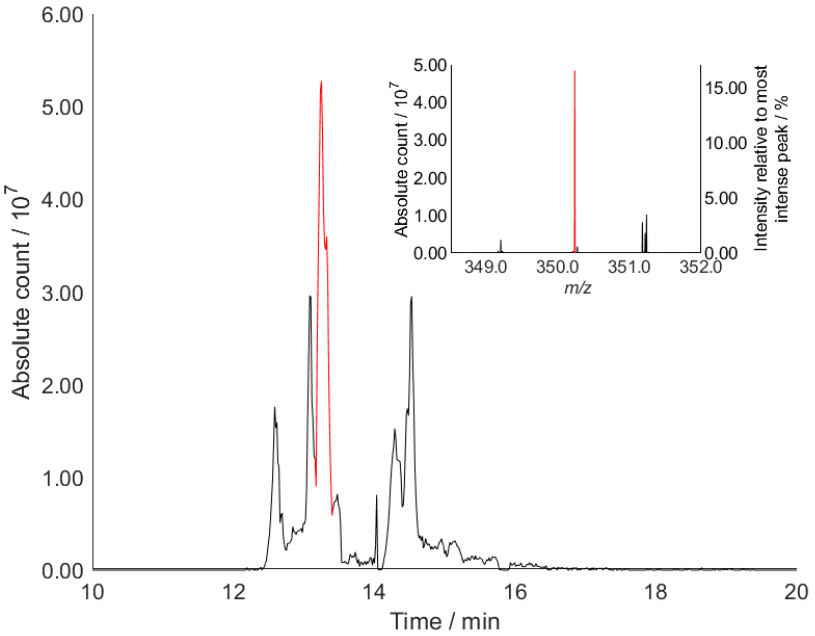


Figure SI93: HPLC-MS chromatogram and mass spectrum (inset) of peaks corresponding to R1.1.1/R1.2.1−ART (*m/z* 350.233±0.002 and *m/z* 372.215±0.002) from TART trapping of α-pinene ozonolysis (11.7.2). MS source was sent to waste between 13.5-14.0 min, to prevent injection of unreacted TART. Mass spectrum of $[R1.1.1/R1.2.1-ART+H]^+$ (red) is at time of maximum intensity (red).

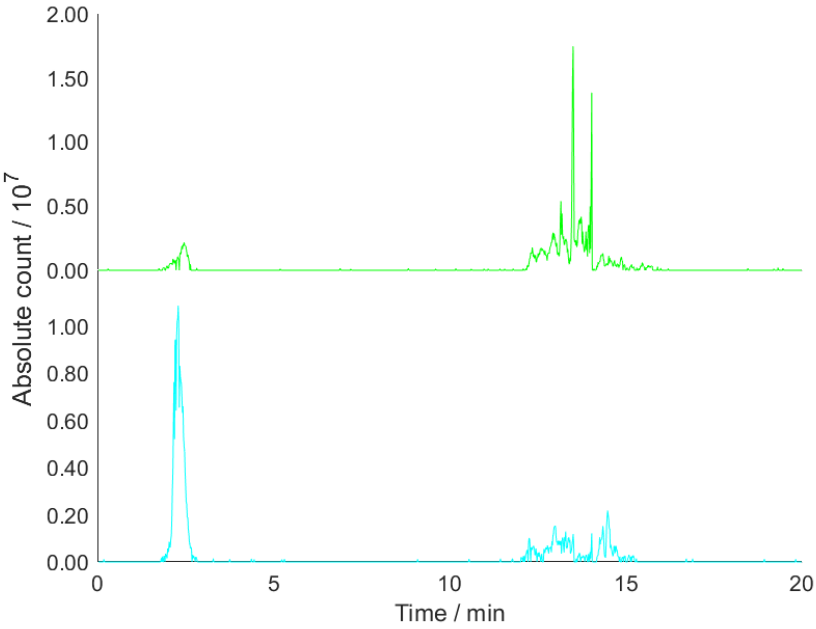


Figure SI94: HPLC-MS chromatograms of peaks corresponding to R5.1/R5.2−ART (*m/z* 384.239±0.002 and *m/z* 406.221±0.002, top, green) and $C_{10}H_{17}O_6$−ART (*m/z* 400.234±0.002 and *m/z* 422.216±0.002, bottom, light blue) from TART trapping of α-pinene ozonolysis (11.7.2). MS source was sent to waste between 13.5-14.0 min, to prevent injection of unreacted TART.

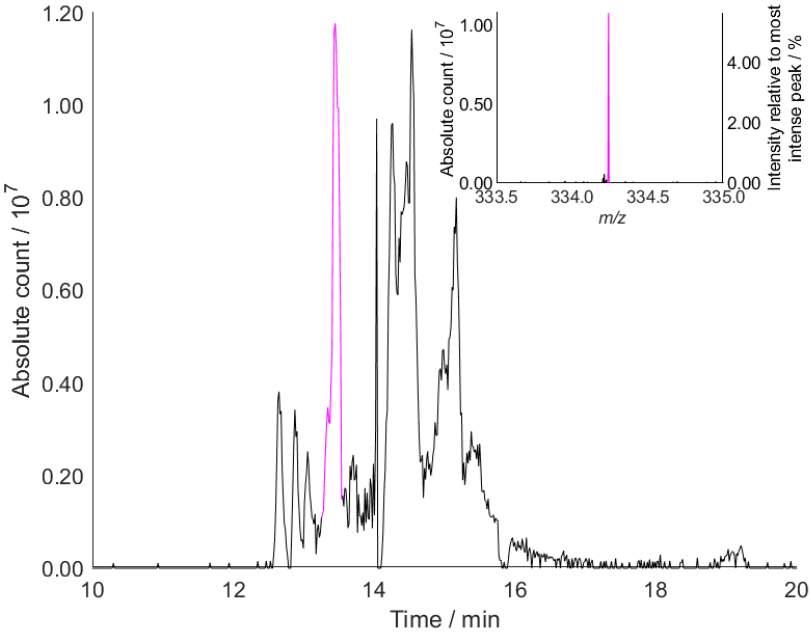


Figure SI95: HPLC-MS chromatogram and mass spectrum (inset) of peaks corresponding to R6/R7−ART (*m/z* 334.238±0.002 and *m/z* 356.220±0.002) from TART trapping of α-pinene ozonolysis (11.7.2). MS source was sent to waste between 13.5-14.0 min, to prevent injection of unreacted TART. Mass spectrum of $[R6/R7-ART+H]^+$ (pink) is at time of maximum intensity (pink).

### SI6.1.2.3. Oligomers

Table SI38: Five most intense peaks believed to correspond to monomeric products from TART trapping of α-pinene ozonolysis, obtained using the Formula Find programme. Molecular formula limits were set as $C_{1\text{-}10}H_{0\text{-}100}O_{0\text{-}15}Na_{0\text{-}1}$ and *m/z* limits 100-1000. Illogical molecular formulae were eliminated.

| Observed *m/z* | Intensity relative to unreacted TART standard / % | Corresponding molecular formula | Structure identified |
|---|---|---|---|
| 225.1098 | 1.74 | $C_{10}H_{18}O_4$ | P5.1.3/P5.2.3/P5.3.1.2/P5.3.2.2 |
| 191.1043 | 1.12 | $C_{10}H_{16}O_2$ | Pinaldehyde/P4.3/P6.2/P7.2 |
| 207.0993 | 0.242 | $C_{10}H_{16}O_3$ | Pinonic acid/P5.3.2.4 |
| 193.1200 | 0.109 | $C_{10}H_{18}O_2$ | P3.3 |
| 209.1152 | 0.104 | $C_{10}H_{18}O_3$ | P3.2/P4.2/P5.3.1.3/P5.3.2.3 |

Table SI39: Dimers from the ten most intense peaks from TART trapping of α-pinene ozonolysis, obtained using the Formula Find programme. Molecular formula limits were set as $C_{1\text{-}40}H_{0\text{-}100}N_{0\text{-}2}O_{0\text{-}15}Na_{0\text{-}1}$ and *m/z* limits 100-1000.

| Observed *m/z* | Intensity relative to unreacted TART standard / % | Corresponding dimer molecular formula | Corresponding monomer cluster molecular formula |
|---|---|---|---|
| 393.2249 | 32.8 | $[C_{20}H_{34}O_6Na]^+$ | $[(C_{10}H_{18}O_4)(C_{10}H_{16}O_2)Na]^+$<br>$[(C_{10}H_{16}O_3)(C_{10}H_{18}O_3)Na]^+$ |
| 409.2200 | 11.9 | $[C_{20}H_{34}O_7Na]^+$ | $[(C_{10}H_{18}O_4)(C_{10}H_{16}O_3)Na]^+$ |
| 391.2094 | 9.16 | $[C_{20}H_{32}O_6Na]^+$ | $[(C_{10}H_{16}O_3)(C_{10}H_{16}O_3)Na]^+$ |
| 375.2144 | 5.06 | $[C_{20}H_{32}O_5Na]^+$ | $[(C_{10}H_{16}O_2)(C_{10}H_{16}O_3)Na]^+$ |
| 425.2149 | 4.83 | $[C_{20}H_{34}O_8Na]^+$ | - |
| 359.2195 | 2.19 | $[C_{20}H_{32}O_4Na]^+$ | $[(C_{10}H_{16}O_2)(C_{10}H_{16}O_2)Na]^+$ |

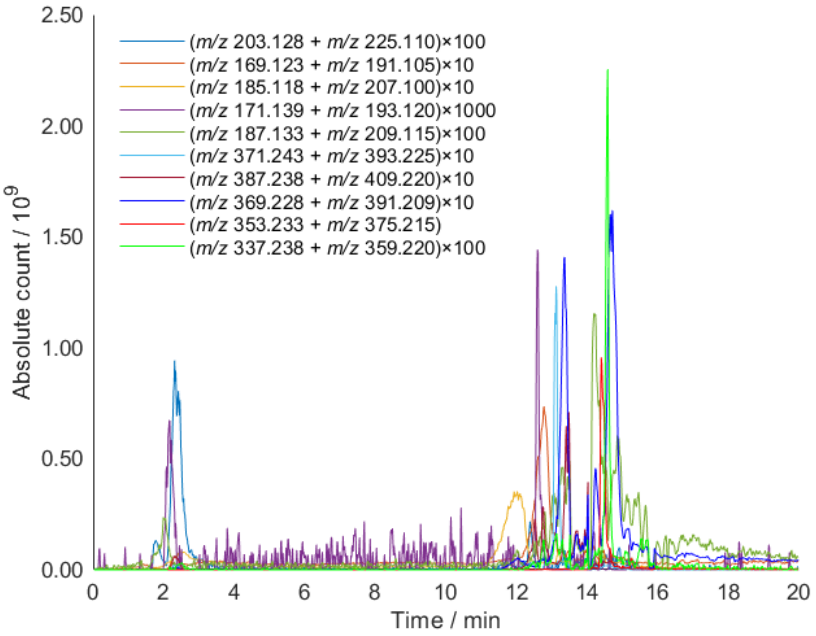


Figure SI96:HPLC-MS chromatograms of peaks (*m/z* ±0.002) corresponding to dimers and their potential cluster-forming monomers from TART trapping of α-pinene ozonolysis (11.7.2). Peaks corresponding to each dimer and their potential cluster-forming monomers either did not overlap or overlap poorly, indicating dimers were formed during TART trapping of α-pinene ozonolysis and not during MS.

Table SI40: Radical-alkene-alkene trimer species identified from TART trapping of α-pinene ozonolysis, using MS for characterisation (11.7.2). Systematic *m/z* error = -0.0005; random *m/z* error = ±0.0012; 100% intensity = $2.01\times10^9$ absolute count. Radical-alkene dimer nomenclature is of the form PR-Trim-x, where R is the index of reactant radical species and x is the total oxygen count in the α-pinene unit, including the bridges between the two units (1-2), two new alkene inner rings (0-2) and new alkene alcohol/hydroperoxide (1-2) functionalisation.

| Species | Predicted *m/z* | Intensity relative to unreacted TART standard / % | | | |
|---|---|---|---|---|---|
| | | No substrate | No $O_2$/ No UV[a] | No TART | Trapping reaction[b] |
| $[CHANT+H]^+$ | 323.2698 | 0.019 | 98.1/ 92.5 | 0 | 29.5±1.2 |
| $[P1.1/1.2\text{-}Trim\text{-}3+Na]^+$ | 511.3399[c] | 0 | 0 | 0.009 | 0.003±0.001 |
| $[P1.1/1.2\text{-}Trim\text{-}4+Na]^+$ | 527.3348[c] | 0.003 | 0 | 0.030 | 0.020±0.001 |
| $[P1.1/1.2\text{-}Trim\text{-}5+Na]^+$ | 543.3297[c] | 0 | 0 | 0.092 | 0.049±0.003 |
| $[P1.1/1.2\text{-}Trim\text{-}6+Na]^+$ | 559.3246[c] | 0 | 0 | 0.752 | 0.66±0.11 |
| $[P1.1/1.2\text{-}Trim\text{-}7+Na]^+$ | 575.3196[c] | 0 | 0 | 0.674 | 0.58±0.04 |
| $[P1.1/1.2\text{-}Trim\text{-}8+Na]^+$ | 591.3145[c] | 0 | 0 | 0.277 | 0.24±0.02 |
| $[P1.1/1.2\text{-}Trim\text{-}9+Na]^+$ | 607.3095 | 0 | 0 | 0.083 | 0.037±0.002 |
| $[P1.1/1.2\text{-}Trim\text{-}10+Na]^+$ | 623.3044 | 0 | 0 | 0.026 | 0 |
| $[P5.1/5.2\text{-}Trim\text{-}3+Na]^+$ | 529.3505 | 0.006 | 0 | 0.019 | 0.013±0.002 |
| $[P5.1/5.2\text{-}Trim\text{-}4+Na]^+$ | 545.3454[c] | 0 | 0 | 0.711 | 0.311±0.005 |
| $[P5.1/5.2\text{-}Trim\text{-}5+Na]^+$ | 561.3403[c] | 0.002 | 0 | 0.250 | 0.120±0.003 |
| $[P5.1/5.2\text{-}Trim\text{-}6+Na]^+$ | 577.3352[c] | 0 | 0 | 3.32 | 3.41±0.14 |
| $[P5.1/5.2\text{-}Trim\text{-}7+Na]^+$ | 593.3301[c] | 0 | 0 | 6.18 | 4.8±0.3 |
| $[P5.1/5.2\text{-}Trim\text{-}8+Na]^+$ | 609.3251[c] | 0 | 0 | 1.57 | 1.15±0.04 |
| $[P5.1/5.2\text{-}Trim\text{-}9+Na]^+$ | 625.3200[c] | 0 | 0 | 0.250 | 0.193±0.013 |
| $[P5.1/5.2\text{-}Trim\text{-}10+Na]^+$ | 641.3150[c] | 0 | 0 | 0.043 | 0.018±0.001 |
| $[PC_{10}H_{17}O_6\text{-}Trim\text{-}3+Na]^+$ | 545.3454[c] | 0 | 0 | 0.711 | 0.311±0.005 |

| | | | | | |
|---|---|---|---|---|---|
| $[PC_{10}H_{17}O_6\text{-Trim-4}+Na]^+$ | 561.3403[c] | 0.002 | 0 | 0.250 | 0.120±0.003 |
| $[PC_{10}H_{17}O_6\text{-Trim-5}+Na]^+$ | 577.3352[c] | 0 | 0 | 3.32 | 3.41±0.14 |
| $[PC_{10}H_{17}O_6\text{-Trim-6}+Na]^+$ | 593.3301[c] | 0 | 0 | 6.18 | 4.8±0.3 |
| $[PC_{10}H_{17}O_6\text{-Trim-7}+Na]^+$ | 609.3251[c] | 0 | 0 | 1.57 | 1.15±0.04 |
| $[PC_{10}H_{17}O_6\text{-Trim-8}+Na]^+$ | 625.3200[c] | 0 | 0 | 0.250 | 0.193±0.013 |
| $[PC_{10}H_{17}O_6\text{-Trim-9}+Na]^+$ | 641.3150[c] | 0 | 0 | 0.043 | 0.018±0.001 |
| $[PC_{10}H_{17}O_6\text{-Trim-10}+Na]^+$ | 657.3099 | 0 | 0 | 0.008 | 0.004±0.001 |
| $[P6/7\text{-Trim-3}+Na]^+$ | 479.3501 | 0 | 0 | 0 | 0 |
| $[P6/7\text{-Trim-4}+Na]^+$ | 495.3450 | 0 | 0 | 0 | 0 |
| $[P6/7\text{-Trim-5}+Na]^+$ | 511.3399[c] | 0 | 0 | 0.009 | 0.003±0.001 |
| $[P6/7\text{-Trim-6}+Na]^+$ | 527.3348[c] | 0.003 | 0 | 0.030 | 0.020±0.001 |
| $[P6/7\text{-Trim-7}+Na]^+$ | 543.3297[c] | 0 | 0 | 0.092 | 0.049±0.003 |
| $[P6/7\text{-Trim-8}+Na]^+$ | 559.3246[c] | 0 | 0 | 0.752 | 0.66±0.11 |
| $[P6/7\text{-Trim-9}+Na]^+$ | 575.3196[c] | 0 | 0 | 0.674 | 0.58±0.04 |
| $[P6/7\text{-Trim-10}+Na]^+$ | 591.3145[c] | 0 | 0 | 0.277 | 0.24±0.02 |

[a]No UV and no $N_2$ controls combined into single column. [b]Three repeats undertaken and an average and associated error calculated. [c]Other table entries have predicted species with same *m/z*.

### SI6.1.2.4. Kinetic modelling

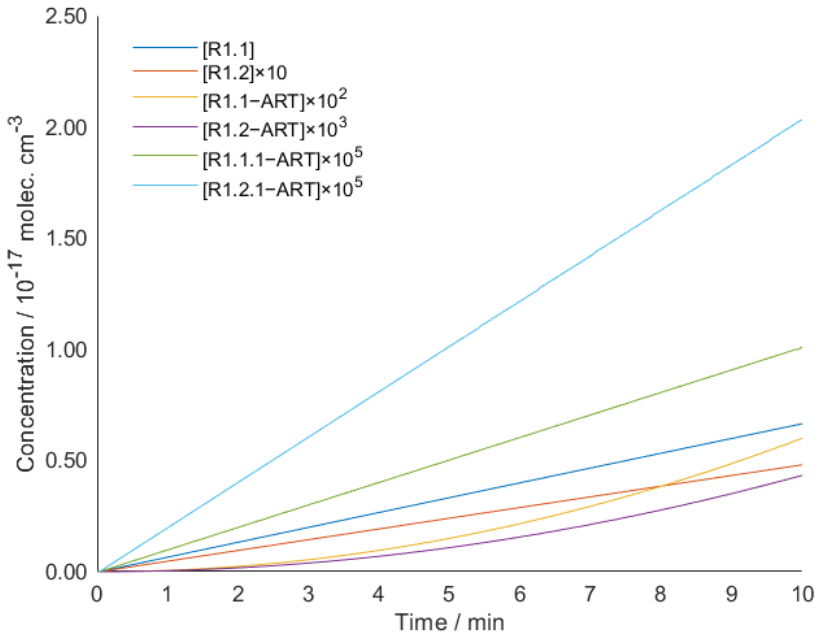


Figure SI97: Liquid phase model of TART trapping of gaseous α-pinene ozonolysis between 0-10 min at residence time 56.5 ms. Simulation indicated [RO•] was extremely low, whilst [$RO_2$•] existed in solution at concentrations greater than TART-trapped $RO_2$•.

# SI7. •OH-initiated alkane degradation

## SI7.1. Using water photolysis as an •OH source

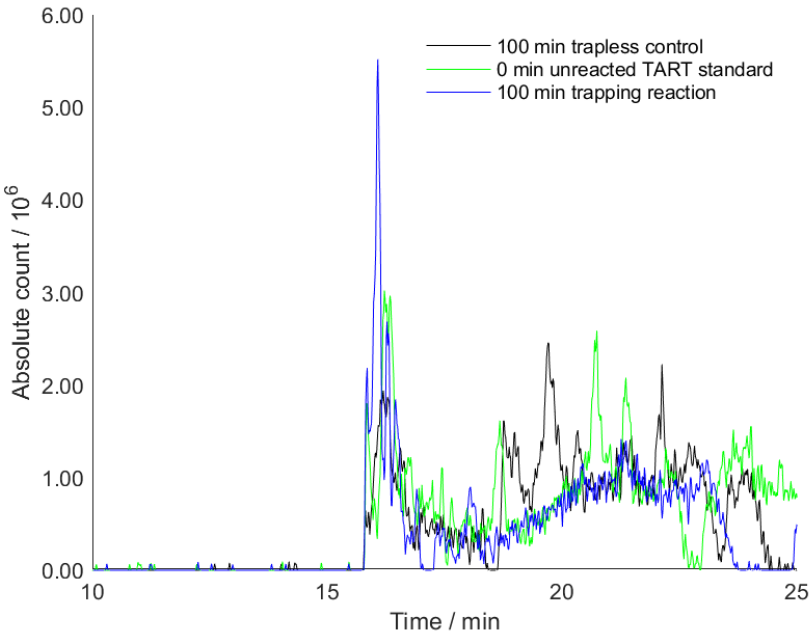


Figure SI98: HPLC-MS chromatograms of peaks corresponding to $RO_2$−ART (*m/z* 326.270±0.002 and *m/z* 348.251±0.002) from TART trapping of •OH-initiated *n*-nonane degradation, using water photolysis as an •OH source and CHANT as TART, after 100 min and with controls (11.8.2). HPLC output was sent to waste between 13.5-14.0 min, to prevent spectrometer contamination by unreacted TART.

Table SI41: Species identified from TART trapping of •OH-initiated *n*-nonane degradation using water photolysis as an •OH source, DEADANT as TART and MS for characterisation after 10 min (11.8.2). Systematic *m/z* error = -0.0005; random *m/z* error = ±0.0005; 100% intensity = $6.11\times10^8$ absolute count.

| Species | | Predicted *m/z* | Intensity relative to unreacted TART standard / % | | |
|---|---|---|---|---|---|
| | | | Trapless control | Unreacted TART standard | Trapping reaction |
| TART | $[CHANT+H]^+$ | 323.2698 | 0.909 | 100 | 120 |
| TART degradation | [N-oxidised CHANT+H]$^+$ | 323.2698 | 0 | 0.067 | 1.91 |
| Trapped radicals | $[RO_2-ART+Na]^+$ | 348.2515 | 0 | 0 | 0 |
| | $[RO-ART+Na]^+$ | 332.2565 | 0 | 0 | 0.041 |
| Products | $[RH+Na]^+$ | 151.1463 | 0 | 0 | 0 |
| | $[ROH+Na]^+$ | 167.1412 | 0 | 0 | 0 |
| | $[RCO+Na]^+$ | 165.1255 | 0 | 0 | 0 |
| | $[ROOH+Na]^+$ | 183.1361 | 0 | 0 | 0 |

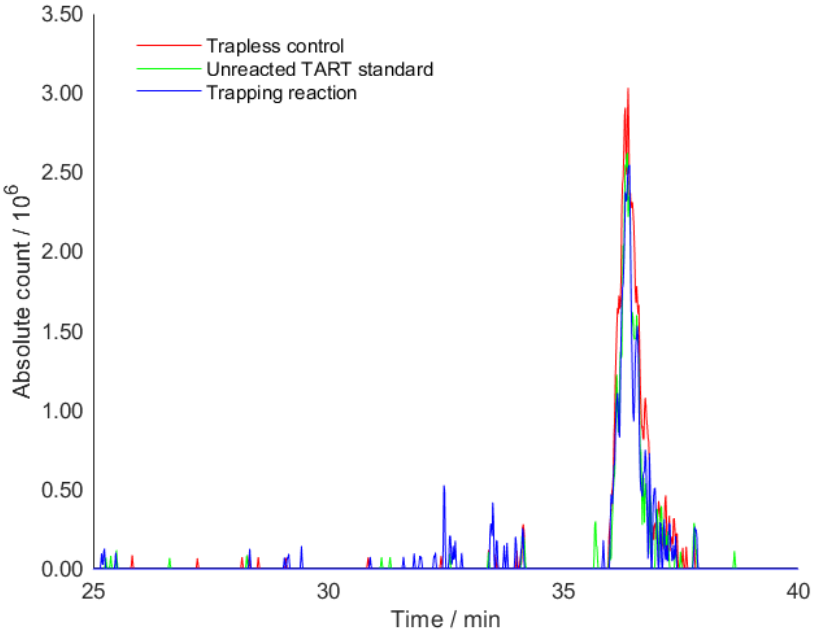


Figure SI99: HPLC-MS chromatograms of the peak corresponding to $RO_2$−ART (*m/z* 315.265±0.002) from TART trapping of •OH-initiated *n*-nonane degradation, using water photolysis as an •OH source and DEADANT as TART, with controls (11.8.2).

# SI8. Modelling equations

## SI8.1. Radical thiol-ene addition

Table SI42: Reactions and their rate constants for TART trapping of radical thiol-ene addition, using styrene (S3.1) and thiols S2.2, S2.3 or S2.5 as substrates (11.5.2.8, 11.10.2). Key parameters: time = 24 h. Concentrations / M: $[thiol]_0$ = 0.400; $[styrene]_0$ = 0.200; $[TART]_0$ = 0.020.

| Reaction[a] | A | | |
|---|---|---|---|
| | S2.2 | S2.3 | S2.5 |
| S==>R1 | 6.81E-06[b] | | |
| R1+A==>R2 | 3.54E+07[c] | 3.54E+09[c] | 3.54E+10[c] |
| R2==>R1+A | 5.31E+07[d] | | |
| R2+S==>P+R1 | 2.48E+06[c] | 2.48E+05[c] | 2.48E+04[c] |
| P+R1==>R2+S | 1.45E+00[d] | | |
| 2R1==>T | 1.00E+08[e] | | |
| R1+R2==>T | 1.00E+08[e] | | |
| 2R2==>T | 1.00E+08[e] | | |
| R1+TART==>R1.ART+TEMPO | 4.35E+06[f] | 3.03E+06[g] | 3.03E+06[g] |
| R2+TART==>R2.ART+TEMPO | 4.50E+02[h] | | |
| R2+TEMPO==>R2.TEMPO | 1.64E+08[i] | | |
| R1+R1.ART==>R1.ART.R1 | 4.35E+06[f] | 3.03E+06[g] | 3.03E+06[g] |
| R1.ART.R1==>R1+R1.ART | 7.99E+06[f] | 1.35E+07[g] | 1.35E+07[g] |
| R1.ART.R1+S==>R1+R1.ART.R1.P | 1.00E+06[f] | 1.32E+07[g] | 1.32E+07[g] |
| R1+R1.ART.R1.P==>R1.ART.R1+S | 5.74E-01[f] | 1.44E+01[g] | 1.44E+01[g] |
| R1.ART.R1+ART==>R1.ART.R1.ART+TEMPO | 4.50E+02[h] | | |
| R1.ART.R1+TEMPO==>R1.ART.R1.TEMPO | 1.64E+08[i] | | |
| R1+R2.ART==>R2.ART.R1 | 4.35E+06[f] | 3.03E+06[g] | 3.03E+06[g] |
| R2.ART.R1==>R1+R2.ART | 7.99E+06[f] | 1.35E+07[g] | 1.35E+07[g] |
| R2.ART.R1+S==>R1+R2.ART.R1.P | 1.00E+06[f] | 1.32E+07[g] | 1.32E+07[g] |
| R1+R2.ART.R1.P==>R2.ART.R1+S | 5.74E-01[f] | 1.44E+01[g] | 1.44E+01[g] |
| R2.ART.R1+ART==>R2.ART.R1.ART+TEMPO | 4.50E+02[h] | | |
| R2.ART.R1+TEMPO==>R2.ART.R1.TEMPO | 1.64E+08[i] | | |
| R1.ART.R1+R1==>T | 1.00E+08[e] | | |
| R1.ART.R1+R2==>T | 1.00E+08[e] | | |
| 2R1.ART.R1==>T | 1.00E+08[e] | | |
| R1.ART.R1+R2.ART.R1==>T | 1.00E+08[e] | | |
| R2.ART.R1+R1==>T | 1.00E+08[e] | | |
| R2.ART.R1+R2==>T | 1.00E+08[e] | | |
| 2R2.ART.R1==>T | 1.00E+08[e] | | |

[a]S = **thiol**, A = **alkene**; P = **thioether product**; T = **terminated product**; R1.ART = **R1−ART**; R2.ART = **R2−ART**; R2.TEMPO = **R2−TEMPO**; R1.ART.R1.P = **R1−ART+S2**. [b]Estimated using experimental data and kinetic modelling. [c]Estimated from literature reaction of thiophenol with styrene[208] and altered by hand until experimental [R1−ART]/[R2−ART] was achieved. [d]Estimated from literature reaction of thiophenol with styrene.[208] [e]Radical-radical termination rate defined by literature.[204] [f]Estimated from literature reaction of thiophenol with methyl methacrylate.[208] [g]Estimated from 4-chlorothiophenol with methyl methacrylate.[208] [h]Estimated from literature reaction of benzyl radical with methyl methacrylate.[209] [i]Estimated from literature reaction of $PhC^{\bullet}HCH_3$ reaction with $TEMPO^{\bullet}$.[210]

Table SI43: Reactions and their rate constants for TART trapping of radical thiol-ene addition, using styrene (S3.1) and thiols S2.1, S2.4 and S2.6 as substrates (11.5.2.8, 11.10.2). Key parameters: time = 24 h. Concentrations / mM: $[thiol]_0$ = 0.400; $[styrene]_0$ = 0.200; $[TART]_0$ = 0.020.

| Reaction[a] | A | | |
|---|---|---|---|
| | S2.1 | S2.4 | S2.6 |
| S==>R1 | 6.81E-06[b] | | |
| R1+A==>R2 | 3.10E+06[c] | 3.10E+07[c] | 3.10E+07[c] |
| R2==>R1+A | 1.30E+03[d] | | |
| R2+S==>P+R1 | 5.00E+02[c] | 5.00E+02[c] | 5.00E+01[c] |
| P+R1==>R2+S | 4.00E+01[d] | | |
| 2R1==>T | 1.00E+08[e] | | |
| R1+R2==>T | 1.00E+08[e] | | |
| 2R2==>T | 1.00E+08[e] | | |
| R1+TART==>R1.ART+TEMPO | 3.20E+06[f] | | |
| R2+TART==>R2.ART+TEMPO | 4.50E+02[g] | | |
| R2+TEMPO==>R2.TEMPO | 1.64E+08[h] | | |
| R1+R1.ART==>R1.ART.R1 | 3.20E+06[f] | | |
| R1.ART.R1==>R1+R1.ART | 1.50E+04[f] | | |
| R1.ART.R1+S==>R1+R1.ART.R1.P | 2.10E+03[f] | | |
| R1+R1.ART.R1.P==>R1.ART.R1+S | 2.30E-01[f] | | |
| R1.ART.R1+ART==>R1.ART.R1.ART+TEMPO | 4.50E+02[g] | | |
| R1.ART.R1+TEMPO==>R1.ART.R1.TEMPO | 1.64E+08[h] | | |
| R1+R2.ART==>R2.ART.R1 | 3.20E+06[f] | | |
| R2.ART.R1==>R1+R2.ART | 1.50E+04[f] | | |
| R2.ART.R1+S==>R1+R2.ART.R1.P | 2.10E+03[f] | | |
| R1+R2.ART.R1.P==>R2.ART.R1+S | 2.30E-01[f] | | |
| R2.ART.R1+ART==>R2.ART.R1.ART+TEMPO | 4.50E+02[g] | | |
| R2.ART.R1+TEMPO==>R2.ART.R1.TEMPO | 1.64E+08[h] | | |
| R1.ART.R1+R1==>T | 1.00E+08[e] | | |
| R1.ART.R1+R2==>T | 1.00E+08[e] | | |
| 2R1.ART.R1==>T | 1.00E+08[e] | | |
| R1.ART.R1+R2.ART.R1==>T | 1.00E+08[e] | | |
| R2.ART.R1+R1==>T | 1.00E+08[e] | | |
| R2.ART.R1+R2==>T | 1.00E+08[e] | | |
| 2R2.ART.R1==>T | 1.00E+08[e] | | |

[a]S = **thiol**, A = **alkene**; P = **thioether product**; T = **terminated product**; R1.ART = **R1−ART**; R2.ART = **R2−ART**; R2.TEMPO = **R2−TEMPO**; R1.ART.R1.P = **R1−ART+S2**. [b]Estimated using experimental data and kinetic modelling. [c]Estimated from literature reaction of methylthiol with styrene[204] and altered by hand until experimental [R1−ART]/[R2−ART] was achieved. [d]Estimated from literature reaction of methylthiol with styrene.[204] [e]Radical-radical termination rate defined by literature.[204] [f]Estimated from literature reaction of methylthiol with methyl acrylate.[204] [g]Estimated from literature reaction of benzyl radical with methyl methacrylate.[209] [h]Estimated from literature reaction of $PhC^{\bullet}HCH_3$ reaction with $TEMPO^{\bullet}$.[210]

Table SI44: Reactions and their rate constants for TART trapping of radical thiol-ene addition, using benzyl mercaptan (S2.1) and alkenes S3.1, S3.4 and S3.6 as substrates (11.5.2.9, 11.10.2). Key parameters: time = 24 h. Concentrations / M: [benzyl mercaptan]$_0$ = 0.400; [alkene]$_0$ = 0.200; [TART]$_0$ = 0.020.

| Reaction[a] | A | | |
|---|---|---|---|
| | S3.1 | S3.4 | S3.6 |
| S==>R1 | 6.81E-06[b] | | |
| R1+A==>R2 | 3.10E+06[c] | 3.10E+05[c] | 3.10E+05[c] |
| R2==>R1+A | 1.30E+03[d] | | |
| R2+S==>P+R1 | 5.00E+02[c] | 5.00E+02[c] | 5.00E+03[c] |
| P+R1==>R2+S | 4.00E+01[d] | | |
| 2R1==>T | 1.00E+08[e] | | |
| R1+R2==>T | 1.00E+08[e] | | |
| 2R2==>T | 1.00E+08[e] | | |
| R1+TART==>R1.ART+TEMPO | 3.20E+06[f] | | |
| R2+TART==>R2.ART+TEMPO | 4.50E+02[g] | | |
| R2+TEMPO==>R2.TEMPO | 1.64E+08[h] | | |
| R1+R1.ART==>R1.ART.R1 | 3.20E+06[f] | | |
| R1.ART.R1==>R1+R1.ART | 1.50E+04[f] | | |
| R1.ART.R1+S==>R1+R1.ART.R1.P | 2.10E+03[f] | | |
| R1+R1.ART.R1.P==>R1.ART.R1+S | 2.30E-01[f] | | |
| R1.ART.R1+ART==>R1.ART.R1.ART+TEMPO | 4.50E+02[g] | | |
| R1.ART.R1+TEMPO==>R1.ART.R1.TEMPO | 1.64E+08[h] | | |
| R1+R2.ART==>R2.ART.R1 | 3.20E+06[f] | | |
| R2.ART.R1==>R1+R2.ART | 1.50E+04[f] | | |
| R2.ART.R1+S==>R1+R2.ART.R1.P | 2.10E+03[f] | | |
| R1+R2.ART.R1.P==>R2.ART.R1+S | 2.30E-01[f] | | |
| R2.ART.R1+ART==>R2.ART.R1.ART+TEMPO | 4.50E+02[g] | | |
| R2.ART.R1+TEMPO==>R2.ART.R1.TEMPO | 1.64E+08[h] | | |
| R1.ART.R1+R1==>T | 1.00E+08[e] | | |
| R1.ART.R1+R2==>T | 1.00E+08[e] | | |
| 2R1.ART.R1==>T | 1.00E+08[e] | | |
| R1.ART.R1+R2.ART.R1==>T | 1.00E+08[e] | | |
| R2.ART.R1+R1==>T | 1.00E+08[e] | | |
| R2.ART.R1+R2==>T | 1.00E+08[e] | | |
| 2R2.ART.R1==>T | 1.00E+08[e] | | |

[a]S = **thiol**, A = **alkene**; P = **thioether product**; T = **terminated product**; R1.ART = **R1−ART**; R2.ART = **R2−ART**; R2.TEMPO = **R2−TEMPO**; R1.ART.R1.P = **R1−ART+S2**. [b]Estimated using experimental data and kinetic modelling. [c]Estimated from literature reaction of methylthiol with styrene[204] and altered by hand until experimental [R1−ART]/[R2−ART] was achieved. [d]Estimated from literature reaction of methylthiol with styrene.[204] [e]Radical-radical termination rate defined by literature.[204] [f]Estimated from literature reaction of methylthiol with methyl acrylate.[204] [g]Estimated from literature reaction of benzyl radical with methyl methacrylate.[209] [h]Estimated from literature reaction of PhC•HCH$_3$ reaction with TEMPO•.[210]

Table SI45: Reactions and their kinetic factors for TART trapping of radical thiol-ene addition, using benzyl mercaptan (S2.1) and alkenes S3.2, S3.3 and S3.5 as substrates (11.5.2.9, 11.10.2). Key parameters: time = 24 h. Concentrations / M: [benzyl mercaptan]$_0$ = 0.400; [alkene]$_0$ = 0.200; [TART]$_0$ = 0.020.

| Reaction[a] | A | | |
|---|---|---|---|
| | S3.2 | S3.3 | S3.5 |
| S==>R1 | 6.81E-06[b] | | |
| R1+A==>R2 | 1.10E+05[c] | 1.10E+05[c] | 1.10E+06[c] |
| R2==>R1+A | 1.10E+07[d] | | |
| R2+S==>P+R1 | 2.30E+05[c] | 2.30E+05[c] | 2.30E+05[c] |
| P+R1==>R2+S | 4.70E-02[d] | | |
| 2R1==>T | 1.00E+08[e] | | |
| R1+R2==>T | 1.00E+08[e] | | |
| 2R2==>T | 1.00E+08[e] | | |
| R1+TART==>R1.ART+TEMPO | 3.20E+06[f] | | |
| R2+TART==>R2.ART+TEMPO | 1.09E+06[g] | | |
| R2+TEMPO==>R2.TEMPO | 7.60E+08[h] | | |
| R1+R1.ART==>R1.ART.R1 | 3.20E+06[f] | | |
| R1.ART.R1==>R1+R1.ART | 1.50E+04[f] | | |
| R1.ART.R1+S==>R1+R1.ART.R1.P | 2.10E+03[f] | | |
| R1+R1.ART.R1.P==>R1.ART.R1+S | 2.30E-01[f] | | |
| R1.ART.R1+ART==>R1.ART.R1.ART+TEMPO | 1.09E+06[g] | | |
| R1.ART.R1+TEMPO==>R1.ART.R1.TEMPO | 7.60E+08[h] | | |
| R1+R2.ART==>R2.ART.R1 | 3.20E+06[f] | | |
| R2.ART.R1==>R1+R2.ART | 1.50E+04[f] | | |
| R2.ART.R1+S==>R1+R2.ART.R1.P | 2.10E+03[f] | | |
| R1+R2.ART.R1.P==>R2.ART.R1+S | 2.30E-01[f] | | |
| R2.ART.R1+ART==>R2.ART.R1.ART+TEMPO | 1.09E+06[g] | | |
| R2.ART.R1+TEMPO==>R2.ART.R1.TEMPO | 7.60E+08[h] | | |
| R1.ART.R1+R1==>T | 1.00E+08[e] | | |
| R1.ART.R1+R2==>T | 1.00E+08[e] | | |
| 2R1.ART.R1==>T | 1.00E+08[e] | | |
| R1.ART.R1+R2.ART.R1==>T | 1.00E+08[e] | | |
| R2.ART.R1+R1==>T | 1.00E+08[e] | | |
| R2.ART.R1+R2==>T | 1.00E+08[e] | | |
| 2R2.ART.R1==>T | 1.00E+08[e] | | |

[a]S = **thiol**, A = **alkene**; P = **thioether product**; T = **terminated product**; R1.ART = **R1−ART**; R2.ART = **R2−ART**; R2.TEMPO = **R2−TEMPO**; R1.ART.R1.P = **R1−ART+S2**. [b]Estimated using experimental data and kinetic modelling. [c]Estimated from literature reaction of methylthiol with propene[204] and altered by hand until experimental [R1−ART]/[R2−ART] was achieved. [d]Estimated from literature reaction of methylthiol with propene.[204] [e]Radical-radical termination rate defined by literature.[204] [f]Estimated from literature reaction of methylthiol with methyl acrylate.[204] [g]Estimated from literature reaction of $(CH_3)_3C^{\bullet}$ with methyl acrylate.[225] [h]Estimated from literature reaction of $(CH_3)_3C^{\bullet}$ reaction with TEMPO$^{\bullet}$.[210]

## SI8.2. α-Pinene ozonolysis

Table SI46: Reactions and their kinetic factors used for gas phase modelling of α-pinene ozonolysis (11.7.5, 11.10.3). Atmospheric reactions of α-pinene were imported into the Kintecus chemical simulation programme[207] from the MCM[57] and truncated to remove late stage pathways. Key parameters: time = 56.5 ms. Concentrations / molec. $cm^{-3}$: $[O_3]_0 = 2.96\times10^{15}$; $[\alpha\text{-pinene}]_0 = 5.20\times10^{16}$.

| Reaction[a,b] | A | $E_a$ |
|---|---|---|
| OH + O3 ==> HO2 | 1.7E-12 | 940 |
| OH + H2 ==> HO2 | 7.7E-12 | 2100 |
| OH + CO ==> HO2 | 1 | 0 |
| OH + H2O2 ==> HO2 | 2.9E-12 | 160 |
| HO2 + O3 ==> OH | 2.03E-16 | -693 |
| OH + HO2 ==> H2O + O2 | 4.8E-11 | -250 |
| HO2 + HO2 ==> H2O2 | 2.2E-13 | 0 |
| APINENE + O3 ==> APINOOA | 4.83E-16 | 640 |
| APINENE + O3 ==> APINOOB | 3.22E-16 | 640 |
| APINENE + OH ==> APINAO2 | 6.864E-12 | -440 |
| APINENE + OH ==> APINBO2 | 4.236E-12 | -440 |
| APINENE + OH ==> APINCO2 | 9E-13 | -440 |
| APINOOA ==> C107O2 + OH | 550000 | 0 |
| APINOOA ==> C109O2 + OH | 450000 | 0 |
| APINOOB ==> APINBOO | 500000 | 0 |
| APINOOB ==> C96O2 + OH + CO | 500000 | 0 |
| APINAO2 + HO2 ==> APINAOOH | 2.65974E-13 | -1300 |
| APINAO2 + RO2 ==> APINAO | 6.44E-14 | 0 |
| APINAO2 + RO2 ==> APINBOH | 2.76E-14 | 0 |
| APINBO2 + HO2 ==> APINBOOH | 2.65974E-13 | -1300 |
| APINBO2 + RO2 ==> APINBCO | 1.76E-13 | 0 |
| APINBO2 + RO2 ==> APINBO | 5.28E-13 | 0 |
| APINBO2 + RO2 ==> APINBOH | 1.76E-13 | 0 |
| APINCO2 + HO2 ==> APINCOOH | 2.65974E-13 | -1300 |
| APINCO2 + RO2 ==> APINCO | 4.69E-15 | 0 |
| APINCO2 + RO2 ==> APINCOH | 2.01E-15 | 0 |
| C107O2 + HO2 ==> C107OOH | 2.65974E-13 | -1300 |
| C107O2 + RO2 ==> C107O | 6.44E-14 | 0 |
| C107O2 + RO2 ==> C107OH | 2.76E-14 | 0 |
| C109O2 + HO2 ==> C109OOH | 2.65974E-13 | -1300 |
| C109O2 + RO2 ==> C109CO | 1E-13 | 0 |
| C109O2 + RO2 ==> C109O | 1.8E-12 | 0 |
| C109O2 + RO2 ==> C109OH | 1E-13 | 0 |
| APINBOO + CO ==> PINAL | 1.2E-15 | 0 |
| APINBOO +M[-H2O(1);] ==> PINAL + H2O2 | 1.4E-17 | 0 |
| APINBOO +M[-H2O(1);] ==> PINONIC | 2E-18 | 0 |
| C96O2 + HO2 ==> C96OOH | 2.5899E-13 | -1300 |
| C96O2 + RO2 ==> C96O | 7.8E-13 | 0 |
| C96O2 + RO2 ==> C96OH | 2.6E-13 | 0 |
| C96O2 + RO2 ==> NORPINAL | 2.6E-13 | 0 |
| APINAOOH + OH ==> APINAO2 | 1.83E-11 | 0 |
| APINAO ==> PINAL + HO2 | 1000000 | 0 |
| APINBOH + OH ==> APINBCO + HO2 | 1.49E-11 | 0 |
| APINBOOH + OH ==> APINBCO + OH | 3.28E-11 | 0 |
| APINBO ==> PINAL + HO2 | 1000000 | 0 |

| | | |
|---|---|---|
| APINBCO + OH ==> C96CO3 | 8.18E-12 | 0 |
| APINCOOH + OH ==> APINCO2 | 1.03E-10 | 0 |
| APINCO ==> CH3COCH3 + C720O2 | 1000000 | 0 |
| APINCOH + OH ==> APINCO | 9.91E-11 | 0 |
| PINAL + OH ==> C96CO3 | 4.0144E-12 | -600 |
| PINAL + OH ==> PINALO2 | 1.1856E-12 | -600 |
| C96CO3 + HO2 ==> C96O2 + OH | 2.288E-13 | -980 |
| C96CO3 + HO2 ==> PERPINONIC | 2.132E-13 | -980 |
| C96CO3 + HO2 ==> PINONIC + O3 | 7.8E-14 | -980 |
| C96CO3 + RO2 ==> C96O2 | 7E-12 | 0 |
| C96CO3 + RO2 ==> PINONIC | 3E-12 | 0 |
| C107OOH + OH ==> C107O2 | 3.01E-11 | 0 |
| C107O ==> C108O2 | 1000000 | 0 |
| C107OH + OH ==> C107O | 2.66E-11 | 0 |
| C109OOH + OH ==> C109CO + OH | 5.47E-11 | 0 |
| C109O ==> C89CO3 + HCHO | 800000 | 0 |
| C109O ==> C920CO3 | 200000 | 0 |
| C109CO + OH ==> C89CO3 + CO | 5.47E-11 | 0 |
| C109OH + OH ==> C109CO + HO2 | 4.45E-11 | 0 |
| PINONIC + OH ==> C96O2 | 6.65E-12 | 0 |
| C96OOH + OH ==> C96O2 | 1.9E-12 | -190 |
| C96OOH + OH ==> NORPINAL + OH | 1.3E-11 | 0 |
| C96O ==> C97O2 | 42000000000 | 3523 |
| C96OH + OH ==> NORPINAL + HO2 | 7.67E-12 | 0 |
| NORPINAL + OH ==> C85CO3 | 2.64E-11 | 0 |
| CH3COCH3 + OH ==> CH3COCH2O2 | 8.8E-12 | 1320 |
| HCC7CO + OH ==> C719O2 | 1.19E-10 | 0 |
| C720O2 + HO2 ==> C720OOH | 2.3862E-13 | -1300 |
| C720O2 + RO2 ==> C720O | 1.5E-13 | 0 |
| C720O2 + RO2 ==> C720OH | 5E-14 | 0 |
| C720O2 + RO2 ==> HCC7CO | 5E-14 | 0 |
| PINALO2 + HO2 ==> PINALOOH | 2.65974E-13 | -1300 |
| PINALO2 + RO2 ==> PINALO | 4.69E-15 | 0 |
| PINALO2 + RO2 ==> PINALOH | 2.01E-15 | 0 |
| PERPINONIC + OH ==> C96CO3 | 9.73E-12 | 0 |
| C108O2 + HO2 ==> C108OOH | 2.65974E-13 | -1300 |
| C108O2 + RO2 ==> C108O | 4.69E-15 | 0 |
| C108O2 + RO2 ==> C108OH | 2.01E-15 | 0 |

[a]RO2 = [APINAO2; APINBO2; APINCO2; C107O2; C109O2; C96O2; C96CO3; C720O2; PINALO2; C108O2]. [b]APINENE = **α-pinene**; APINOOA = **R1**; APINOOB = **R2**; APINAO2 = **R3**; APINBO2 = **R4**; APINCO2 = **R5**; C107O2 = **R1.1**; C109O2 = **R1.2**; C96O2 = **R2.1**; APINAOOH = **P3.2**; APINAO = **R3.1**; APINBOH = **P3.3**; APINBOOH = **P4.2**; APINBCO = **P4.3**; APINBO = **R4.1**; APINCO = **R5.3**; C107OOH = **P1.1.2**; C107O = **R1.1.1**; C107OH = **P1.1.3**; C109OOH = **P1.2.2**; C109CO = **P1.2.4**; C109O = **R1.2.1**; C109OH = **P1.2.3**; PINAL = **pinaldehyde**; PINONIC = **pinonic acid**; C96OOH = **P2.1.2**; C96O = **R2.1.1**; C96OH = **P2.1.3**; NORPINAL = **P2.1.4**; C108O2 = **R1.1.1.1**; C89CO3 = **R1.2.1.1**; C920CO3 = **R1.2.1.2**; C97O2 = **R2.1.1.1**.

Table SI47: Reactions and their kinetic factors used for liquid phase modelling of TART trapping of α-pinene ozonolysis (11.7.5). These rate constants were estimated from assorted literature sources between reactions of $RO_2^{\bullet}$ with methyl methacrylate[226] and $RO^{\bullet}$ with alkenes[228] respectively. $[Trap]_0 = 3.01\times10^{17}$ molec. $cm^{-3}$. For liquid phase, key parameters: time = 2 min. Concentrations added / molec. $cm^{-3}$ $s^{-1}$. For gas-liquid interface, key parameters: time = 6.79 ms; scaled to time = 2 min. Initial concentrations / molec. $cm^{-3}$.

| Reaction | A | $E_a$ |
|---|---|---|
| APINAO2 + Trap ==> APINAO2.Trap + TEMPO | 1.00E-22 | 0 |
| APINBO2 + Trap ==> APINBO2.Trap + TEMPO | 1.00E-22 | 0 |
| APINCO2 + Trap ==> APINCO2.Trap + TEMPO | 1.00E-22 | 0 |
| C107O2 + Trap ==> C107O2.Trap + TEMPO | 1.00E-22 | 0 |
| C109O2 + Trap ==> C109O2.Trap + TEMPO | 1.00E-22 | 0 |
| C96O2 + Trap ==> C96O2.Trap + TEMPO | 1.00E-22 | 0 |
| APINAO + Trap ==> APINAO.Trap + TEMPO | 1.00E-15 | 0 |
| APINBO + Trap ==> APINBO.Trap + TEMPO | 1.00E-15 | 0 |
| APINCO + Trap ==> APINCO.Trap + TEMPO | 1.00E-15 | 0 |
| C107O + Trap ==> C107O.Trap + TEMPO | 1.00E-15 | 0 |
| C109O + Trap ==> C109O.Trap + TEMPO | 1.00E-15 | 0 |
| C96O + Trap ==> C96O.Trap + TEMPO | 1.00E-15 | 0 |

[a]APINAO2 = **R3**; APINBO2 = **R4**; APINCO2 = **R5**; C107O2 = **R1.1**; C109O2 = **R1.2**; C96O2 = **R2.1**; APINAO = **R3.1**; APINBO = **R4.1**; APINCO = **R5.3**; C107O = **R1.1.1**; C109O = **R1.2.1**; C96O = **R2.1.1**.

## SI8.3. $^{\bullet}$OH-initiated *n*-nonane degradation

Table SI48: Reactions and their kinetic factors used for gas phase modelling of $^{\bullet}$OH-initiated *n*-nonane degradation (11.8.2, 11.10.4). Atmospheric reactions of *n*-nonane were imported into the Kintecus chemical simulation programme[207] from the MCM[57] and truncated to remove late stage pathways. Key parameters: residence time = 129 ms. Concentrations / molec. $cm^{-3}$: $[^{\bullet}OH]_0 = 3.4\pm0.5\times10^{11}$; $[HO_2^{\bullet}]_0 = 3.4\pm0.5\times10^{11}$; $[n\text{-nonane}]_0 = 1.01\times10^{16}$.

| Reaction[a,b] | A | $E_a$ |
|---|---|---|
| OH + O3 ==> HO2 | 1.7E-12 | 940 |
| OH + H2 ==> HO2 | 7.7E-12 | 2100 |
| OH + CO ==> HO2 | 1 | 0 |
| OH + H2O2 ==> HO2 | 2.9E-12 | 160 |
| HO2 + O3 ==> OH | 2.03E-16 | -693 |
| OH + HO2 ==> H2O + O2 | 4.8E-11 | -250 |
| HO2 + HO2 ==> H2O2 | 2.2E-13 | 0 |
| OH + NC9H20 ==> NONO2 | 2.51E-17 | -447 |
| NONO2 + HO2 ==> NONOOH | 2.5899E-13 | -1300 |
| NONO2 + RO2 ==> NON3ONE | 5.00E-14 | 0 |
| NONO2 + RO2 ==> NONO | 1.5E-13 | 0 |
| NONO2 + RO2 ==> NONOH | 5E-14 | 0 |
| OH + NONOOH ==> NON3ONE + OH | 3.65E-11 | 0 |
| NONO ==> HO3C96O2 | 2.58E+11 | 3430 |
| OH + NON3ONE ==> C91O2 | 1.07E-11 | 0 |
| OH + NONOH ==> NON3ONE + HO2 | 1.87E-11 | 0 |
| HO3C96O2 + HO2 ==> HO3C96OOH | 2.5899E-13 | -1300 |
| HO3C96O2 + RO2 ==> HO36C9 | 5E-14 | 0 |
| HO3C96O2 + RO2 ==> HO3C96O | 1.5E-13 | 0 |
| HO3C96O2 + RO2 ==> HO4CO7C9 | 5E-14 | 0 |
| C91O2 + HO2 ==> C91OOH | 2.5899E-13 | -1300 |
| C91O2 + RO2 ==> C91O | 2.5E-13 | 0 |
| OH + HO3C96OOH ==> HO4CO7C9 + OH | 4.55E-11 | 0 |
| HO3C96O ==> HO4CO7C9 + HO2 | 5.55E+11 | 2945 |
| OH + HO36C9 ==> HO4CO7C9 + HO2 | 2.43E-11 | 0 |

| | | |
|---|---|---|
| OH + HO4CO7C9 ==> C93O2 | 6.0496E-12 | 0 |
| OH + HO4CO7C9 ==> CO36C9 + HO2 | 1.38504E-11 | 0 |
| OH + C5H11CHO ==> C5H11CO3 | 2.88E-11 | 0 |
| OH + C91OOH ==> C91O2 | 8.8E-11 | 0 |
| C91O ==> C92O2 | 1.15E+11 | 3430 |
| OH + CO36C9 ==> C94O2 | 1.14E-11 | 0 |

[a]RO2 = [NONO2; HO3C96O2; C91O2; C2H5O2; HO5C6O2; C93O2; HO1C6O2; C5H11CO3; C92O2; C94O2].
[b]NC9H20 = ***n*-nonane**; NONO2 = **$RO_2^{\bullet}$**; NONOOH = **ROOH**; NON3ONE = **RCO**; NONO = **$RO^{\bullet}$**; NONOH = **ROH**; HO3C96O2 = **$R(OH)O_2^{\bullet}$**.

# References


1 J. Fossey, D. Lefort and J. Sorba, *Free Radicals in Organic Chemistry*, Wiley, New York, 1995.

2 A. F. Parsons, *An Introduction to Free Radical Chemistry*, Blackwell Science, Oxford, 2000.

3 W. A. Braunecker and K. Matyjaszewski, *Prog. Polym. Sci.*, 2007, **32**, 93–146.

4 K. Matyjaszewski and J. Xia, *Chem. Rev.*, 2001, **101**, 2921–2990.

5 C. K. Prier, D. A. Rankic and D. W. C. MacMillan, *Chem. Rev.*, 2013, **113**, 5322–5363.

6 M. H. Shaw, J. Twilton and D. W. C. MacMillan, *J. Org. Chem.*, 2016, **81**, 6898–6926.

7 N. A. Romero and D. A. Nicewicz, *Chem. Rev.*, 2016, **116**, 10075–10166.

8 K. Apel and H. Hirt, *Annu. Rev. Plant Biol.*, 2004, **55**, 373–399.

9 M. Valko, D. Leibfritz, J. Moncol, M. T. D. Cronin, M. Mazur and J. Telser, *Int. J. Biochem. Cell Biol.*, 2007, **39**, 44–84.

10 M. Hallquist, J. C. Wenger, U. Baltensperger, Y. Rudich, D. Simpson, M. Claeys, J. Dommen, N. M. Donahue, C. George, A. H. Goldstein, J. F. Hamilton, H. Herrmann, T. Hoffmann, Y. Iinuma, M. Jang, M. E. Jenkin, J. L. Jimenez, A. Kiendler-Scharr, W. Maenhaut, G. McFiggans, T. F. Mentel, A. Monod, A. S. H. Prévôt, J. H. Seinfeld, J. D. Surratt, R. Szmigielski and J. Wildt, *Atmos. Chem. Phys.*, 2009, **9**, 5155–5236.

11 B. Nozière, M. Kalberer, M. Claeys, J. Allan, B. D'Anna, S. Decesari, E. Finessi, M. Glasius, I. Grgić, J. F. Hamilton, T. Hoffmann, Y. Iinuma, M. Jaoui, A. Kahnt, C. J. Kampf, I. Kourtchev, W. Maenhaut, N. Marsden, S. Saarikoski, J. Schnelle-Kreis, J. D. Surratt, S. Szidat, R. Szmigielski and A. Wisthaler, *Chem. Rev.*, 2015, **115**, 3919–3983.

12 A. L. Zanocco, A. Cañete M. and M. X. Melendez, *Bol. Soc. Chil. Quím.*, 2000, **45**, 123–129.

13 H. Togo, *Advanced Free Radical Reactions for Organic Synthesis*, Elsevier B.V., 2004.

14 K. J. Romero, M. S. Galliher, D. A. Pratt and C. R. J. Stephenson, *Chem. Soc. Rev.*, 2018, **47**, 7851–7866.

15 P. Nesvadba, in *Encyclopedia of Radicals in Chemistry, Biology and Materials*, John Wiley & Sons Ltd., 2012.

16 K. C. Berger, P. C. Deb and G. Meyerhoff, *Macromolecules*, 1977, **10**, 1075–1080.

17 T. Posner, *Berichte der Dtsch. Chem. Gesellschaft*, 1905, **1**, 646–657.

18 N. B. Cramer and C. N. Bowman, *J. Polym. Sci. Part A Polym. Chem.*, 2001, **39**, 3311–3319.

19 O. Okay and C. N. Bowman, *Macromol. Theory Simul.*, 2005, **14**, 267–277.

20 A. B. Lowe, *Polym. Chem.*, 2010, **1**, 17–36.

21 C. E. Hoyle and C. N. Bowman, *Angew. Chem. Int. Ed.*, 2010, **49**, 1540–1573.

22 B. H. J. Bielski, D. E. Cabelli, R. L. Arudi and A. B. Ross, *J. Phys. Chem. Ref. Data*, 1985, **14**, 1041–1100.

23 L. Gaohua, X. Miao and L. Dou, *Expert Opin. Drug Metab. Toxicol.*, 2021, **17**, 1103–1124.

24 S. Yoshikawa, K. Muramoto, K. Shinzawa-itoh and H. Aoyama, *Biochim. Biophys. Acta*, 2006, **1757**, 1110–1116.

25 K. Schmidt-Rohr, *ACS Omega*, 2020, **5**, 2221–2233.

26 X. Li, P. Fang, J. Mai, E. T. Choi, H. Wang and X. F. Yang, *J. Hematol. Oncol.*, 2013, **6**, 1–19.

27 A. W. Segal, *Annu. Rev. Immunol.*, 2005, **23**, 197–223.

28 M. Herb and M. Schramm, *Antioxidants*, 2021, **10**, 1–39.

29 J. F. Curtin, M. Donovan and T. G. Cotter, *J. Immunol. Methods*, 2002, **265**, 49–72.

30 T. Ozben, *J. Pharm. Sci.*, 2007, **96**, 2181–2196.

31 M. Hayyan, M. A. Hashim and I. M. Alnashef, *Chem. Rev.*, 2016, **116**, 3029–3085.

32 M. J. Davies, *Biochim. Biophys. Acta - Proteins Proteomics*, 2005, **1703**, 93–109.

33 S. B. Nimse and D. Pal, *RSC Adv.*, 2015, **5**, 27986–28006.

34 P. Sharma, A. B. Jha, R. S. Dubey and M. Pessarakli, *J. Bot.*, 2012, **2012**, 1–26.

35 P. Chelikani, I. Fita and P. C. Loewen, *Cell. Mol. Life Sci.*, 2004, **61**, 192–208.

36 A. Meister and M. E. Anderson, *Ann. Rev. Biochem.*, 1983, **52**, 711–760.

37 F. Q. Schafer and G. R. Buettner, *Free Radic. Biol. Med.*, 2001, **30**, 1191–1212.

38 N. Couto, N. Malys, S. J. Gaskell and J. Barber, *J. Proteome Res.*, 2013, **12**, 2885–2894.

39 C. E. Ofoedu, L. You, C. M. Osuji, J. O. Iwouno, N. O. Kabuo, M. Ojukwu, I. M. Agunwah, J. S. Chacha, O. P. Muobike, A. O. Agunbiade, G. Sardo, G. Bono, C. O. R. Okpala and M. Korzeniowska, *Foods*, 2021, **10**, 699.

40 Y. P. A. de Oliveira, L. C. Pontes-de-Carvalho, R. D. Couto and A. A. Noronha-Dutra, *Brazilian J. Infect. Dis.*, 2017, **21**, 19–26.

41 F. Ahmadinejad, S. Geir Møller, M. Hashemzadeh-Chaleshtori, G. Bidkhori and M.-S. Jami, *Antioxidants*, 2017, **6**, 51.

42 Y. Liu, Q. Jia, Q. Guo, A. Jiang and J. Zhou, *Anal. Chem.*, 2017, **89**, 12299–12305.

43 D. Harman, *J. Gerontol.*, 1956, **11**, 298–300.

44 H. C. Birnboim, *Carcinogenesis*, 1986, **7**, 1511–1517.

45 J. Cadet, T. Delatour, T. Douki, D. Gasparutto, J. P. Pouget, J. L. Ravanat and S. Sauvaigo, *Mutat. Res.*, 1999, **424**, 9–21.

46 L. C. Colis, P. Raychaudhury and A. K. Basu, *Biochemistry*, 2008, **47**, 8070–8079.

47 H. C. Box, E. E. Budzinski, J. D. Dawidzik, J. C. Wallace, S. Marianne, J. S. Gobey, H. C. Box, E. E. Budzinski, D. Dawidzik, C. Wallace, S. Evans and S. Gobey, *Radiat. Res.*, 2014, **145**, 641–643.

48 A. Parent, A. Benjdia, A. Guillot, X. Kubiak, C. Balty, B. Lefranc, J. Leprince and O. Berteau, *J. Am. Chem. Soc.*, 2017, **140**, 2469–2477.

49 C. N. Hewitt and R. M. Harrison, *Atmos. Environ.*, 1985, **19**, 545–554.

50 S. Gligorovski, R. Strekowski, S. Barbati and D. Vione, *Chem. Rev.*, 2015, **115**, 13051–

13092.

51 C. M. Spivakovsky, J. A. Logan, S. A. Montzka, Y. J. Balkanski, M. Foreman-Fowler, D. B. A. Jones, L. W. Horowitz, A. C. Fusco, C. A. M. Brenninkmeijer, M. J. Prather, S. C. Wofsy and M. B. McElroy, *J. Geophys. Res. Atmos.*, 2000, **105**, 8931–8980.

52 R. P. Adamsa and J. W. Wrightb, *J. Essent. Oil Res.*, 2012, **24**, 435–440.

53 H. J. Kim, K. Kim, N. S. Kim and D. S. Lee, *J. Chromatogr. A*, 2000, **902**, 389–404.

54 H. Wittcoff and B. Reuben, *Industrial Organic Chemicals*, John Wiley, New York, NY, 1996.

55 R. E. Dunmore, J. R. Hopkins, R. T. Lidster, J. D. Lee, M. J. Evans, A. R. Rickard, A. C. Lewis and J. F. Hamilton, *Atmos. Chem. Phys.*, 2015, **15**, 9983–9996.

56 P. Ciccioli, E. Brancaleoni, R. Mabilia and A. Cecinato, *J. Chromatogr. A*, 1997, **777**, 267–274.

57 Master Chemical Mechanism, MCM v3.3.1 (Jenkin *et al*., *Atmos. Environ.*, 1997, **31**, 81; Saunders *et al*., *Atmos. Chem. Phys.*, 2003, **3**, 161; Jenkin *et al*., *Atmos. Chem. Phys.*, 2015, **15**, 11433), http://mcm.york.ac.uk.

58 D. Zhang and R. Zhang, *J. Chem. Phys.*, 2005, **122**, 114308.

59 M. Camredon, J. F. Hamilton, M. S. Alam, K. P. Wyche, T. Carr, I. R. White, P. S. Monks, A. R. Rickard and W. J. Bloss, *Atmos. Chem. Phys.*, 2010, **10**, 2893–2917.

60 S. D. Tetali, *Planta*, 2019, **249**, 1–8.

61 K. Sindelarova, C. Granier, I. Bouarar, A. Guenther, S. Tilmes, T. Stavrakou, J. F. Müller, U. Kuhn, P. Stefani and W. Knorr, *Atmos. Chem. Phys.*, 2014, **14**, 9317–9341.

62 A. Guenther, C. Nicholas Hewitt, E. David, R. Fall, G. Chris, G. Tom, H. Peter, L. Klinger, L. Manuel, W. A. Mckay, P. Tom, B. Scholes, R. Steinbrecher, R. Tallamraju, J. Taylor and P. Zimmerman, *J. Geophys. Res.*, 1995, **100**, 8873–8892.

63 G. I. Gkatzelis, M. M. Coggon, B. C. McDonald, J. Peischl, J. B. Gilman, K. C. Aikin, M. A. Robinson, F. Canonaco, A. S. H. Prevot, M. Trainer and C. Warneke, *Environ. Sci. Technol.*, 2021, **55**, 4332–4343.

64 C. Stönner, A. Edtbauer and J. Williams, *Indoor Air*, 2018, **28**, 164–172.

65 M. Ehn, J. A. Thornton, E. Kleist, M. Sipilä, H. Junninen, I. Pullinen, M. Springer, F. Rubach, R. Tillmann, B. Lee, F. Lopez-Hilfiker, S. Andres, I. H. Acir, M. Rissanen, T. Jokinen, S. Schobesberger, J. Kangasluoma, J. Kontkanen, T. Nieminen, T. Kurtén, L. B. Nielsen, S. Jørgensen, H. G. Kjaergaard, M. Canagaratna, M. D. Maso, T. Berndt, T. Petäjä, A. Wahner, V. M. Kerminen, M. Kulmala, D. R. Worsnop, J. Wildt and T. F. Mentel, *Nature*, 2014, **506**, 476–479.

66 A. Mutzel, L. Poulain, T. Berndt, Y. Iinuma, M. Rodigast, O. Böge, S. Richters, G. Spindler, M. Sipilä, T. Jokinen, M. Kulmala and H. Herrmann, *Environ. Sci. Technol.*, 2015, **49**, 7754–7761.

67 F. Bianchi, T. Kurtén, M. Riva, C. Mohr, M. P. Rissanen, P. Roldin, T. Berndt, J. D. Crounse, P. O. Wennberg, T. F. Mentel, J. Wildt, H. Junninen, T. Jokinen, M. Kulmala, D. R. Worsnop, J. A. Thornton, N. Donahue, H. G. Kjaergaard and M. Ehn, *Chem. Rev.*, 2019, **119**, 3472–3509.

68 D. Johnson and G. Marston, *Chem. Soc. Rev.*, 2008, **37**, 699–716.

69 R. Criegee, *Angew. Chem. Int. Ed.*, 1975, **14**, 745–752.

70 C. A. Taatjes, G. Meloni, T. M. Selby, A. J. Trevitt, D. L. Osborn, C. J. Percival and D. E. Shallcross, *J. Am. Chem. Soc.*, 2008, **130**, 11883–11885.

71 O. Welz, J. D. Savee, D. L. Osborn, S. S. Vasu, C. J. Percival, D. E. Shallcross and C. A. Taatjes, *Science*, 2012, **335**, 204–207.

72 Y. Te Su, Y. H. Huang, H. A. Witek and Y. P. Lee, *Science*, 2013, **340**, 174–176.

73 M. J. Newland, A. R. Rickard, M. S. Alam, L. Vereecken, A. Muñoz, M. Ródenas and W. J. Bloss, *Phys. Chem. Chem. Phys.*, 2015, **17**, 4076–4088.

74 E. Zavoisky, *J. Phys. USSR*, 1945, **9**, 211–245.

75 V. Parish, *NMR, NQR, EPR and Mössbauer Spectroscopy in Inorganic Chemistry*, Ellis Horwood Limited, Chichester, UK, 1990.

76 C. A. Rice-Evans, A. T. Diplock and M. C. R. Symons, in *Techniques in Free Radical Research*, Elsevier Science Publishers B.V., Amsterdam, 1991, pp. 51–100.

77 V. Chechik, E. Carter and D. Murphy, *Electron Paramagnetic Resonance*, Oxford University Press, Oxford, UK, 2016.

78 A. Yamada, M. Abe, Y. Nishimura, S. Ishizaka, M. Namba, T. Nakashima, K. Shimoji and N. Hattori, *Beilstein J. Org. Chem.*, 2019, **15**, 863–873.

79 A. C. Eslami, W. Pasanphan, B. A. Wagner and G. R. Buettner, *Chem. Cent. J.*, 2010, **4**, 1–4.

80 D. Mihelcic, D. H. Ehhalt, G. F. Kulessa, J. Klomfass, M. Trainer, U. Schmidt and H. Röhrs, *Pure Appl. Geophys.*, 1978, **116**, 530–536.

81 D. Mihelcic, P. Müsgen and D. H. Ehhalt, *J. Atmos. Chem.*, 1985, **3**, 341–361.

82 D. Mihelcic, D. Klemp, P. Müsgen, H. W. Pätz and A. Volz-Thomas, *J. Atmos. Ocean. Technol.*, 1993, **16**, 313–335.

83 E. G. Janzen, *Acc. Chem. Res.*, 1971, **4**, 31–40.

84 D. F. Church, *Anal. Chem.*, 1994, **66**, 419–427.

85 R. Kaptein and J. L. Oosterhoff, *Chem. Phys. Lett.*, 1969, **4**, 195–197.

86 M. Goez, in *Annual Reports on NMR Spectroscopy*, Elsevier Ltd., 2009, vol. 66, pp. 77–147.

87 C. Karunakaran, P. Santharaman and M. Balamurugan, *1H and 13C nuclear magnetic resonance spectroscopy*, Elsevier Inc., 2018.

88 O. A. Krumkacheva, V. R. Gorelik, E. G. Bagryanskaya, N. V. Lebedeva and M. D. E. Forbes, *Langmuir*, 2010, **26**, 8971–8980.

89 J. A. McCloskey, *Mass Spectrometry*, Academic Press, San Diego, 1990.

90 J. R. Chapman, *Practical Organic Mass Spectrometry: A Guide for Chemical and Biological Analysis*, John Wiley, Chichester, UK, 1993.

91 E. de Hoffmann and V. Stroobant, *Mass Spectrometry: Principles and Applications*, John Wiley & Sons Ltd., Chichester, UK, 2007.

92 G. L. Glish and R. W. Vachet, *Nat. Rev. Drug Discov.*, 2003, **2**, 140–150.

93 F. W. McLafferty, *Annu. Rev. Anal. Chem.*, 2011, **4**, 1–22.

94 H. Awad, M. M. Khamis and A. El-Aneed, *Appl. Spectrosc. Rev.*, 2015, **50**, 158–175.

95 A. Gaudel-Siri, C. Marchal, V. Ledentu, D. Gigmes, D. Siri and L. Charles, *Eur. J. Mass Spectrom.*, 2019, **25**, 229–238.

96 M. J. Eirod, *J. Phys. Chem. A*, 1999, **103**, 4378–4384.

97 D. Hanson, J. Orlando, B. Nozière and E. Kosciuch, *Int. J. Mass Spectrom.*, 2004, **239**, 147–159.

98 B. Nozière and D. R. Hanson, *J. Phys. Chem. A*, 2017, **121**, 8453–8464.

99 B. Nozière and L. Vereecken, *Angew. Chem. Int. Ed.*, 2019, **58**, 13976–13982.

100 C. Zhu, K. Kawamura and B. Kunwar, *Atmos. Chem. Phys.*, 2015, **15**, 1959–1973.

101 H.-H. Perkampus, *UV-Vis Spectroscopy and Its Applications*, Springer-Verlag, New York, 1992.

102 J. R. Lakowicz, *Principles of Fluorescence Spectroscopy*, Springer, New York, 2006.

103 A. Celebioglu and T. Uyar, *J. Agric. Food Chem.*, 2017, **65**, 5404–5412.

104 Y. Beldjoudi, M. A. Nascimento, Y. J. Cho, H. Yu, H. Aziz, D. Tonouchi, K. Eguchi, M. M. Matsushita, K. Awaga, I. Osorio-Roman, C. P. Constantinides and J. M. Rawson, *J. Am. Chem. Soc.*, 2018, **140**, 6260–6270.

105 V. Sick and N. Wermuth, *Appl. Phys. B Lasers Opt.*, 2004, **79**, 139–143.

106 X. Ren, H. Harder, M. Martinez, I. C. Faloona, D. Tan, R. L. Lesher, P. Di Carlo, J. B. Simpas and W. H. Brune, *J. Atmos. Chem.*, 2004, **47**, 169–190.

107 D. E. Heard, *Annu. Rev. Phys. Chem.*, 2006, **57**, 191–216.

108 D. Stone, L. K. Whalley and D. E. Heard, *Chem. Soc. Rev.*, 2012, **41**, 6348–6404.

109 Y. Gong and L. Andrews, *J. Phys. Chem. A*, 2011, **115**, 3029–3033.

110 H. Li, Y. Cheng, H. Tang, Y. Bi, Y. Chen, G. Yang, S. Guo, S. Tian, J. Liao, X. Lv, S. Zeng, M. Zhu, C. Xu, J. X. Cheng and P. Wang, *Adv. Sci.*, 2020, **7**, 1903644.

111 A. Saiz-Lopez, A. S. Mahajan, R. A. Salmon, S. J. B. Bauguitte, A. E. Jones, H. K. Roscoe and J. M. C. Plane, *Science*, 2007, **317**, 348–351.

112 M. Sangwan and L. Zhu, *J. Phys. Chem. A*, 2018, **122**, 1861–1872.

113 N. Wei, B. Fang, W. Zhao, C. Wang, N. Yang, W. Zhang, W. Chen and C. Fittschen, *Anal. Chem.*, 2020, **92**, 4334–4339.

114 P. L. Zamora and F. A. Villamena, *J. Phys. Chem. A*, 2012, **116**, 7210–7218.

115 M. Pelletier, V. Lavastre and D. Girard, *Toxicol. Sci.*, 2002, **69**, 210–216.

116 F. Poulhès, E. Rizzato, P. Bernasconi, R. Rosas, S. Viel, L. Jicsinszky, A. Rockenbauer, D. Bardelang, D. Siri, A. Gaudel-Siri, H. Karoui, M. Hardy and O. Ouari, *Org. Biomol. Chem.*, 2017, **15**, 6358–6366.

117 M. Cassien, C. Petrocchi, S. Thétiot-Laurent, M. Robin, E. Ricquebourg, C. Kandouli, A. Asteian, A. Rockenbauer, A. Mercier, M. Culcasi and S. Pietri, *Eur. J. Med. Chem.*, 2016, **119**, 197–217.

118 K. Abbas, M. Hardy, F. Poulhès, H. Karoui, P. Tordo, O. Ouari and F. Peyrot, *Free Radic. Biol. Med.*, 2014, **71**, 281–290.

119 M. A. Rudat and C. N. McEwen, *J. Am. Chem. Soc.*, 1981, **103**, 4349–4354.

120 H. Iwahashi, C. E. Parker, R. P. Mason and K. B. Tomer, *Rapid Commun. Mass Spectrom.*, 1990, **4**, 352–354.

121 C. E. Parker, H. Iwahashi and K. B. Tomer, *J. Am. Soc. Mass Spectrom.*, 1991, **2**, 413–418.

122 Q. Guo, S. Y. Qian and R. P. Mason, *J. Am. Soc. Mass Spectrom.*, 2003, **14**, 862–871.

123 P. Domingues, C. Fonseca, A. Reis and M. R. M. Domingues, *Biomed. Chromatogr.*, 2012, **26**, 51–60.

124 Y. Wang, M. Liu, Y. Zhu, K. Cheng, W. Da, B. Liu and F. Li, *Talanta*, 2016, **160**, 106–112.

125 C. Giorio, S. J. Campbell, M. Bruschi, F. Tampieri, A. Barbon, A. Toffoletti, A. Tapparo, C. Paijens, A. J. Wedlake, P. Grice, D. J. Howe and M. Kalberer, *J. Am. Chem. Soc.*, 2017, **139**, 3999–4008.

126 A. Zaytsev, M. Breitenlechner, A. Novelli, H. Fuchs, D. Knopf, J. Kroll and F. Keutsch, *Atmos. Meas. Tech. Discuss.*, 2020, **14**, 1–20.

127 F. Leinisch, J. Jiang, E. F. Derose, V. V. Khramtsov and R. P. Mason, *Free Radic. Biol. Med.*, 2013, **65**, 1497–1505.

128 S. Pou, D. J. Hassett, B. E. Britigan, M. S. Cohen and G. M. Rosen, *Anal. Biochem.*, 1989, **177**, 1–6.

129 G. R. Buettner and L. W. Oberley, *Biochem. Biophys. Res. Commun.*, 1978, **83**, 69–74.

130 N. Sankuratri, Y. Kotake and E. G. Janzen, *Free Radic. Biol. Med.*, 1996, **21**, 889–894.

131 N. Khan, C. M. Wilmot, G. M. Rosen, E. Demidenko, J. Sun, J. Joseph, J. O'Hara, B. Kalyanaraman and H. M. Swartz, *Free Radic. Biol. Med.*, 2003, **34**, 1473–1481.

132 K. Stolze, N. Udilova, T. Rosenau, A. Hofinger and H. Nohl, *Biochem. Pharmacol.*, 2003, **66**, 1717–1726.

133 T. Vogler and A. Studer, *Synthesis*, 2008, **13**, 1979–1993.

134 Y. Matsuoka, Y. Izumi, M. Takahashi, T. Bamba and K. Yamada, *Anal. Chem.*, 2020, **92**, 6993–7002.

135 X. F. Xia, S. L. Zhu, Y. N. Niu, D. Zhang, X. Liu and H. Wang, *Tetrahedron*, 2016, **72**, 3068–3072.

136 H. Yan, G. Rong, D. Liu, Y. Zheng, J. Chen and J. Mao, *Org. Lett.*, 2014, **16**, 6306–6309.

137 A. P. Dobbs, P. Jones, M. J. Penny and S. E. Rigby, *Tetrahedron*, 2009, **65**, 5271–5277.

138 P. J. Wright and A. M. English, *J. Am. Chem. Soc.*, 2003, **125**, 8655–8665.

139 Y. R. Luo, *Comprehensive Handbook of Chemical Bond Energies*, CRC Press, Boca Raton, FL, 2007.

140 D. H. R. Barton, V. N. Le Gloahec and J. Smith, *Tetrahedron Lett.*, 1998, **39**, 7483–7486.

141 C. D. Cook and R. C. Woodworth, *J. Am. Chem. Soc.*, 1953, **75**, 6242–6244.

142 V. A. Khizhnyi and G. A. Goloverda, *Teor Eksperim Khim*, 1988, **24**, 154–159.

143 P. Griva and E. T. Dexisov, *Int. J. Chem. Kinet.*, 1973, **5**, 869–877.

144 M. A. DaRooge and L. R. Mahoney, *J. Org. Chem.*, 1967, **32**, 1–6.

145 M. Tomita, T. Okuyama, S. Watanabe and H. Watanabe, *Arch. Toxicol.*, 1994, **68**, 428–433.

146 X. Yang, M. Zhan, L. Kong and L. Wang, *J. Environ. Sci.*, 2004, 16, 687–689.

147 H. Jian, *Chinese J. Chem.*, 2005, **23**, 1273–1274.

148 H. Karoui, F. Le Moigne, O. Ouari and P. Tordo, in *Stable Radicals: Fundamentals and Applied Aspects of Odd-Electron Compounds*, ed. R. G. Hicks, John Wiley & Sons, Inc., 2010, vol. 12, pp. 173–229.

149 E. G. Bagryanskaya and S. R. A. Marque, *Chem. Rev.*, 2014, **114**, 5011–5056.

150 Y.-M. Dang and X.-Q. Guo, *Appl. Spectrosc.*, 2006, **60**, 203–207.

151 R. Toba, H. Gotoh and K. Sakakibara, *Org. Lett.*, 2014, **16**, 3868–3871.

152 A. Grantham, PhD thesis, University of York, 2017.

153 J. F. Van Humbeck, S. P. Simonovich, R. R. Knowles and D. W. C. Macmillan, *J. Am. Chem. Soc. Commun.*, 2010, **132**, 10012–10014.

154 M. E. Jenkin, T. P. Murrells, S. J. Shalliker and G. D. Hayman, *J. Chem. Soc. Faraday Trans.*, 1993, **89**, 433–446.

155 T. Wang, G. Kehr, L. Liu, S. Grimme, C. G. Daniliuc and G. Erker, *J. Am. Chem. Soc.*, 2016, **138**, 4302–4305.

156 D. E. Bergbreiter and B. Walchuk, *Macromolecules*, 1998, **31**, 6380–6382.

157 O. Ito, Y. Arito and M. Matsuda, *J. Chem. Soc. Perkin Trans. 2*, 1988, 869–873.

158 A. M. Tsedilin, A. N. Fakhrutdinov, D. B. Eremin, S. S. Zalesskiy, A. O. Chizhov, N. G. Kolotyrkina and V. P. Ananikov, *Mendeleev Commun.*, 2015, **25**, 454–456.

159 S. J. Gaskell, *J. Mass Spectrom.*, 1997, **32**, 677–688.

160 S. Banerjee and S. Mazumdar, *Int. J. Anal. Chem.*, 2012, **2012**, 1–40.

161 P. Liigand, J. Liigand, K. Kaupmees and A. Kruve, *Anal. Chim. Acta*, 2021, **1152**, 238117.

162 S. Indelicato, D. Bongiorno and L. Ceraulo, *Front. Chem.*, 2021, **8**, 1–6.

163 F. W. McLafferty, *Acc. Chem. Res.*, 1980, **13**, 33–39.

164 J. J. Coon, J. E. P. Syka, J. Shabanowitz and D. F. Hunt, *Biotechniques*, 2005, **38**, 519–523.

165 A. R. Johnson and E. E. Carlson, *Anal. Chem.*, 2015, **87**, 10668–10678.

166 J. F. Parcher, M. Wang, A. G. Chittiboyina and I. A. Khan, *Drug Test. Anal.*, 2018, **10**, 28–36.

167 J. W. Flora, J. C. Hannis and D. C. Muddiman, *Anal. Chem.*, 2001, **73**, 1247–1251.

168 K. A. Herrmann, A. Somogyi, V. H. Wysocki, L. Drahos and K. Vekey, *Anal. Chem.*, 2005, **77**, 7626–7638.

169 W. A. Korfmacher, *Drug Discov. Today*, 2005, **10**, 1357–1367.

170 J. J. Pitt, *Clin. Biochem. Rev.*, 2009, **30**, 19–34.

171 N. A. Pratima, *Arch. Org. Inorg. Chem. Sci.*, 2018, **1**, 26–34.

172 I. M. Klotz and B. H. Frank, *J. Am. Chem. Soc.*, 1965, **87**, 2721–2728.

173 N. Hogg, *J. Biol. Chem.*, 1996, **271**, 6000–6009.

174 L. Engman, J. Lind and G. Merényi, *J. Phys. Chem.*, 1994, **98**, 3174–3182.

175 P. Carloni, E. Damiani, M. Iacussi, L. Greci, P. Stipa, D. Cauzi, C. Rizzoli and P. Sgarabotto, *Tetrahedron*, 1995, **51**, 12445–12452.

176 M. Méndez, J. S. Francisco and D. A. Dixon, *Chem. Eur. J.*, 2014, **20**, 10231–10235.

177 D. H. R. Barton and J. M. Beaton, *J. Am. Chem. Soc.*, 1961, **83**, 4083–4089.

178 D. R. Barton, J. M. Beaton, L. E. Geller and M. M. Pechet, *J. Am. Chem. Soc.*, 1961, **83**, 4076–4083.

179 D. H. R. Barton, R. H. Hesse, M. M. Pechet and L. C. Smith, *J. Chem. Soc., Perkin Trans. 1*, 1979, 1159–1165.

180 M. Akhtar and M. M. Pechet, *J. Am. Chem. Soc.*, 1964, **86**, 265–268.

181 A. W. Hofmann, *Chem. Ber.*, 1885, **18**, 109–131.

182 K. Löffler and C. Freytag, *Chem. Ber.*, 1909, **42**, 3427–3431.

183 E. J. Corey and W. R. Hertler, *J. Am. Chem. Soc.*, 1960, **82**, 1657–1668.

184 C. Martínez and K. Muñiz, *Angew. Chem. Int. Ed.*, 2015, **54**, 8287–8291.

185 P. Becker, T. Duhamel, C. J. Stein, M. Reiher and K. Muñiz, *Angew. Chem. Int. Ed.*, 2017, **56**, 8004–8008.

186 P. Becker, T. Duhamel, C. Martínez and K. Muñiz, *Angew. Chem. Int. Ed.*, 2018, **57**, 5166–5170.

187 S. Shkunnikova, H. Zipse and D. Šakić, *Org. Biomol. Chem.*, 2021, **19**, 854–865.

188 A. Artaryan, A. Mardyukov, K. Kulbitski, I. Avigdori, G. A. Nisnevich, P. R. Schreiner and M. Gandelman, *J. Org. Chem.*, 2017, **82**, 7093–7100.

189 A. E. Bosnidou, T. Duhamel and K. Muñiz, *European J. Org. Chem.*, 2020, 6361–6365.

190 S. Wawzonek and P. J. Thelen, *J. Am. Chem. Soc.*, 1950, **72**, 2118–2120.

191 A. Borodine, *Justus Liebigs Ann. Chem.*, 1861, **119**, 121–123.

192 H. Hunsdiecker and C. Hunsdiecker, *Berichte der Dtsch. Chem. Gesellschaft*, 1942, **75**, 291–297.

193 R. G. Johnson and R. K. Ingham, *Chem. Rev.*, 1956, **56**, 219–269.

194 J. A. den Hollander and J. P. M. van der Ploeg, *Tetrahedron*, 1976, **32**, 2433–2436.

195 J. W. Hilborn and J. A. Pincock, *J. Am. Chem. Soc.*, 1991, **113**, 2683–2686.

196 A. Bhattacherjee, M. Sneha, L. Lewis-Borrell, O. Tau, I. P. Clark and A. J. Orr-Ewing, *Nat. Commun.*, 2019, **10**, 1–7.

197 J. C. Bevington and J. Leech, *Eur. Polym. J.*, 1980, **16**, 917–920.

198 J. Chateauneuf, J. Lusztyk and K. U. Ingold, *J. Am. Chem. Soc.*, 1987, **109**, 897–899.

199 J. Chateauneuf, J. Lusztyk and K. U. Ingold, *J. Am. Chem. Soc.*, 1988, **110**, 2886–2893.

200 Y. Wang, W. Wang, R. Tang, Z. Liu, W. Tao and Z. Fang, *Org. Biomol. Chem.*, 2018, **16**, 7782–7786.

201 G. J. P. Perry, J. M. Quibell, A. Panigrahi and I. Larrosa, *J. Am. Chem. Soc.*, 2017, **139**, 11527–11536.

202 L. Buzzetti, G. E. M. Crisenza and P. Melchiorre, *Angew. Chem. Int. Ed.*, 2019, **58**, 3730–3747.

203 J. R. Donald and S. L. Berrell, *Chem. Sci.*, 2019, **10**, 5832–5836.

204 B. H. Northrop and R. N. Coffey, *J. Am. Chem. Soc.*, 2012, **134**, 13804–13817.

205 E. L. Tyson, M. S. Ament and T. P. Yoon, *J. Org. Chem.*, 2013, **78**, 2046–2050.

206 C. M. Q. Le, F. Morlet-Savary and A. Chemtob, *Polym. Chem.*, 2021, **12**, 6594–6605.

207 J. C. Ianni, Kintecus, Windows Version 6.50, www.kintecus.com.

208 V. Fındık, I. Degirmenci, Ş. Çatak and V. Aviyente, *Eur. Polym. J.*, 2019, **110**, 211–220.

209 G. S. Prementine and D. A. Tirrell, *Macromolecules*, 1989, **22**, 52–55.

210 J. Chateauneuf, J. Lusztyk and K. U. Ingold, *J. Org. Chem.*, 1988, **53**, 1629–1632.

211 I. Degirmenci and M. L. Coote, *J. Phys. Chem. A*, 2016, **120**, 7398–7403.

212 H. E. Ho, A. Pagano, J. A. Rossi-Ashton, J. R. Donald, R. G. Epton, J. C. Churchill, M. J. James, P. O'Brien, R. J. K. Taylor and W. P. Unsworth, *Chem. Sci.*, 2020, **11**, 1353–1360.

213 M. S. Cooke, M. D. Evans, M. Dizdaroglu and J. Lunec, *FASEB J.*, 2003, **17**, 1195–1214.

214 B. Halliwell, *Biochem. J.*, 2007, **401**, 1–11.

215 M. Dizdaroglu and P. Jaruga, *Free Radic. Res.*, 2012, **46**, 382–419.

216 J. Cadet and J. Richard Wagner, *Cold Spring Harb. Perspect. Biol.*, 2013, **5**, 1–18.

217 G. V. Buxton, C. L. Greenstock, W. P. Helman and A. B. Ross, *J. Phys. Chem. Ref. Data*, 1988, **17**, 513–886.

218 L. M. Smith, H. M. Aitken and M. L. Coote, *Acc. Chem. Res.*, 2018, **51**, 2006–2013.

219 M. Dorfman L. and E. Adams G., *Reactivity of the Hydroxyl Radical in Aqueous Solutions*, Columbus, OH, 1973.

220 B. Maillard, K. U. Ingold and J. C. Scaiano, *J. Am. Chem. Soc.*, 1983, **105**, 5095–5099.

221 P. Neta, R. E. Huie and A. B. Ross, *J. Phys. Chem. Ref. Data*, 1988, **17**, 1027–1284.

222 S. Korcek, J. H. B. Chenier, J. A. Howard and K. U. Ingold, *Can. J. Chem.*, 1972, **50**, 2285–2297.

223 J. K. Thomas, *J. Phys. Chem.*, 1967, **71**, 1919–1925.

224 K. Münger and H. Fischer, *Int. J. Chem. Kinet.*, 1985, **17**, 809–829.

225 H. Rubin, PhD Thesis, University of Zurich, 1993.

226 J. A. Howard, *Can. J. Chem.*, 1972, **50**, 2298–2304.

227 P. Koelewijn, *Recl. des Trav. Chim. des Pays-Bas*, 1972, **91**, 759–779.

228 P. C. Wong, D. Griller and J. C. Scaiano, *J. Am. Chem. Soc.*, 1982, **104**, 5106–5108.

229 C. Wang, Z. Wang, B. Zeng, M. Zheng, N. Xiao and Z. Zhao, *Chem. Commun.*, 2021, **57**, 12293–12296.

230 I. H. Madshus, *Biochem. J.*, 1988, **250**, 1–8.

231 A. Fischbacher, C. von Sonntag and T. C. Schmidt, *Chemosphere*, 2017, **182**, 738–744.

232 M. Kimura, M. Tohma and T. Tomita, *Chem. Pharm. Bull.*, 1972, **20**, 2185–2190.

233 J. Woodward, K. W. Lennon, G. Zanin, M. Wagner and M. A. Scott, *Biotechnol. Lett.*, 1985, **7**, 197–202.

234 S.-S. Liang, Y.-L. Shiue, C.-J. Kuo, S.-E. Guo, W.-T. Liao and E.-M. Tsai, *Sci. World J.*, 2013, 189162.

235 C. P. Rao and K. Geetha, *BioMetals*, 1994, **7**, 25–29.

236 Y. S.H., Y. H. and J. P., *Handbook of Aqueous Solubility Data*, CRC Press, 2010.

237 J. Cadet and J. R. Wagner, *Cold Spring Harb. Perspect. Biol.*, 2013, **5**, 1–18.

238 C. L. Hawkins and M. J. Davies, *Biochim. Biophys. Acta - Bioenerg.*, 2001, **1504**, 196–219.

239 A. E. Counterman, A. E. Hilderbrand, C. A. Srebalus Barnes and D. E. Clemmer, *J. Am. Soc. Mass Spectrom.*, 2001, **12**, 1020–1035.

240 M. N. Schuchmann and C. Von Sonntag, *J. Chem. Soc. Perkin Trans. 2*, 1977, 1958–1963.

241 R. A. M. Vreeburg, O. B. Airianah and S. C. Fry, *Biochem. J.*, 2014, **463**, 225–237.

242 A. Matros, D. Peshev, M. Peukert, H. P. Mock and W. Van Den Ende, *Plant J.*, 2015, **82**, 822–839.

243 W. D. Kumler and T. C. Daniels, *J. Am. Chem. Soc.*, 1935, **57**, 1929–1930.

244 D. J. Stewart, S. H. Almabrok, J. P. Lockhart, O. M. Mohamed, D. R. Nutt, C. Pfrang and G. Marston, *Atmos. Environ.*, 2013, **70**, 227–235.

245 D. L. Baulch, C. T. Bowman, C. J. Cobos, R. A. Cox, T. Just, J. A. Kerr, M. J. Pilling, D. Stocker, J. Troe, W. Tsang, R. W. Walker and J. Warnatz, *J. Phys. Chem. Ref. Data*, 2005, **34**, 757–1397.

246 R. X. Fernandes, K. Luther and J. Troe, *J. Phys. Chem. A*, 2006, **110**, 4442–4449.

247 N. M. Panich and B. G. Ershov, *J. Mol. Liq.*, 2021, **340**, 117318.

248 A. Hansel, W. Scholz, B. Mentler, L. Fischer and T. Berndt, *Atmos. Environ.*, 2018, **186**, 248–255.

249 L. Vereecken and J. Peeters, *J. Phys. Chem. A*, 2004, **108**, 5197–5204.

250 V. K. Yadav and K. G. Babu, *European J. Org. Chem.*, 2005, 452–456.

251 L. Vereecken, J. F. Müller and J. Peeters, *Phys. Chem. Chem. Phys.*, 2007, **9**, 5241–5248.

252 T. Berndt, S. Richters, T. Jokinen, N. Hyttinen, T. Kurtén, R. V. Otkjær, H. G. Kjaergaard, F. Stratmann, H. Herrmann, M. Sipilä, M. Kulmala and M. Ehn, *Nat. Commun.*, 2016, **7**, 1–8.

253 T. Jokinen, T. Berndt, R. Makkonen, V. M. Kerminen, H. Junninen, P. Paasonen, F. Stratmann, H. Herrmann, A. B. Guenther, D. R. Worsnop, M. Kulmala, M. Ehn and M. Sipilä, *Proc. Natl. Acad. Sci. U. S. A.*, 2015, **112**, 7123–7128.

254 J. Kirkby, J. Duplissy, K. Sengupta, C. Frege, H. Gordon, C. Williamson, M. Heinritzi, M. Simon, C. Yan, J. Almeida, J. Trostl, T. Nieminen, I. K. Ortega, R. Wagner, A. Adamov, A. Amorim, A. K. Bernhammer, F. Bianchi, M. Breitenlechner, S. Brilke, X. Chen, J. Craven, A. Dias, S. Ehrhart, R. C. Flagan, A. Franchin, C. Fuchs, R. Guida, J. Hakala, C. R. Hoyle, T. Jokinen, H. Junninen, J. Kangasluoma, J. Kim, M. Krapf, A. Kurten, A. Laaksonen, K. Lehtipalo, V. Makhmutov, S. Mathot, U. Molteni, A. Onnela, O. Perakyla, F. Piel, T. Petaja, A. P. Praplan, K. Pringle, A. Rap, N. A. D. Richards, I. Riipinen, M. P. Rissanen, L. Rondo, N. Sarnela, S. Schobesberger, C. E. Scott, J. H. Seinfeld, M. Sipila, G. Steiner, Y. Stozhkov, F. Stratmann, A. Tomé, A. Virtanen, A. L. Vogel, A. C. Wagner, P. E. Wagner, E. Weingartner, D. Wimmer, P. M. Winkler, P. Ye, X. Zhang, A. Hansel, J. Dommen, N. M. Donahue, D. R. Worsnop, U. Baltensperger, M. Kulmala, K. S. Carslaw and J. Curtius, *Nature*, 2016, **533**, 521–526.

255 J. Peeters, L. Vereecken and G. Fantechi, *Phys. Chem. Chem. Phys.*, 2001, **3**, 5489–5504.

256 A. Zaytsev, M. Breitenlechner, A. Novelli, H. Fuchs, D. A. Knopf, J. H. Kroll and F. N. Keutsch, *Atmos. Meas. Tech.*, 2021, **14**, 2501–2513.

257 E. S. C. Kwok and Atkinson, *Science*, 1995, **29**, 1685–1695.

258 J. W. Raymonda and W. T. Simpson, *J. Chem. Phys.*, 1967, **47**, 430–448.

259 M. S. Alam, A. R. Rickard, M. Camredon, K. P. Wyche, T. Carr, K. E. Hornsby, P. S. Monks and W. J. Bloss, *J. Phys. Chem. A*, 2013, **117**, 12468–12483.

260 L. Onel, A. Brennan, P. W. Seakins, L. Whalley and D. E. Heard, *Atmos. Meas. Tech.*, 2017, **10**, 3985–4000.

261 S. Goldstein and A. Samuni, *J. Phys. Chem. A*, 2007, **111**, 1066–1072.

262 L. Whalley, E. Slater, C. Ye, R. Woodward-Massey, J. Lee, F. Squires, J. Hopkins, R. Dunmore, J. Hamilton, A. Lewis, L. Crilley, L. Kramer, W. Bloss and D. Heard, *Geophys. Res. Abstr.*, 2018, **20**, 7409.

263 L. P. E. Yunker, Z. Ahmadi, J. R. Logan, W. Wu, T. Li, A. Martindale, A. G. Oliver and J. S. McIndoe, *Organometallics*, 2018, **37**, 4297–4308.

264 L. E. Greene, R. Lincoln and G. Cosa, *J. Am. Chem. Soc.*, 2017, **139**, 15801–15811.

265 M. Braun, U. Hartnagel, E. Ravanelli, B. Schade, C. Böttcher, O. Vostrowsky and A. Hirsch, *European J. Org. Chem.*, 2004, 1983–2001.

266 X. Chen, L. Henschke, Q. Wu, K. Muthoosamy, B. Neumann and T. Weil, *Org. Biomol. Chem.*, 2013, **11**, 353–361.

267 R. Göttlich, *Synthesis*, 2000, **11**, 1561–1564.

268 S. Pandiancherri and D. W. Lupton, *Tetrahedron Lett.*, 2011, **52**, 671–674.

269 Y. Xie, M. Sun, H. Zhou, Q. Cao, K. Gao, C. Niu and H. Yang, *J. Org. Chem.*, 2013, **78**, 10251–10263.

270 S. L. Titouani, J.-P. Lavergne, P. Viallefont and R. Jacquier, *Tetrahedron*, 1980, **36**, 2961–2965.

271 J. Cason, M. J. Kalm and R. H. Mills, *J. Org. Chem.*, 1953, **18**, 1670–1674.

272 H. Merten and H. Gilman, *J. Am. Chem. Soc.*, 1954, **76**, 5798–5799.

273 H. J. Perera, H. Mortazavian and F. D. Blum, *Langmuir*, 2017, **33**, 2799–2809.

274 J. Ortega, C. González and S. Galván, *J. Chem. Eng. Data*, 2001, **46**, 904–912.